ESTIMATION OF THE SEISMIC REPONSE OF BUILDINGS AND THE EFFECT OF DIFFERENT SCALING METHODS FOR GROUND MOTION

Sundar Ram Krishna Murthy Mohan Ram

A Thesis
In
The Department
Of
Building, Civil and Environmental Engineering

Presented in Partial Fulfillment of the Requirements
For the degree of Master of Applied Science (Civil Engineering) at
Concordia University
Montreal, Quebec, Canada

December 2012

CONCORDIA UNIVERSITY

School of Graduate Studies

This is to certify that the thesis prepared

By: **Sundar Ram Krishna Murthy Mohan Ram**

Entitled: **ESTIMATION OF THE SEISMIC REPONSE OF BUILDINGS AND THE EFFECT OF DIFFERENT SCALING METHODS FOR GROUND MOTION**

And submitted in partial fulfillment of the requirements for the degree of

Master of Applied Science (Civil Engineering)

Complies with the regulations of the University and meets the accepted standards with respect to originality and quality.

Signed by the final examining committee:

_____ Chair (Dr. L. Tirca, BCEE)

_____Examiner External to the Program
(Dr. A. Dolatabadi, MIE)

_____Examiner (Dr. L. Tirca, BCEE)

_____Examiner (Dr. A. Bhowmick, BCEE)

_____Supervisor (Dr. A. Bagchi, BCEE)

Approved by _____
Chair of Department or Graduate Program Director

_____20_____ _____
Dean of Faculty

ESTIMATION OF THE SEISMIC REPONSE OF BUILDINGS AND THE EFFECT OF DIFFERENT SCALING METHODS FOR GROUND MOTION

Sundar Ram Krishna Murthy Mohan

ABSTRACT

The Seismic design code of Canada is changing rapidly to accommodate the needs of the future generation of buildings for management of earthquake hazard mitigation. In this context the recent advancement in Earthquake Technology and Structural Engineering has emphasized on the need for a better methodology and in-depth investigation into the area of structural performance evaluation in order to ensure that structures designed for the areas of high and moderate seismic hazard to the expected standards and meet the objective of life safety and collapse prevention in a real life scenario. In order to ensure the above performance objectives for a building structure, it is necessary to estimate its capacity with respect to the demand, and the dynamic response corresponding to the design levels of earthquakes. The research carried out here aims to investigate: (i) the earthquake demand and capacity profiles of a set of set of moment frame buildings designed according to the latest version of the National Building Code of Canada, and (ii) the effect of scaling and spectral matching techniques commonly applied to ground motions on the seismic demand parameters determined using the dynamic time history analysis. A set of buildings with steel moment resisting frames of 5, 10, 15, 20 stories in height and located in Vancouver area of Canada have been considered in this study. An extensive review has been conducted to determine the existing methods for performance-based design and the techniques available to selecting and scaling suite of earthquake

records to perform a fully non-linear dynamic analysis in time domain. Based on that, a range of scaling techniques including linear scaling techniques, and spectral matching technique have been considered for an ensemble of recorded ground motion time histories. In addition a set of artificially generated spectrum-compatible earthquake records are also considered. The static pushover analysis has been carried out and the corresponding capacity curves have been obtained and interpreted with commonly used performance-based design methods. It is observed that all the methods considered here confirm that the existing design based on the code procedure is adequate and conservative. The pushover curves are also compared to the results obtained from the Time history analysis to determine the performance achievements of the buildings. The interstory drift obtained from the time history analysis using different scaling methods show a uniform and consistent pattern of deformation in low rise to medium rise frames whereas dispersion greater dispersion of the results has been observed in tall buildings. Other response quantities such as the lateral drift, base shear and bending moment show similar patterns. Based on the results from the research it is suggested to use the artificial records if site specific real ground motion records are unavailable. The scope for further research lies in exploring ways to the possibility of new scaling techniques that can control the dispersion in the response more effectively.

Acknowledgements

It's my deepest pleasure to express my sincere gratitude and heartfelt thanks to my program supervisor *Dr.Ashutosh Bagchi*, Associate Professor at Concordia University for having been the foremost source of inspiration, guidance and support through my M.A.Sc. program. "*Sir, please accept my sincere regards and heartfelt thanks for all that you have done for me through the course of my M.A.Sc., program"*

I fully acknowledge and convey my sincere gratitude and heartfelt appreciation to my mother *Smt.Sugandha* for her timeless encouragement and support in my student life.

Acknowledgement of thanks goes to my course work supervisors *Dr. Oscar Pekau, Dr. Lucia Tirca, Dr. Kinh H. Ha*, *Dr. Mohammed Ali* and *Mr.Adel Zaki***.** I also thank Jenny, Olga and the staff at BCEE department, Concordia University for their support during my graduate study.

The research was partially funded by Dr. Bagchi's research grant from the Natural Sciences and Engineering Research Council of Canada (NSERC) and Concordia University which is highly appreciated and acknowledged with thanks. Support from Canara Bank, India is also acknowledged. My sincere thanks and appreciation goes to my family and my colleagues in the Building, Civil and Environmental engineering department and to for their encouragement through my M.A.Sc. Program. Last but not the least, I whole heartedly pray and thank to pay my due respects to the Supreme *God* in guiding me to complete my graduate program with success.

TABLE OF CONTENTS

LIST OF FIGURES

LIST OF TABLES

My Loving Mother

Chapter 1

Introduction

1.1 Preface

Earthquake is described a seismic event involving sudden release of energy in the earth crust giving rise to seismic waves which causes ground motion or shaking of the ground, In the history of the mankind several strong earthquake incidents and their aftermaths have led to massive damage of property, destructive fires, tsunami and huge loss of human life. The recent earthquake in Japan (2011) of magnitude 9.0 is one such catastrophic scenario where in the aftermath effects provoked nuclear hazard in the region. Although the occurrence of an earthquake cannot be predicted to take precautionary measures and avoid loss of life and damage to property, the need of the hour is to aim for a possible response preparedness to deal with such a scenario in future in case of occurrence.

Earthquake engineering is an inter-disciplinary area which developed in the late 20^{th} century; it is a branch of civil engineering dealing in mitigating earthquake hazards by applying mainly the principles and knowledge of engineering sciences and seismology. The scope of the earthquake engineering include (a) Investigation of regional earthquake hazard to select a suitable location for the proposed structure (b) Estimation of the hazard at the selected location considering an adequate time interval and the local site conditions (c) Estimation of the structural response under the imposed hazard forces beforehand to facilitate adequate design of structure in whole and its members to resist such forces in order to prevent failure or collapse.

Looking back into the history of the built environment, many buildings, bridges and other facilities were designed by engineers to improve the performance during earthquakes However, the technology and the construction methods for earthquake resistant design of structures are still evolving. There is still a need for the development of effective tools for engineering analysis to compute the design seismic demands of the structural components and carry out performance-based seismic design.

It is important to note that earthquake engineering has been widely acknowledged and received well by researchers and engineers all over the world in the late 20^{th} century, and the knowledge database has been growing in a significant rate supported by advancing technologies, building code regulations, education and training professionals, and by public support. Fig.1 shows the worldwide growth trend of seismic design codes.

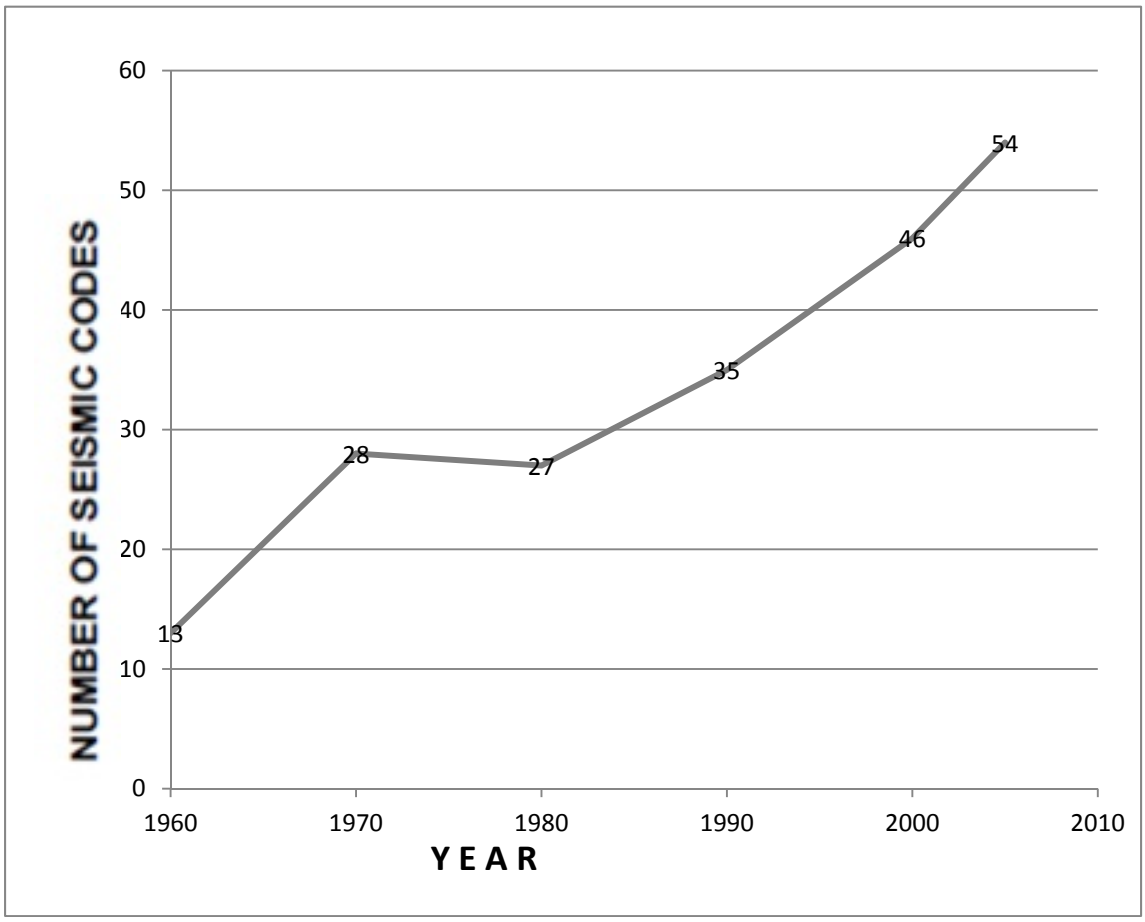

Figure 1.1: Growth in Worldwide Number of Seismic Codes (Source: International Association for Earthquake Engineering (2004, 2000, 1996, 1992, 1980a, 1980b, 1976, 1973, 1966, 1963, 1960))

Fig. 1.1 shows the development of seismic codes worldwide this led to subsequent growth in knowledge and research for technology to make buildings and structures more earthquake resistant, which were later investigated and adopted quickly by many developed and developing countries. Under the Canadian scenario the NBCC 2010 being the latest version was revised to a large extent in its previous edition NBCC 2005 to streamline seismic deign provisions for practicing engineers., The latest Canadian code recommends the use of dynamic analysis for seismic performance evaluation of existent

and new structures. While NBCC 2010 is not a performance-based design code, it is said to be an objective-based code that allows the use of new materials or design processes based on acceptable solutions to achieve the stated objectives in the design. In the context of performance-based design procedure, it is necessary to determine if a building designed according to the current provisions of the code actually is capable of achieving the given performance objectives assumed in the design and determine possible modifications to incorporate multiple levels of performance corresponding to various levels of seismic hazard. The research presented here looks at a number of buildings designed according to the current seismic provisions in Canada in the context of their performance achievements under the design level of seismic hazard utilizing various methods of response prediction and performance evaluation.

1.2 NBCC 2010 - Seismic Design Provisions

The seismic design of buildings in Canada is required to be performed according to the provisions of the National Building Code of Canada (NBCC). NBCC 2010 is the latest version of the building code which is based on the revision of NBCC 2005. It allows for the use of Equivalent Static Load Method (ESLM) for estimating the lateral forces due to seismic hazard for buildings with simple and regular shape and geometric configurations, and of a limited height. While dynamic analysis is recommended for all buildings, it is mandatory for structures of irregular, complex geometry and buildings of height above 60 m.

NBCC 2010 addresses the overall building performance in a broader perspective, by considering the parameters of ground motions, site soil effects, analysis and design

methodologies (De Vall, 2003). The important features and noteworthy points for seismic design under NBCC 2010 are as follows

- It provides the Uniform hazard spectra for the specific site to be used for Seismic design purpose, the hazard spectrum has 2% probability of exceedance in 50 years with a recurrence interval of 2500 years (Humar and Mahgoub, 2003), further the probability of exceedance of the Uniform hazard spectra is said to be a function of time, with similar characteristics to that of the hazard spectra.
- NBCC 2010 has a broader objective to achieve the required performance and safety of the structure, hence it allows for use for alternate methods of analysis and design to meet the acceptable levels of performance, which may not be specified in the code.
- NBCC 2010 also provides a description and guidelines for structural irregularity

1.3 Performance–based Seismic Design

Recent innovation and advancement in the area of earthquake engineering have led to development of new state-of–art approaches towards performance evaluation and design of structures called Performance-Based Seismic Design. Here, the emphasis is given to *a priori* evaluation of performance of a structure related to the site specific seismic hazard. Seismic hazard includes ground fault, rupture, ground-shaking liquefaction, lateral spreading and land sliding. The new approach helps in pre-emption of the structural performance through qualitative and quantitative means based on controlling the response and damage parameters at the time of the design.

Performance-based seismic design is a two-step process which involves performance evaluation and structural design. The main purpose of performance evaluation is to check the performance of structure up to a desired level under dynamic forces induced by ground motion. The aim of performance-based design is to design the structure based on the desired or assumed performance level to be achieved under seismic excitation. The capacity and the seismic response need to be determined accurately to estimate the level of damage and corresponding performance of a structure. Damage parameters such as the interstorey drift, roof-drift, joint rotation etc. which are displacement based quantities are among the most widely used parameters (Bagchi, 2001) to determine the level of seismic performance. These damage parameters can be determined using static and dynamic analyses of a structure. Usually a nonlinear time history analysis of a structure subjected to seismic ground acceleration is considered a more appropriate method to determine the response parameters accurately. However, the selection of seismic ground motion and scaling them appropriately for the use in the nonlinear time history analysis are important issues which still require further research.

In order to achieve the required performance level by design, a performance objective is predefined and consists of specification of performance level of the structure and a corresponding probability that this performance level may exceed (Yun et al 2002).

The Structural Engineers Association of California have laid down guidelines for Performance objectives under different seismic hazard levels Table (1.1) and a description of different types of structural performances in Table (1.2).

Table 1.1: Design Earthquakes (SEAOC Vision 2000, 1995)

Earthquake Design Level	Recurrence Interval	Probability of Exceedance
Frequent	43 years	50% in 30 years
Occasional	72 years	50% in 50 years
Rare	475 years	10% in 50 years
Very Rare	970 years	10% in 100 years
Extremely Rare	2500 years	2% in 50 years

Table 1.2: Structural Performance Level (Vision 2000)

Performance Level	Description	Transient drift	Permanent drift
Fully Functional	No significant damage has occurred to structural and non-structural components. Building is suitable for normal intended occupancy and use.	<0.2%	Negligible
Operational	No significant damage has occurred to structure, which retains nearly all of its pre-earthquake strength and stiffness. Non-structural components are secure and most would function, if utilities available. Building may be used for intended purpose, albeit in an impaired mode.	<0.5%	Negligible
Life Safe	Significant damage to structural elements, with substantial reduction in stiffness, however, margin remains against collapse. Non-structural elements are secured but may not function. Occupancy may be prevented until repairs can be instituted.	< 1.5%	<0.5%
Near Collapse	Substantial structural and non-structural damage. Structural strength and stiffness substantially degraded. Little margin against collapse. Some falling debris hazards may occur.	<2.5%	< 2.5

It is noteworthy to recognize that NBCC 2010 does not provide guidelines for seismic performance evaluation but specifies the maximum allowable interstorey drift as 2.5% beyond which the structure is assumed to have failed.

1.4 Ground Motion Scaling Techniques

The next generation of design codes, especially those adopting the framework of performance based seismic design, shall include the option of design based on displacement parameters rather than forces. Non-linear dynamic time history analysis conducted as part of a performance-based seismic design approach typically involves the following steps

- Obtain site specific input accelerograms for dynamic analysis
- Perform nonlinear dynamic analysis to compute internal forces and displacements
- Check for the strength of structural elements by computing capacity ratios
- Take adequate steps to ensure structural integrity, safety and performance

It is however noted that suitable Ground Motion Records (GMR) which are site specific are usually unavailable and uncertain. Nonlinear dynamic analysis require the ground motion acceleration time histories which cover the spectral ordinates of the site specific target spectrum prescribed in the codes. In this scenario the ground motion records are obtained using one of the three alternative procedures.

- Selection of a real accelerogram from a GMR database with site specific conditions and characteristics (e.g., magnitude [M], distance [R], duration [D], soil condition [SSI]);
- Simulate GMR from seismological model of fault rupture mechanisms; or
- Artificial or synthetic ground motions generated from filtered noise.

Nonlinear dynamic analysis requires scaling of the real accelerograms for a GMR to that of the target spectrum, which can be done by scaling spectral ordinates without altering the spectral shape or scaling the spectral ordinates and modifying the spectral shape to match the target spectrum. Ideally, the analysis requires scaled real accelerograms without altering the spectral shape. This is because nonlinear displacement and ductility demands are sensitive to the details of the ground motions containing sequences of peaks and valleys as well as long duration pulses. The scaling of spectral ordinates and modification of the spectral shape could however be done in frequency domain or in time domain. From the structural damage assessment point of view, the effect of spectral matching and scaling techniques used to obtain the site specific ground motion characteristics and the related damage potential needs to be studied as there is lack of knowledge in this area. The present research attempts to address the above need.

1.5 Thesis Objectives and Scope

The objectives and scope of the research carried out are outlined below

- To determine the capacity and the seismic demand characteristics of steel moment-frame buildings designed according to the Canadian code provisions
- To determine the effect of ground motion scaling techniques on the seismic performance parameters of the above steel moment resisting frames
- To develop a methodology or guideline to reduce the effect of scaling techniques on the seismic demand of a structure.

In order to achieve the above goals, the following tasks have been undertaken:

- Design a set of building with steel moment resisting frames according NBCC 2010, where the buildings are assumed to be located in Vancouver;
- Select a set of GMRs to represent the seismicity of Vancouver;
- Implement a number of established GMR Scaling Techniques to scale the selected GMRs which are used for carrying out Nonlinear Time History analysis of the Steel moment resisting frame buildings mentioned above;
- Perform a statistical analysis of the seismic demand parameters corresponding to all the GMRs and compare them for different scaling methods; and
- Based on the results, provide a guideline for the selection and scaling of GMRs for time history analysis and evaluation of the seismic response of buildings.

1.6 Thesis Outline and Structure

The thesis has been organized into seven chapters. Objective of the thesis with some introductory materials are presented in the current chapter i.e Chapter 1. A review of literature on this topic is provided in the Chapter 2. Design of the Steel moment resisting frame buildings considered in the research has been presented in Chapter 3. Chapter 4 details the Selection and Scaling of Seismic Ground Motion Records. Chapter 5 discusses the response of the building frames to Static Pushover Analysis under which, it is interpreted using various Performance-based Seismic Design (PBSD) procedures. Chapter 6 presents and discusses the seismic response of the building frames obtained using Non-linear dynamic analysis and the summary of the present thesis and conclusions are presented in the Chapter 7. A list of references used in the thesis has been provided at the end.

Chapter 2

Literature Review

2.1 Introduction

Earthquake engineering in the context of civil engineering deals with seismic hazards assessment and design of structures to cope with the expected levels of hazard. It lays down guidelines for planning, analysis and design of structures in such a way that are capable of achieving an expected level of performance to a given level of seismic hazard. These principles have been the basis of most seismic codes over the decades which are broadly classified towards the following three goals according to the Structural Engineering Association of California (SEAOC 1959-1999):

a.) A minor level of earthquake ground motion without damage;

b.) A moderate level of ground motion without structural damage but possibly experience some non-structural damage;

c.) A major level of ground motion having an intensity equal to the strongest , either experienced or forecast for the building site without collapse , but possibly with some structural as well as non-structural damage.

The recent research advancement in earthquake engineering has often advocated for an innovative performance-based design code instead of the current code which prescribes design guidelines in a simplistic methodology. The aim of performance-based design is to design the structure for a no-collapse condition after evaluating the seismic performance of the structure under a suitable ground motion record which is site specific, and also

ensure different levels of performance corresponding to different levels of seismic hazard. The seismic performance of a structure is assessed and evaluated using inter-storey drifts, inelastic deformations, strains and many other damage indices. Several simplified methods are developed for performance-based design such as displacement based design method, damage spectrum (Bozorgnia and Bertero, 2004) and yield point spectra, to name a few. Although several simplified methods are developed for such design, these methods are still very approximate and differ significantly from each other, since no reliable and robust performance-based design method is available, NBCC 2010 still allows for the traditional force-based design for simple and regular buildings However, NBCC 2010 requires the use of dynamic analysis for complex structures or structures exceeding 60 m in height. While dynamic analysis is required to deal with seismic design, it is still not very practical for everyday office use as it requires significant time in solving for representative ground motion records and in data processing. Given that there is a wide range of uncertainties related to selection of appropriate ground motion records, material modeling and analysis algorithms, significant training and experience is required for a design engineer to carry out such assessment and interpret the results carefully. On the other hand, design codes are required to be simple and robust, and their procedures are expected to be directly based on sound understanding of the physical nature of the problem. Achieving this is difficult, especially when large, nonlinear, and uncertain dynamic response is involved.

In these circumstances it is noted that to reach the goal of performance-based design the performance levels need to be defined, which can be done through rigorous performance evaluation. Hence, it is evaluation of the seismic performance of a structure which is

considered as an important step in realizing a reliable and robust performance-based design. The literature reviewed here mainly focuses on the available techniques on seismic performance evaluation and ground motion scaling techniques which is an important aspect of dynamic response evaluation of a structure subjected to seismic forces.

2.2 Seismic Performance Evaluation

FEMA-350 (2000) provides a reliability-based probabilistic approach to performance evaluation, considering the uncertainties involved in the judgment and prediction of the characteristics of the earthquake parameters. In FEMA-273 (1997) four levels of structural performance are mentioned. In FEMA-273 (1997), both the peak and residual interstorey drifts are utilized in defining the performance levels as an indicator of damage. But only two, Immediate Occupancy (IO) and Collapse Prevention (CP) levels are mostly used in the evaluation of performance. The characteristic parameters of these two performance levels for Steel moment resisting frames are given in the Table 1.3.

Table 1.3: FEMA-273,1997 - Performance Level for SMRF

Performance Level/Limit State	Limit Drift (%)	Limit Residual drift (%)
Immediate Occupancy (IO)	0.7	-
Life Safety (LS)	2.5	1.0
Collapse Prevention (CP)	5.0	5.0

Structures designed according to the current design codes are found to undergo significant inelastic deformation under a strong earthquake which is generally defined in the form of a response spectrum of the ground acceleration history. The elastic analysis of structures subjected to seismic actions typically in the form of response spectrum

analysis, do not always predict the hierarchy of failure mechanisms. It is also not possible to predict the amount of energy absorption and the force redistribution pattern that result from the plastic hinge formation in a structure. This information can only be obtained by studying the inelastic structural response in the time domain. Inelastic analytical procedures help to understand the actual behavior of structures by identifying failure modes and the potential for progressive collapse (Priestley, 2000). Inelastic analysis procedures basically include inelastic time history analysis and inelastic static analysis which is also known as *pushover* analysis. Pushover analysis is very useful in determining the capacity of a structure, the failure mechanism and the sequence of yielding. It also forms a basis for many performance-based seismic design procedures (e.g., Chopra and Goel 1999; Fajfar 2000; Aschheim, 2004; Humar and Ghorbanie-Asl 2005). During the last decade, elastic and inelastic dynamic analyses in the time domain have been made feasible for complex structures because of the rapidly increasing computational power and the evolution of engineering software. Linear elastic dynamic time history analysis is very useful when the dominant modes of vibration are closely spaced or for multiply supported structures (i.e., bridges) where higher modes are excepted to be excited due to the random nature of the incoming seismic waves (Katsanos et al. 2010). The information on behavior of the structure obtained specially from inelastic structural response in the time domain is critical for the assessment of existing or new structures of high importance (i.e., tall and high-rise buildings, storage tanks and nuclear power plants), with complexity (coupled soil–structure systems, massive and irregular buildings), of high degree of inelasticity (i.e., structures designed to

exhibit large deformations), and having geometrical nonlinearity (i.e., base-isolated structures).

Nonlinear dynamic analysis in time-domain is necessary to capture the response of the structure to severe ground motion and obtain reasonable estimates of the demands on the structure. This analysis method is considered to be the most accurate method provided the structure (and constituent elements) and the seismic input to the structure can be modeled to be representative of the reality. The ground motion records can be obtained from natural earthquake records, or can be generated synthetically and artificially.

2.3 Selection of Ground Motion Records (GMR)

2.3.1 Real Accelerograms

The advantage of using real accelerograms is that they are genuine records of seismic shaking produced by earthquakes. Hence, they carry all the ground motion characteristics (amplitude, frequency and energy content, duration and phase characteristics) and reflect all the factors that influence accelerograms. However, the real accelerograms are often not smooth as compared to that of the target or design response spectrum of seismic hazard for a given site. In the design codes, the seismic scenario, which is based on a pair of magnitude, distance and soil conditions, is generally represented by means of a spectral target shape. Guidance given in seismic design codes on how to select appropriate real records is usually focused on compatibility with this response spectrum rather than seismological parameters. Therefore, real earthquake records, which have similar characteristics (magnitude, distance, site condition, and fault type) with the site under consideration, have to be selected to match elastic response spectrum given in the

code. When selecting the earthquake records, it is desirable to use earthquake magnitudes within 0.25 magnitude units of the target magnitude (Stewart et al, 2001). Selection of records having appropriate fault-site distances is important especially for near-fault sites. Site conditions have a major effect on the characteristics and frequency content of the strong ground motion records. Even though the ground motions are amplified in soft soils, the high frequency motions are attenuated. Also, in order to preserve non-stationary characteristics of the initial time history, it is essential to start with an acceleration time history whose spectrum is as close to the target spectrum as possible in the period range of interest. A close initial fit also ensures a speedy convergence to the design values (Fahjan and Ozdemir, 2008). Although using real earthquake records has many advantages, there may exist a lack of strong motion earthquake records to satisfy the seismological and geological conditions and site-specific requirements defined in seismic codes.

2.3.2 Artificial Records

Artificial accelerograms whose response spectra is closely compatible to the design response spectra can be generated in either time or frequency domain (Gupta and Krawinkler, 1999). Artificial spectrum-compatible accelerograms can be generated using programs such as SIMQKE (Gasparini and Vanmarcke, 1979) and TARSCTHS (Papageorgiou et al. 2002). The program SIMQKE computes a power spectral density function from a specified smooth response spectrum and uses this function to derive the amplitudes of sinusoidal signals which have random phase angles uniformly distributed between 0 and 2π. The sinusoidal motions are then summed and an iterative procedure can be invoked to improve the match the target response spectrum, by calculating the

ratio between the target and actual response ordinates at selected frequencies. The power spectral density function is then adjusted by: the square of the ordinate ratio and a new motion is generated. In order to get other characteristics of artificial spectrum-compatible record, such as the duration, it is necessary to obtain supplementary information about the expected earthquake motion apart from the response spectrum. The computer code TARSCTHS (Papageorgiou et al., 2002) uses non-stationary stochastic vector processes to generate artificial time histories from a user defined elastic response spectrum. Here the iterative scheme is applied in the frequency domain where the phase angles of the desired motion are randomly generated.

2.3.3 Synthetic Accelerograms

The accelerograms were found to be largely unavailable during the earlier decades due to the absence of data recordings of the earthquakes, hence synthetic records were used instead of real earthquake records, synthetic accelerograms are mainly made up deterministic or stochastic ground-motion modeling methods. While short–period motions behave stochastically, long-period motions mainly behave in a deterministic manner, where the period of transition from deterministic to stochastic is assumed to be 1.0 s (Stewart.et al. 2001). A number of computer programs were developed for generating synthetic ground-motions (e.g. Zeng et al, 1994; Beresnev and Atkinson, 1998; Boore, 2003). The simulation is based on stochastic point source approach of which the specified Fourier spectrum of the ground motion is a function of magnitude and distance. The simulation model also includes the source parameters characteristic for the geographic region considered, and takes into account the effect of the magnitude and distance on the duration of the ground motion summed (with a proper time delay) in the

time domain to obtain the ground motion from the entire fault. Using this method, Atkinson (2009) simulated accelerograms for western and eastern Canada for earthquake with various magnitudes a wide range of source-to-site distances.

2.4 Spectral Matching and GMR Scaling

2.4.1 Target Spectral Matching

Once an initial search in terms of magnitude, distance and site classification has been performed, depending on the number of records retrieved, further pruning then needs to be carried out to acquire the number of records deemed necessary to obtain stable results from the inelastic dynamic analyses. If there are far more records than actually needed, the obvious choice would be to apply a second sweep of the search using more restrictive criteria, such as a smaller distance range or insisting on a close match with the site classification. There are three methods for further modifying actual time histories to match the target spectrum. Matching techniques are based on scaling of the selected time history records in time domain after filtering the actual motion in frequency domain by its spectral ratio with the design target spectrum; or elementary wavelets are added or subtracted from the real time history to match a target design spectrum

2.4.2 Ground Motion Scaling in Time Domain

In this approach, recorded motion is simply scaled up or down by a constant scaling factor uniformly to find out the best matches to the target spectrum over a period range of interest, without changing its frequency content. It could be stated that the accelerograms should only be scaled in terms of amplitude. There are procedures which minimize the differences between the scaled motion's response spectrum and target spectrum in a least-square sense (e.g., Nikolaou 1998; Somerville et al. 1997a,b).

2.4.3 Spectral Matching in Frequency Domain

A frequency domain matching methodology uses an actual record to produce a similar motion that matches almost perfectly a target (design) spectrum. In this method, an actual motion is filtered in frequency domain by its spectral ratio with the design target spectrum. Fourier spectral amplitudes of an input motion are modified while the Fourier phases of that remain unchanged during the entire procedure. Preservation of phase characteristics is important for non-linear time domain analyses, because the non-linear solution can be sensitive to the phasing of the individual time history. In order to keep the phases one applies to the signal a real-only "transfer function" (i.e., with a zero-imaginary component), to rescale the Fourier amplitudes. The technique is repeated iteratively until the desired matching is achieved for a certain range of periods. The more iterations results with better compatibility with the target design spectrum (Ozdemir and Fahjan, 2007).

2.4.4 Spectral Matching in Time Domain

One approach for spectral matching is to adjust the original record iteratively in the time domain to achieve compatibility with a specified target acceleration response spectrum by adding wavelets having specified period ranges and limited durations to the input time history. These wave packets are added at times where there is already significant amplitude in that period range in the time history. This method preserves the overall phasing characteristics and as the time varying (i.e., non-stationary) frequency content of the ground motion (Somerville, 1998). The resulting records each have an elastic response spectrum that is coincident (within a tolerance) with the target spectrum. This procedure was first proposed by Kaul (1978) and was extended to simultaneously match

spectra at multiple damping values by Lilhanand and Tseng (1987). Although this procedure is more complicated than the frequency domain matching procedure as in most cases it can preserves the non-stationary character of the reference time history. Abrahamson (1992) developed RSPMATCH software modifying the Lilhanand and Tseng (1987) algorithm that preserves non-stationary character of the reference ground motion for a wider range of time histories. Mukherjee and Gupta (2002) proposed a method in which the accelerogram is divided into a finite number of time-histories of distinct frequency bands, the time-histories are then iteratively scaled to match the target spectrum.

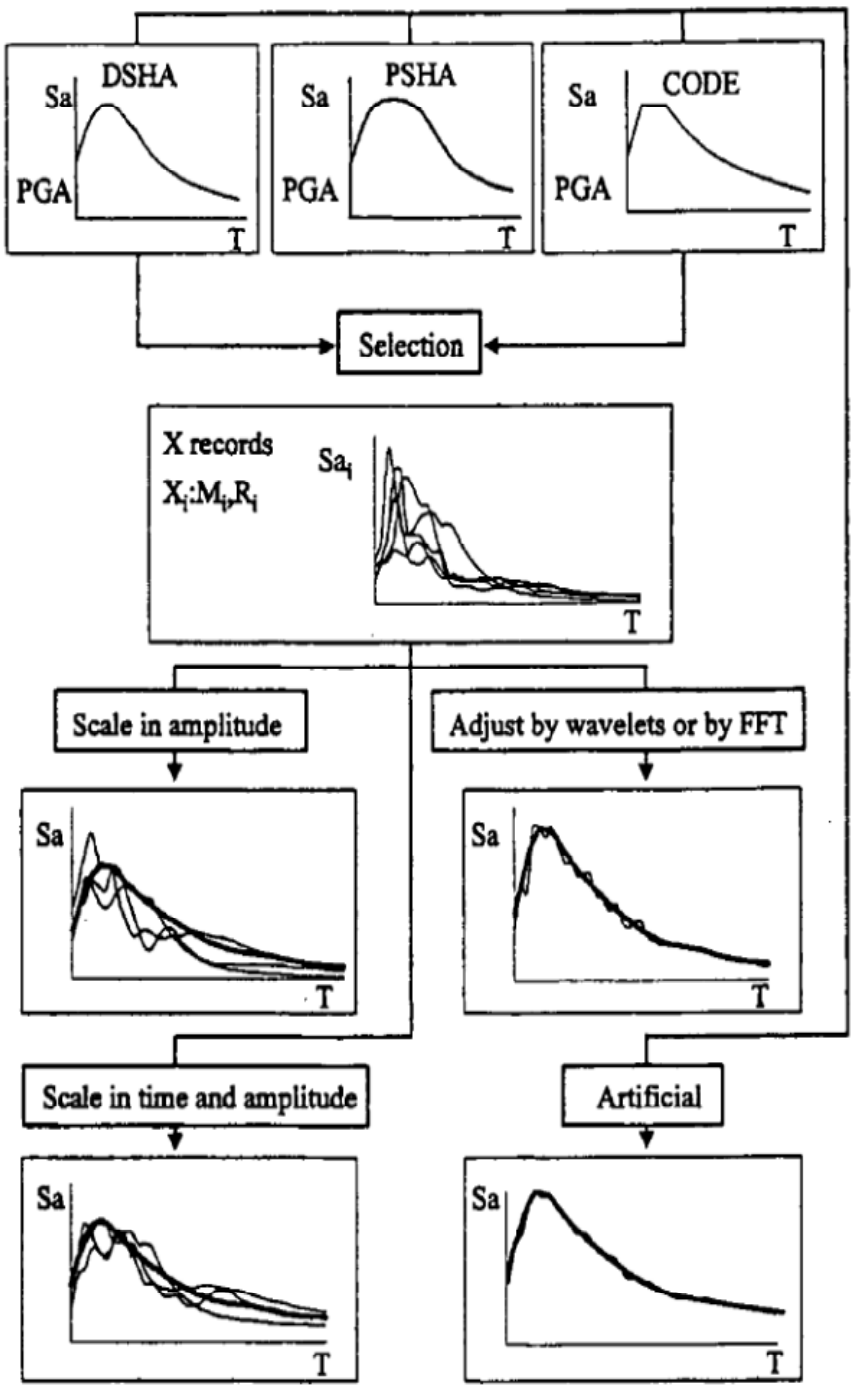

Figure 2.1: The use of real earthquake accelerograms (Bommer and Acevedo, 2004)

2.5 Modal Pushover Scaling (MPS)

MPS scaling procedure was developed and proposed by Kalkan and Chopra (2011). This method serves the purpose of scaling earthquake records near a fault site where inelastic spectral deformation dominates predominantly over the corresponding elastic spectral deformation (Bozorgnia and Mahin 1998; Alavi and Krawinkler 2000; Baez and Miranda 2000; Chopra and Chintanapakdee 2004). It is known to explicitly consider the strength of the structure obtained from the first-mode pushover curve and determine the scaling factors for each record to match a target value of the deformation of the first-mode inelastic SDF system estimated by standard procedures. The MPS method is further considered to be appropriate for analysis of first-mode dominated structures and is found to be sufficient to accurately estimate the seismic response of low-rise to mid-rise structures.

The intensity-based scaling procedures provides scale factors for a small number of ground-motion records, so that nonlinear Response History Analysis (RHA) of a structure for these scaled records remains reliable to estimate the median value of the seismic demand parameters (SDPs) such that the record-to record variations in the EDP (Engineering Demand Parameters) is kept low. However, none of the procedures like scaling based on PGA (Peak Ground Acceleration), intensity or peak velocity take into account the properties of the structure to be analyzed. As the intensity-based scaling depends on elastic responses of the structure, it is found to produce inaccurate estimates

with wide dispersion in Seismic EDP values for structures responding in the nonlinear range (Nau and Hall 1984; Miranda 1993; Vidic et al. 1994; Shome and Cornell 1998). In this context a recent study conducted by Kalkan and Chopra (2011) considering three sets of 7 ground motions scaled by MPS procedure and the code recommended ASCE/SEI 7-05 procedure — for a 4 , 6 , and 13 storey Steel Moment Resisting Frame (SMRF) buildings showed that the median values of EDPs like interstorey drift, and floor displacement obtained from MPS procedure were within admissible dispersion levels of about 20%, whereas the the EDPs from the code based procedure overestimated the demand ranging by 20% to 50% in the 4- and 6-storey buildings and about 50% for the 13-storey building. Thus, the MPS method is deemed an accurate and efficient procedure as compared to the ASCE/SEI 7-05 scaling method. Extension of the MPS method to include higher vibration modes is expected to provide improved estimates for mid-rise and high-rise buildings (Tothong and Cornell 2008; Tothong and Luco 2007; Luco and Cornell 2007).

2.6 Steel Moment Resisting Frame (SMRF)

A large number of modern high-rise buildings have Steel Moment Resisting Frame (SMRF) as the primary earthquake resisting system. This type of construction was considered as an efficient way to resist lateral forces induced during earthquakes since the steel elements are expected to be able to sustain large plastic deformation in bending and shear. However, the failure of more than 150 SMRF during the 1994 Northridge earthquake and the 1995 Kobe earthquake primarily in the form of brittle fractures at welded beam to column connections raised serious concerns regarding the seismic

behavior of code compliant SMRF structures. The critical issues were then broadly classified into the following three points (Gupta and Krawlinker, 1999):

- The observed behavior of SMRF structures was found to be largely deviant from the expected code compliant designs.
- The immediate need for predicting the seismic demand for the very large number of existing SMRF structures in different geographic locations and under different levels of shaking to enable retrofit and rehabilitation if required.
- The immediate need to predict the structural safety at various seismic hazard levels due to potential connection fractures.

The solution for the existing problem highlighted can be brought about through in-depth understanding of the basic factors controlling the seismic behavior of SMRF structures. The answers or solutions developed should provide an estimate of the structural performance and the reliability for the very large inventory of existing SMRF systems in order to facilitate the decision process for the seismic rehabilitation of these structures to acceptable performance levels, thus there is a pressing need for a systematic evaluation of SMRF structures in order to better understand the core structural behavior characteristics and address performance expectations at different hazard levels .

2.7 Review of NBCC 2010 Code Provisions

According to NBCC (2010) the minimum lateral earthquake force V, is calculated by using the following equation -

$$V \geq \frac{S(2.0)M_V I_E W}{R_d R_0} \quad \text{.....} \quad 1.1$$

where $S(T_a)$ is the spectral acceleration corresponding to the building's fundamental period T_a; M_V is the factor to account for multistorey effect, I_E is the importance factor, W is the total weight of the building, R_d ductility related force modification factor, R_0 is the over strength related force modification factor. Table 1.4 shows the revised value of higher mode factor M_V in NBCC 2010.

Table 1.4: Values of higher mode factor M_v for various structural systems (NBCC 2005)

Sa(0.2)/Sa(2.0)	TYPE OF LATERAL RESISTING SYSTEMS	M_v for T_a<1.0	M_v for T_a>2.0
<8.0	Moment Resisting Frame or " coupled walls "	1.0	1.0
	Braced Frame	1.0	1.0
	Walls, wall-frame systems , other systems	1.0	1.2
	Moment Resisting Frame or " coupled walls "	1.0	1.2
≥8.0	Braced Frame	1.0	1.5
	Walls, wall-frame systems , other systems	1.0	2.5
Note : Linear Interpolation should be used for intermediate values			

The design spectral response acceleration values $S(T_a)$ is given by the following formula, which holds good for linear interpolation for intermediate values.

$S(T_a)$ = $F_aS_a(0.2)$ for $T \leq 0.2$ s

= $F_vS_a(0.5)$ or $F_aS_a(0.2)$ whichever is smaller for $T_a = 0.5$ s

= $F_vS_a(1.0)$ for $T_a = 1.0$ s ……………………………………………(1.2)

= $F_vS\ (2.0)$ for $Ta = 2.0$ s

= $F_vS_a(2.0)/2$ for $Ta \geq 4.0$ s

where $S(T_a)$ is the 5% damped spectral response acceleration expressed as a ratio to the acceleration due to gravity, g for a period T_a; F_a is an acceleration based site coefficient, and F_v accounts for velocity based site coefficient. The lateral load distribution along the height of a building is given by the Eq. 1.3

$$F_x = \frac{(V - F_t)W_x h_x}{\sum_{i=1}^{n} W_i h_i} \quad \ldots\ldots\ldots\ldots\ldots\ldots\ldots\ldots \quad \ldots\ldots. \quad (1.3)$$

F_x is the lateral force applied at level x, n is the total number of storeys, h_x and h_i are the heights above the Ground level to level x and i, respectively. F_t is given by the Eq. 1.4 considering the portion of V concentrated at top storey.

$$F_t = 0.07 T_a V \leq 0.25\ V \quad \ldots\ldots\ldots\ldots\ldots\ldots\ldots\ldots\ldots\ldots\ldots\ldots \quad (1.4)$$

$$F_t = 0\ (T_a \leq 0.7\ \text{s}) \quad \ldots\ldots\ldots\ldots\ldots\ldots\ldots\ldots\ldots\ldots\ldots\ldots\ldots\ldots\ldots\ldots \quad (1.4a)$$

The graph of spectral acceleration versus period for Vancouver as given in NBCC 2010 is shown in Figure 1.3, and the design values of spectra for Vancouver are shown in Table 1.2. The spectral values in between the periods reported in Table 1.2 are obtained by linear interpolation.

Table 1.5: Design Spectra of NBCC 2005 (Adams and Atkinson, 2003)

Location	Sa(0.2)	Sa(0.5)	Sa(1.0)	Sa(2.0)	Sa(≥4.0)
Vancouver	0.96	0.66	0.34	0.18	0.09

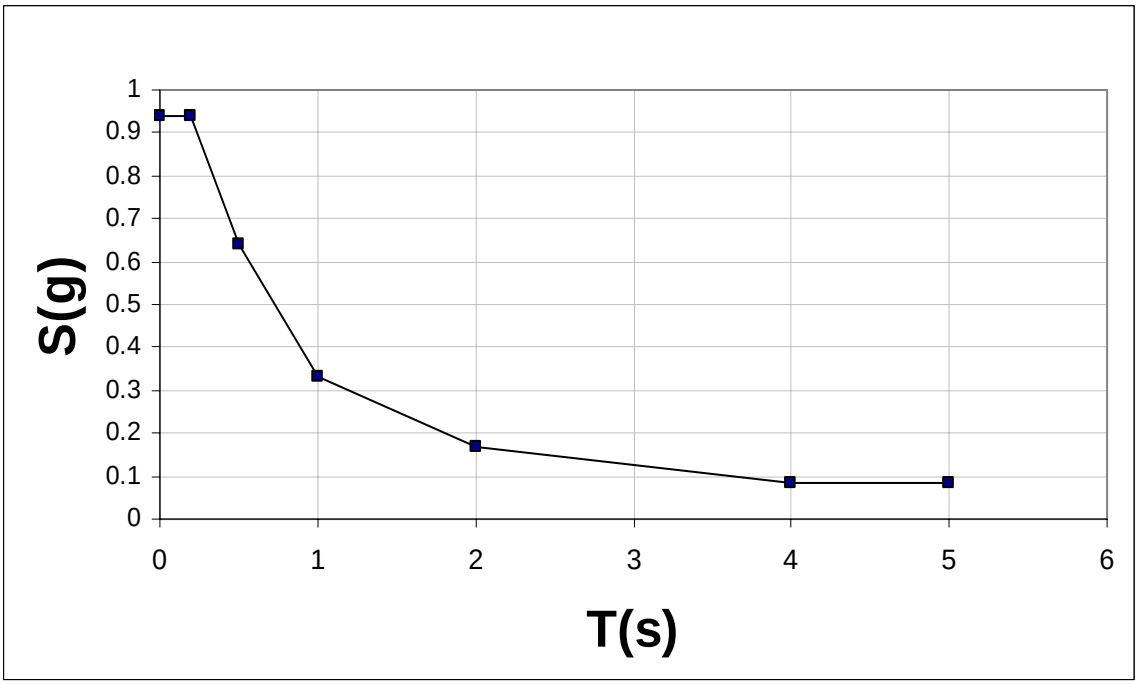

Figure 2.2: Design Spectra for Vancouver (NBCC 2010)

2.8 Summary

Performing fully dynamic nonlinear structural analysis is time-consuming (and therefore costly) in engineering practice. The use of spectrum-compatible records, which allow fewer analysis runs to be made, will perhaps be preferred by design engineers. There is no consensus yet on the number of real accelerograms required to obtain stable measures of inelastic response from time history analysis. It is generally recommended that a suite of seven to ten records are sufficient (Bommer and Acevedo, 2004). Currently, there is a lack of knowledge in the area of damage potential due to the effect of spectral matching and scaling of GMR (Leger and Tremblay, 2009). One of the goals of the present research is evaluate the currently available scaling methods for GMRs used in RHA and investigate their implications on the seismic response.

Chapter 3

Design of Steel Moment Resisting Frames

3.1 Introduction

The buildings chosen for the performance evaluation and the research presented here are of steel moment resisting frames, located in Vancouver, Canada. The Vancouver region in Canada is classified as high seismic zone as compared to the other parts of the country. Four buildings of five, ten, fifteen and twenty storey height, symmetrical along the vertical center line of the steel frames are designed according to the seismic provisions of NBCC 2010. Each building has a series of frames in the east-west (E-W) direction and three bays in the north-south (N-S) direction. The center to center spacing of the frames in the E-W direction is 6 meters whereas in the N-S direction the two exterior bays are of 9 meters and the interior bay is 6 meters. The first storey height in the buildings is 4.85 meter and the remaining floors are spaced at 3.65 meter each. A typical layout plan is shown in Figure 3.1, the elevation views are shown in Figures 3.2 and 3.3. The building frames along the north-south direction have been chosen for the design but the effect of accidental torsion is not considered in the process as the building is configured in a symmetrical and regular geometric manner.

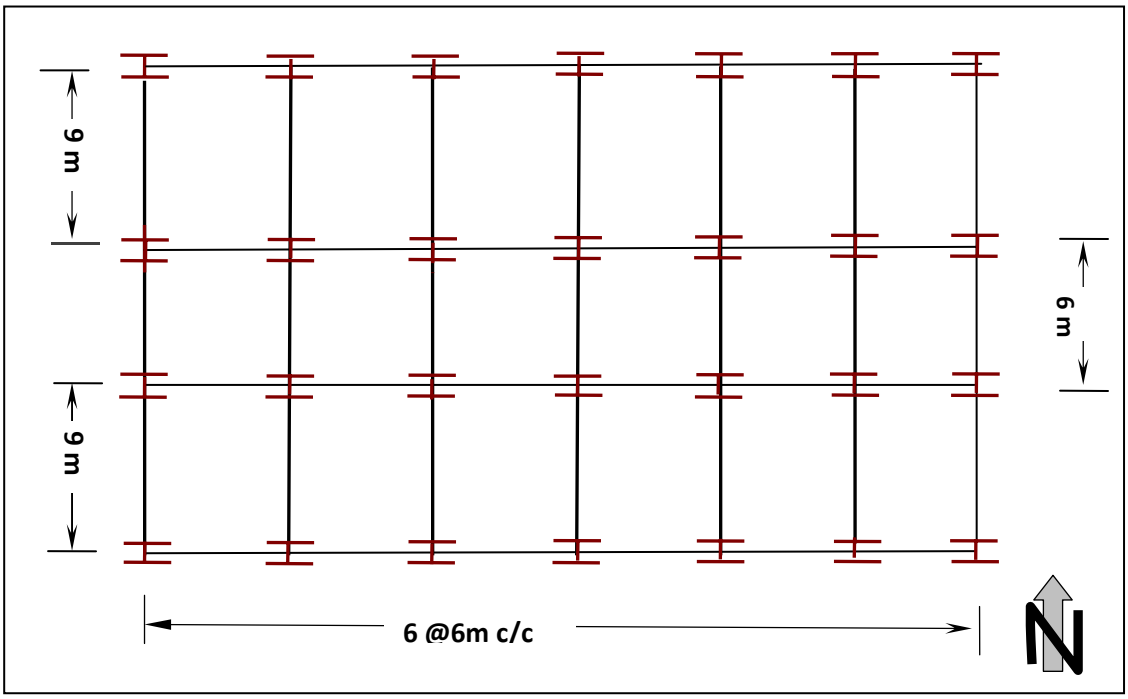

Figure 3.1 - Layout Plan of the Building

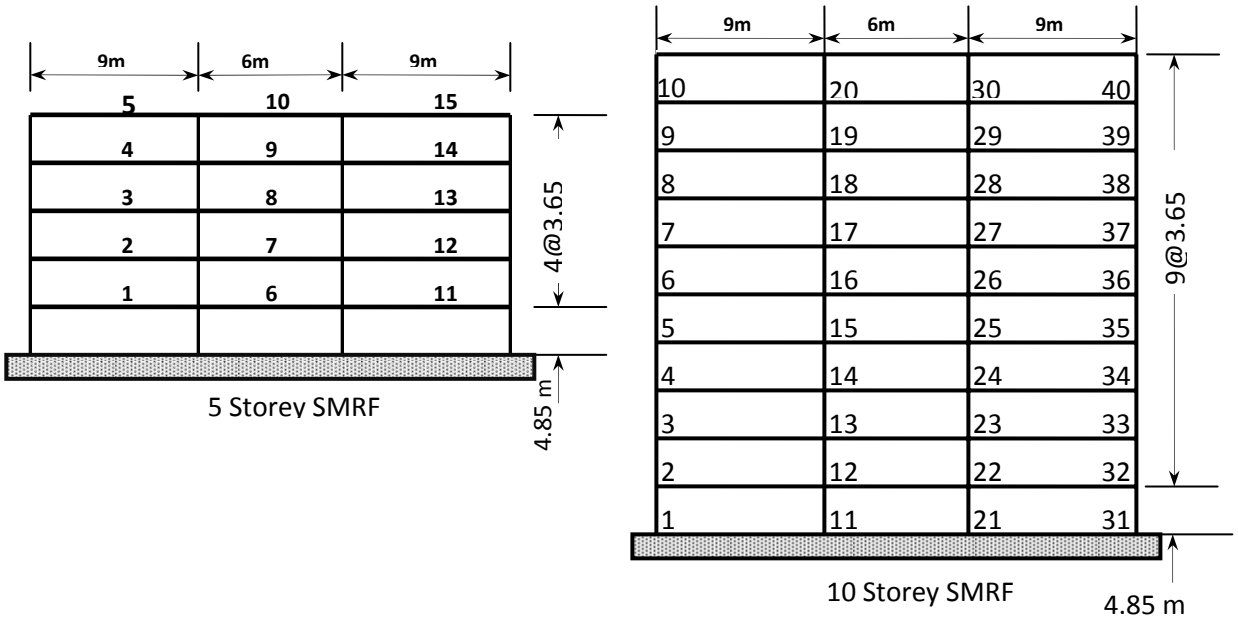

Figure 3.2 - Elevation of 5 & 10 Storey frames

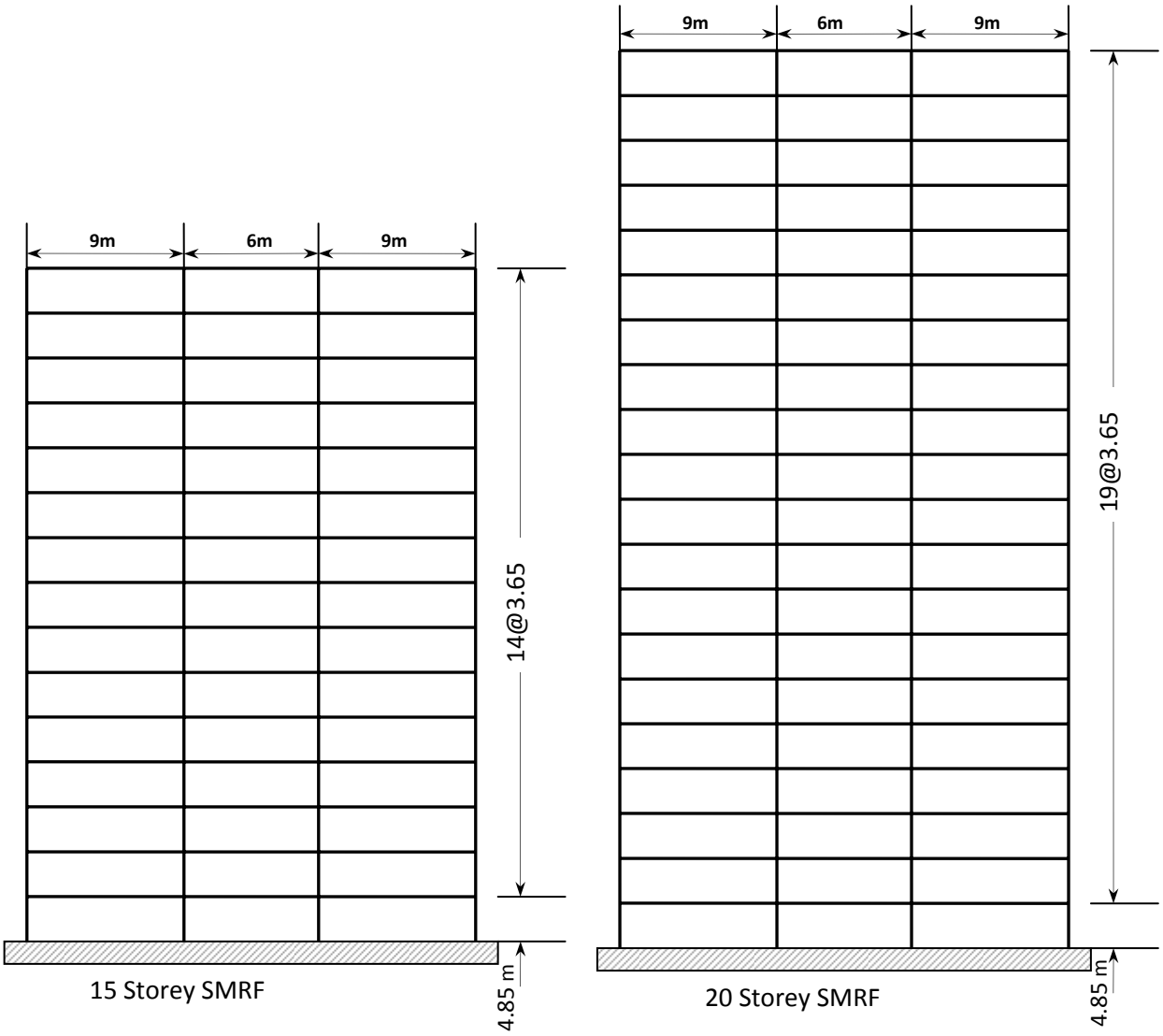

Figure 3.3 - Elevation of 15 & 20 Storey Frames.

The equivalent static force-based design process as per the code has been adopted for the design which involves the calculation of member forces prior to designing the members as per the specified provisions. NBCC 2010 specifies a seismic hazard level under which probability of exceedance is of 2% in 50 years.

3.2 Structural analysis and design

A number of commercial and non-commercial software programs are available for linear and nonlinear analysis of structural systems. Some of the popular ones include DRAIN-2DX (Prakash *et al.*, 1993), DRAIN-3DX (Static and Dynamic Analysis of Inelastic 3D Structures), DRAIN-BUILDING (Static and Dynamic Analysis of Inelastic Building Structures), SAP-2000, ETABS and PERFORM 3D (Computer and Structures, 2012). To facilitate the nonlinear dynamic analysis of the 2D frame structures considered for the research, the DRAIN-2DX software has been employed since it is known to produce reliable results and simple to use for plane structures. The program has been used in the present research to carry out the response spectrum analysis of the frames in the unstressed state, the modal analysis to compute the fundamental frequency of the frames, the pushover analysis to determine the maximum deflection and strength of the structure as well as the nonlinear dynamic analysis in the time domain. The modeling of the structure in the DRAIN 2DX software is done by defining the planar coordinates of the frame. The beam members of the same floor level are grouped in the same section type and the column sections are changed at an interval of five floors, i.e. columns are spliced at every fifth floor. The modeling of the frame has been done using Element type- 2 (Beam-Column Element) available in DRAIN-2DX element library. It also allows for defining the effect of axial force on bending strength by considering the P-M interaction curve and the

yield surface. Element Type 2 is shown in the Fig 3.4, which possess Linearized Geometric Stiffness and allows for axial-flexural interaction. The connections of beam to column are modeled as rigid zones as defined in FEMA 440 under predefined connections.

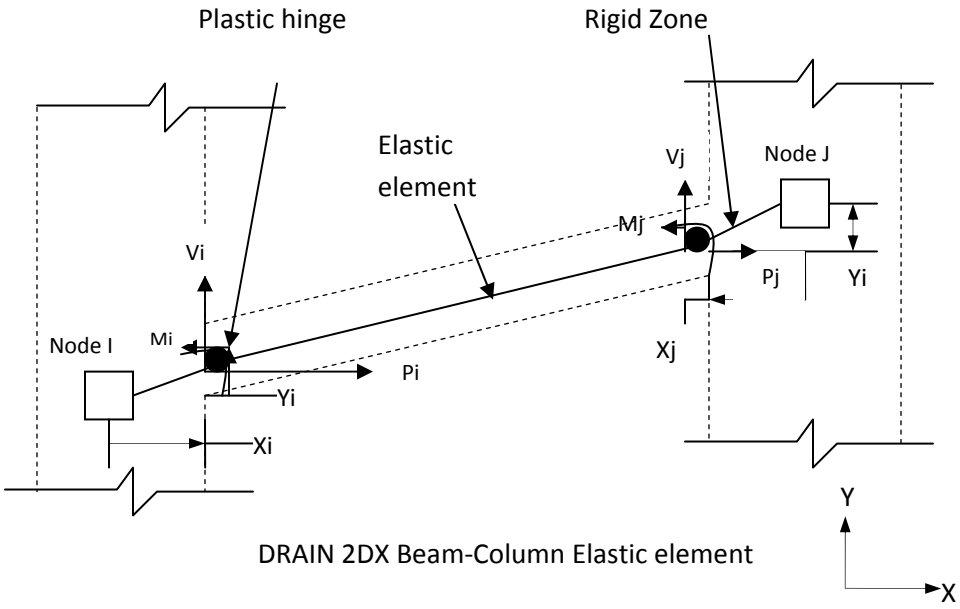

Figure 3.4 - Model of DRAIN-2DX Element Type-2 (Prakash *et al.,* 1995)

3.3 Design of Steel Moment Resisting Frames (SMRF)

The equivalent static lateral load procedure for the seismic load as prescribed by NBCC 2010 has been used in the preliminary design the buildings which then revised using the modal and response spectrum analysis. Building frames are designed to satisfy the NBCC 2010 requirements and the steel structural elements have been designed as per CSA S16-09 (CSA, 2010). The following loadings have been considered in the design of the buildings: gravity

loads (dead load *(D)*, live load *(L)*) and seismic load *(E)*. The dead loads comprise the self-weight of the frame elements and other non-structural components the live loads are obtained as per the specification from NBCC 2010. Table 3.1 gives the values of Dead loads and Live loads. The total weight of the building has also been calculated using the static design procedure and is found to remain constant at each iteration of the static design process. Live load at the roof is mainly the snow load *(S)*.

Table 3.1:Design loads.

Dead Load (kPa)		Live Load (kPa)		
Roof	Floor	Roof	Interior typical floor	Corridor
3.4	4.05	2.32	2.4	4.8

Linear static analysis of frames has been performed using DRAIN-2DX to determine the member forces. Load combination of the forces has been used to evaluate the design force for both beam and column of the frames. The combinations of different loads are given in Equations 3.4 and 3.5.

$$1.25D+1.5L \quad \text{.....3.4}$$

$$1.0D\pm 1.0E+(0.5L+0.25S) \quad \text{.....3.5}$$

In static analysis-based design it has been checked that the structure designed to be safe for the combination of gravity loads also remains safe to withstand the earthquake loads. In the case where structure is designed for gravity load fails to withstand the seismic load, the design has been further modified to satisfy the both load combinations in Equations 3.4 and 3.5. During the design process, the empirical fundamental periods of the frames has been calculated by using the Equation 3.6.

$$Ta = 0.085(h_n)3/4 \text{ (NBCC, 2010)} \quad \text{.....} \quad 3.6$$

where, T_a is the empirical fundamental period and h_n is the total height of the building frame. This period has been used to calculate the equivalent seismic force for the first iteration of the static design. After designing of frames by using the empirical fundamental period, a detail modal analysis of the frames has been carried out. The fundamental periods of frames obtained from the modal analysis if found to be more than T_a obtained from the empirical period using Equation 3.6, the seismic force is revised using the modal period or $1.5T_a$, whichever is smaller (NBCC, 2010). A summary of the periods of different frames is presented in the Table 3.2

Table 3.2: Fundamental Periods of the Buildings.

Frame Height	By Empirical Equation (Eq.3.6), (T_a), s	Period from Modal Analysis,	$1.5T_a$, s
5 storey	0.787	1.412	1.181
10 Storey	1.293	2.528	1.939
15 Storey	1.739	3.571	2.609
20 Storey	2.149	4.789	3.224

The design base shear is calculated by using Equation 1.1 as provided in NBCC 2010. The base shear is then distributed along the height of the building in the form of inverted triangle as per code requirement, and the lateral force is computed for each storey level according to the weight and the height at the storey level. Seismic force at the specified storey level is computed by using Equation 1.3 and the non-linear static pushover analysis is performed including the effect of P-Δ to determine the capacity and yielding sequence of the structure. The buildings are considered to be of normal importance and the frames are assumed to be ductile.

The equivalent base shear of the four buildings is given by the Eq.1.1 in which the parameters are I_E (importance factor)=1.0, M_V (factor for higher mode effect)=1.0, R_d (ductility factor) =5.0

and the R_0 (overstrength factor)=1.5. The soil is of type- C is assumed which is dense soil with soft rock, hence F_v=F_a=1.0 (site specification factor). Further, the design spectral acceleration value *S(T)* is equal to the spectral acceleration value $S_a(T_a)$ provided in the code. The design values of the base shear of the four buildings as determined using the empirical period are as shown in Table 3.3.

Table 3.3: Base shear of SMRF.

Steel Moment Resisting Frame	Base Shear V (KN) Bare Frame
5 storey	154.70
10 Storey	192.44
15 Storey	293.75
20 Storey	400.96

However, the fundamental period determined by the modal analysis and 1.5T_a whichever is smaller is used for recalculating the base shear. If any variation is found in the base shear, the design of the buildings is revised with the new base shear and the sections of the frames are modified suitably.

3.4 Modal Analysis

The software DRAIN-2DX has been employed to obtain the fundamental frequency and the mode shapes of the frames. The mode shapes for different frames are shown in Figs. 3.5 and 3.6.

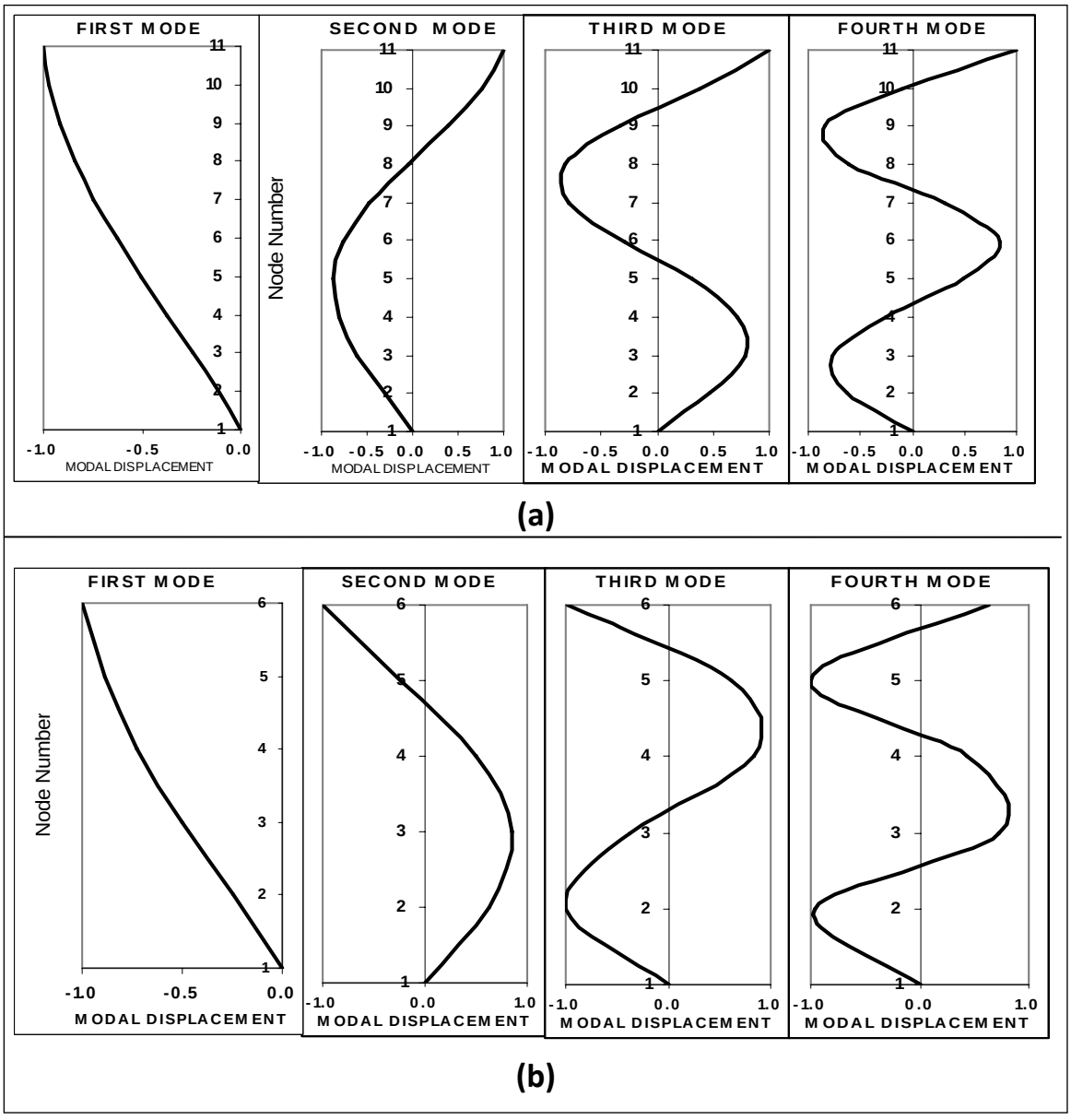

Figure 3.5: Mode Shapes of 10 and 5 Storey Building Frames; (a) Mode Shapes of 10 Storey Building Frame, (b) Mode Shapes of 5 Storey Building Frame.

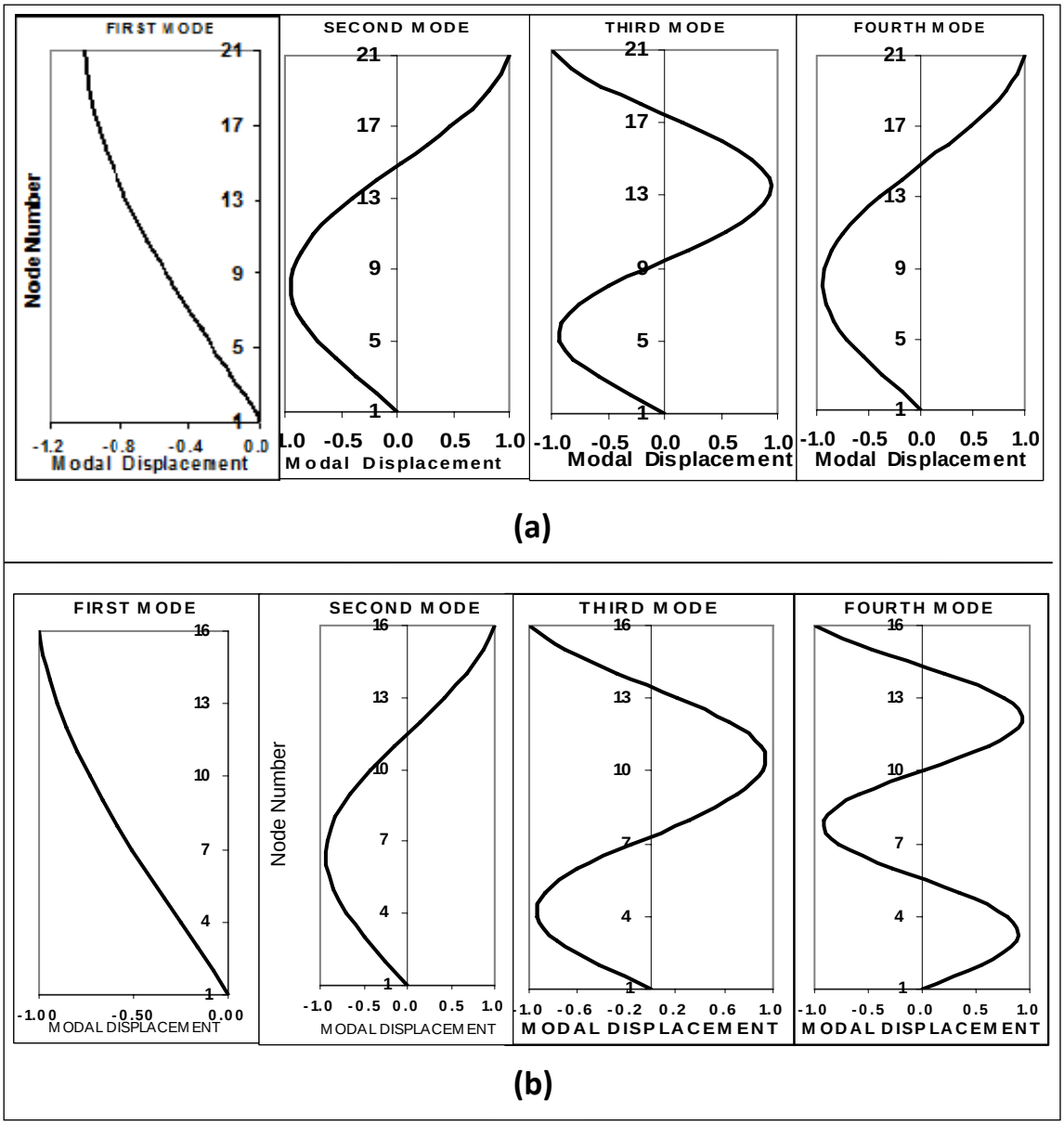

Figure 3.6: Mode Shapes of 20 and 15 Storey Building Frames; (a) Mode Shapes of 20 Storey Building Frame, (b) Mode Shapes of 15 Storey Building Frame

Table 3.4 depicts a sample calculation of the base shear post the modal analysis.

Table 3.4: A sample calculation of base shear after modal analysis.

Modal Period	1.5 T_a	Selected Period	S(1.0)g	S(2.0), g	S(Design), g	M_v (1.0)	M_v (2.00)
4.789	3.223	3.223	0.340	0.180	0.180	1.00	1.10
M_v (Design)	Weight, W (kN)	Factor R_d	Factor R_0	Base shear after modal analysis, V_m (kN)		Base shear before modal analysis, V_s (kN)	
1.10	15187	1.50	5.00	400.96		601.44	

In the steel frame design it has been checked that the selected design base shear is greater than or equal to the base shear calculated for spectral acceleration S(2.0)g and less than 2/3 of base shear corresponding to acceleration S(0.2)g. Ductile frames of Type-D are designed as per the guidelines presented in the CISC (2010) Handbook of Steel Construction and the steel sections used in the design are of CSA G40.21 grade with yield strength, F_y=350 MPa and modulus of elasticity *(E)* = 200x10^3 Mpa ,for both beam and column. The columns in the ductile frames are designed as beam-column elements to avoid yielding and flexural buckling.

The column strengths are further computed by using the Equation 3.7 as prescribed in CISC (2010) which is applicable to plane and unbraced frames.

$$\frac{C_f}{C_r} + \frac{0.85U_{1x}M_{fx}}{M_{rx}} \leq 1.0 \quad \ldots\ldots\ldots\ldots\ldots\ldots\ldots\ldots\ldots\ldots 3.7$$

In the Equation 3.7, the constants U_{lx} is = 1.0 in case of the unbraced frames. The factored moment (M_{fx}) and the factored axial compressive force (C_f) are obtained from the analysis. The resistive bending moment (Mrx) and the resistive compressive axial force (C_r) for the individual columns are taken from the CISC (2010) Handbook.

The steel beams are designed to comply to the limit states specified in CAN/CSA-S16-01(2001) and the computed factored resistance is compared to the specified factored resistance using the condition $V_r > V_f$ and $M_r > M_f$, where the factored beam shear (V_r) and moment resistant (M_r) are obtained from the CISC (2010) Handbook. The design iteration is carried out till the condition is satisfied. The deflection in beams has been checked for live and dead loads to satisfy the serviceability limit state, and the deflection has been calculated by using Equation 3.8.

$$\left.\begin{aligned} I_{reqd} &= WC_d B_d \\ \Delta &= \left(I_{reqd} / I\right)\Delta_m \end{aligned}\right\} \quad \text{..... 3.8}$$

where I_{reqd} is the required moment of inertia of area, I is the gross moment of inertia, Δ_m is the specified maximum deflection, Δ is the computed deflection, C_d is the deflection constant, B_d *is* a constant pertaining to the load and support, and W is the total live load on the beam. In light of the shake-down condition under which the frame system behaves elastically after initially yielding in case of cyclic loading, the mandatory check for capacity-based design the column and beam strength at the shake-down condition have been computed by using the formulae given in CISC (2010) Handbook.

$$\sum M_{rc} \geq \sum \left(1.1\, R_y\, M_{pb} + V_h \left[x + \frac{d_c}{2} \right] \right) \text{.....3.9}$$

$$M_{rc} = 1.18\, \phi\, M_{pc} \left(1 - \frac{C_f}{\phi C_y} \right) \leq \phi M_{pc} \text{ .....3.10}$$

where M_{rc} and M_{pb} are the plastic moment of resistance of the column and the beam respectively. Ø is the resistance factor, V_h is the shear acting upon the plastic hinge location

when plastic hinging occurs, C_f is the factored axial compressive load of column, C_y is the axial compressive load at yield. R_y is a factor applied to yield stress F_y to estimate the probable yield stress and F_y is the minimum specified yield stress. It is noted that the shake-down condition in frames causes columns to carry all the loads, resulting in formation of plastic hinges mainly in the beams at a certain specified distance from column center line and where the distance depends on the type of connection of beam and column. The distance of plastic hinge from the center of the column for the connection chosen for the presented frame is $x+d_c/2$ (Fig.2.1 and 2.2), in which, d_c is the depth of column and x is the distance between the plastic hinge and the face of the column. It has been checked that all joints of every frame considered here have satisfied this capacity design criteria. As a part of the dynamic analysis, a response spectrum analysis of each frame has been performed to determine the base shear and the design base shear is reduced further according to the NBCC provision. The finalized sections for different elements of the frames are presented in the Table 3.6 and 3.7.

Table 3.5 - Sections of Columns.

Building Height	Column Row	Storey 1 to 5	Storey 6 to10	Storey 11 to 15	Storey 16 to 20
5 Storey	External	W310x179			
	Internal	W310x253			
10 Storey	External	W310x283	W310x158		
	Internal	W310x314	W310x202		
15 Storey	External	W310x283	W310x253	W310x179	
	Internal	W360x314	W360x260	W310x283	
20 Storey	External	W310x283	W310x253	W310x202	W310x179
	Internal	W360x314	W360x287	W360x262	W360x262

Table 3.6 - Section of Beams.

Storey Level	Building Height			
	5 Storey	10 Storey	15 Storey	20 Storey
Top Storey	W310x79	W310x79	W310x107	W310x107
Other Storey	W310x86	W310x107	W310x129	W310x129

A flow chart of the above design methodology is presented in the Figure 3.8. It has been adapted from (Hannan, 2006) and has been revised for the present work. The flowchart is described here briefly.

Step1 – Select the member sections for the Steel moment resisting frame based on experience and proceed further with the design and recalculation process.

Step 2 – Compute the empirical fundamental period of the structure along with other design parameters to finally obtain the design base shear, distributed base shear as along the height of the structure to get the lateral force.

Step 3 - Perform the Static analysis for the given loads and load combinations using the DRAIN-2DX program and obtain the shear, bending and axial forces for individual member .

Step 4 - Check the obtained member forces with the code specified values , if the members pass the check , further perform the modal analysis of the structure and revise the base shear with the new fundamental period and proceed with Step 5, if the members fail the test redesign the structure with new sections and repeat the design procedure from Step 1.

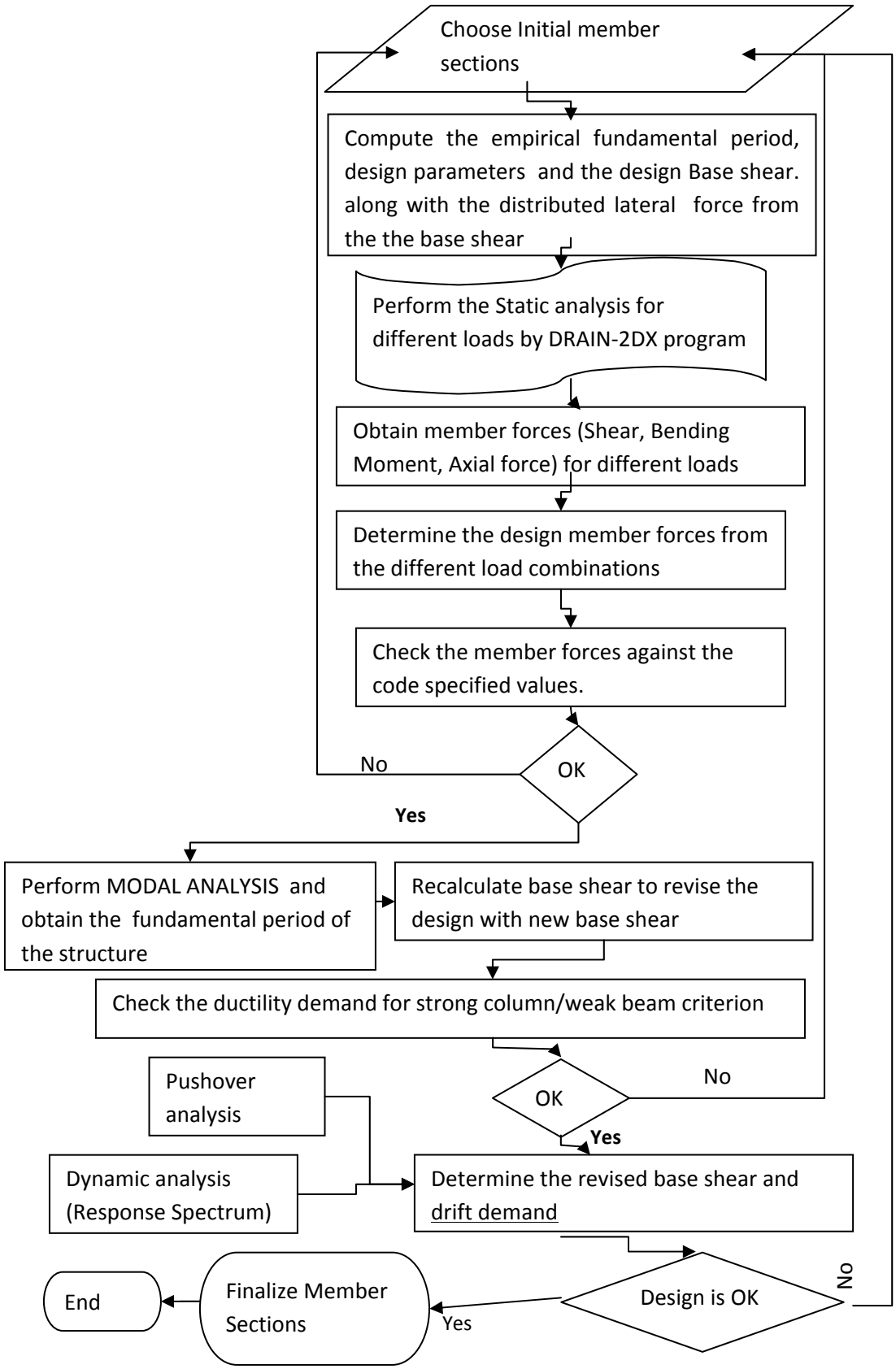

Figure 3.7: Flow-chart for the design and evaluation of Steel Moment Resisting Frames

Step 5 – Check for ductility demands of the individual members in the structure designed, if the members pass the ductility tests proceed with Step 6, else redesign the structure from Step 1.

Step 6 – Conduct the Non-linear static pushover analysis and response spectrum analysis on the structure designed and compute the base shear to obtain revised values, calculate the drift demand and check if the drift demands are within the code specified or acceptable limits.if the drift demands are within limits revise the sections of the members if required and finalize the design sections, if the results are unsatisfactory redesign the structure from Step 1.

3.5 Modal Analysis using a 3D model in ETABS Software

A 5 storey building was considered to be analyzed using the ETABS software in order to compare the modes from the DRAIN 2DX modal analysis. A 3D model of the building is developed using in the ETABS software and modal characteristics of the building model have been compared to the 2D model developed in the DRAIN-2DX model in order to establish the validity of the 2D models. ETABS is a reputed software in the as per the industry standards known for its innovative features and reliability in Building analysis and design. It provides the user with an Integrated Building Analysis and Design Environment. The software can analyze variety of structures including Moment Resisting Frames, Braced Frames, Staggered Truss Systems, Frames with Reduced Beam Sections or Side Plates, Rigid and Flexible Floors, Sloped Roofs, Ramps and Parking Structures, Mezzanine Floors Composite or Steel Joist Floor Framing Systems. ETABS is easy to use in designing a simple building or for performing a dynamic analysis of a complex high-rise building that utilizes non-linear dampers for inter-storey drift control.

3.5.1 Modeling

The modeling phase in ETABS involves the representation of the entire structure by elements to which physical and material properties are assigned. This building has 5 stories with 19.45m meter height. The dimension in X direction is 36 m and in Y direction is 24 m. Fig 3.8 shows the plan vie of the building in ETABS and Fig.3.9 shows the 3d view of the model structure in ETABS

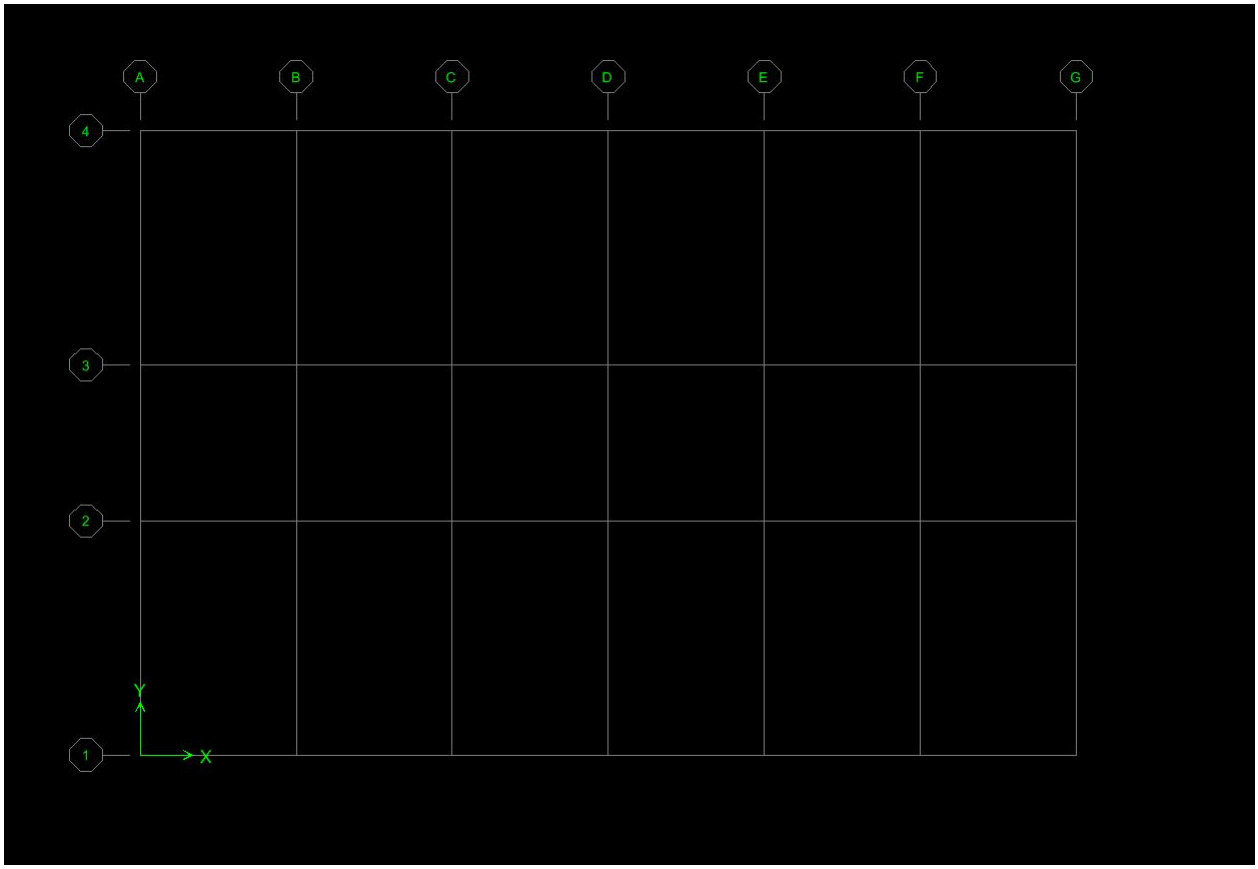

Fig.3.8 – Plan view of the building in ETABS

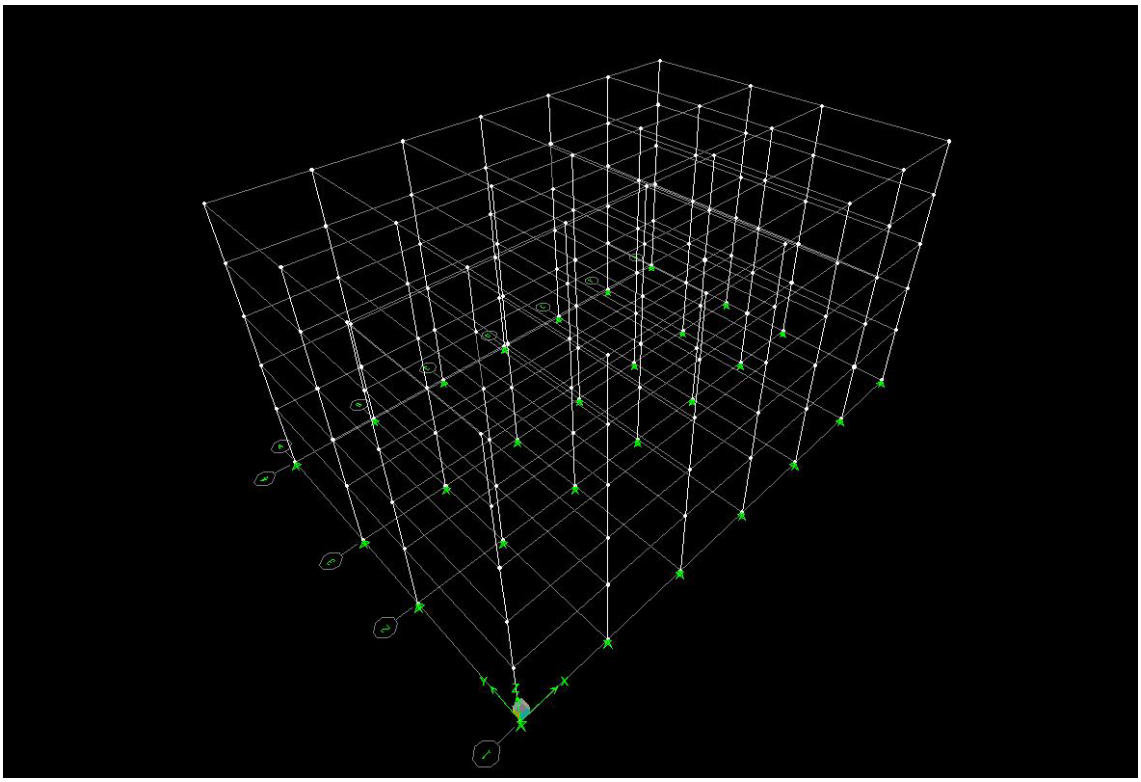

Fig.3.9 3-Dimensional view of the structure in ETABS

3.5.2 Loading

The modeling phase in ETABS involves the representation of the entire structure by elements to which physical and material properties are assigned. This building has 5 stories with 19.45m meter height. The dimension in X direction is 36 m and in Y direction is 24 m, the loads given in Table 3.1 has been adopted for the ETABS analysis and the Load combination has been chosen as per the equations 3.4 and 3.5, the base shear distribution or the lateral load distribution in the 5 storey SMRF at each storey level has been given in the Table 5.8 .

3.5.3 ETABS Analysis

Comparison of Mode periods from the DRAIN 2DX software and the ETABS software has been given in the Table 3.7. It is observed from Table 3.7 that the modal frequencies of the building

obtained from the 3D model (ETABS) and the 2D model (DRAIN 2DX) are in good agreement. This indicates that the 2D models can provide acceptable results. This expected in all the buildings as all of them have symmetrical plan. For the static and dynamic analysis, the 2D models are also expected to give acceptable results since the loads are applied symmetrically and structures, which are symmetrical would deform in a symmetrical manner. The effect of accidental torsion is expected to be minimal as suggested in NBCC 2010. Hence the static and dynamic analysis of all the buildings considered here are performed using the 2D models in the DRAIN 2DX software.

Table 3.7 – Modal periods from DRAIN 2DX and ETABS .

Modal Periods	**DRAIN 2DX**	**ETABS**
1	1.4123	1.396
2	0.42427	0.3782
3	0.21304	0.20024
4	0.12495	0.13452
5	0.084307	0.11047

3.6 Summary

The model of the building and the layout plan selected is symmetrical along the X and the Y axis hence a 2D analysis holds good for analyzing the effect of gravity, lateral and earthquake induced forces, ductile moment resisting frames are used in the building with direction of secondary beams running from right to left, and to allow for non-linear deformations. For the design of the building the frame or the bay in the N-S direction has been considered and Class I columns have been used in the design and has been shown to be in agreement with the CSA-S16-

09 standards, as the building is symmetrical in both the directions the columns have been spliced at every 5 floors instead of 3 floors and it is found to be optimal for design purpose, the rotation demands and the load carrying capacities of beams and columns of the ductile moment resisting frame have been checked to satisfy the design . The building was further modeled in ETABS under gravity, lateral and earthquake forces to verify and the check the results from the DRAIN 2D analysis and the results were found to be in agreement from both the cases .The designed members have been strictly checked to satisfy the guidelines from CSA (2009) for CSA-S16-09.

Chapter 4

Selection and Scaling of Ground Motions

4.1 Introduction

Non-linear dynamic analysis in time domain performed as part of performance-based design requires recorded acceleration as input data. The ground motion records selected for the analysis are expected to possess all the characteristics of a real earthquake records anticipated at the given site. Seismic waves, however are found to traverse in a complex path from the source or the plane fault to different sites, and are considered to have random characteristics in space and time. The code guidelines, on the other hand, are found to be simple and inadequate to serve as a guide for selecting earthquake records as it underestimates the potential effect of selecting appropriate records to be used for performance evaluation of structures. Furthermore, when time history analysis is performed, the response of a structure is captured for a suite of different ground motion records to obtain a reasonable engineering solution.

4.2 Selection of Ground Motion Records (GMR)

The presently available literature on the selection of earthquake records are deficient in engineering standards and the responsibility of selecting appropriate representative records for dynamic analysis rests upon the design engineer who in turn depends on the data of the seismic hazard at the site of the interest. Very few building codes which requires the use of dynamic analysis of structures, may not necessarily address the critical aspect of the number and type of records to be used in the analysis. The codes that specify the same are rare and the most common recommendation is for 3 records where maximum structural response must be used as per Eurocode 8 (EC8, 2004) and ASCE 7-05 (ASCE, 2005). However, Reyes and Kalkan (2011) suggested that seven or more records are preferable. The following figure (Fig. 4.1) shows a flowchart outlining the available options for Seismic Hazard Analysis (SHA) procedures that can be performed by an engineer. In the Fig.4.1 refers M,R,Ɛ refer to Magnitude (M), Source to site distance (R), and the soil profile at the specific site, respectively; and X_i, Mi and R_i indicate the selected and required number of records based on soil properties, Magnitude and Source to site distance, respectively .

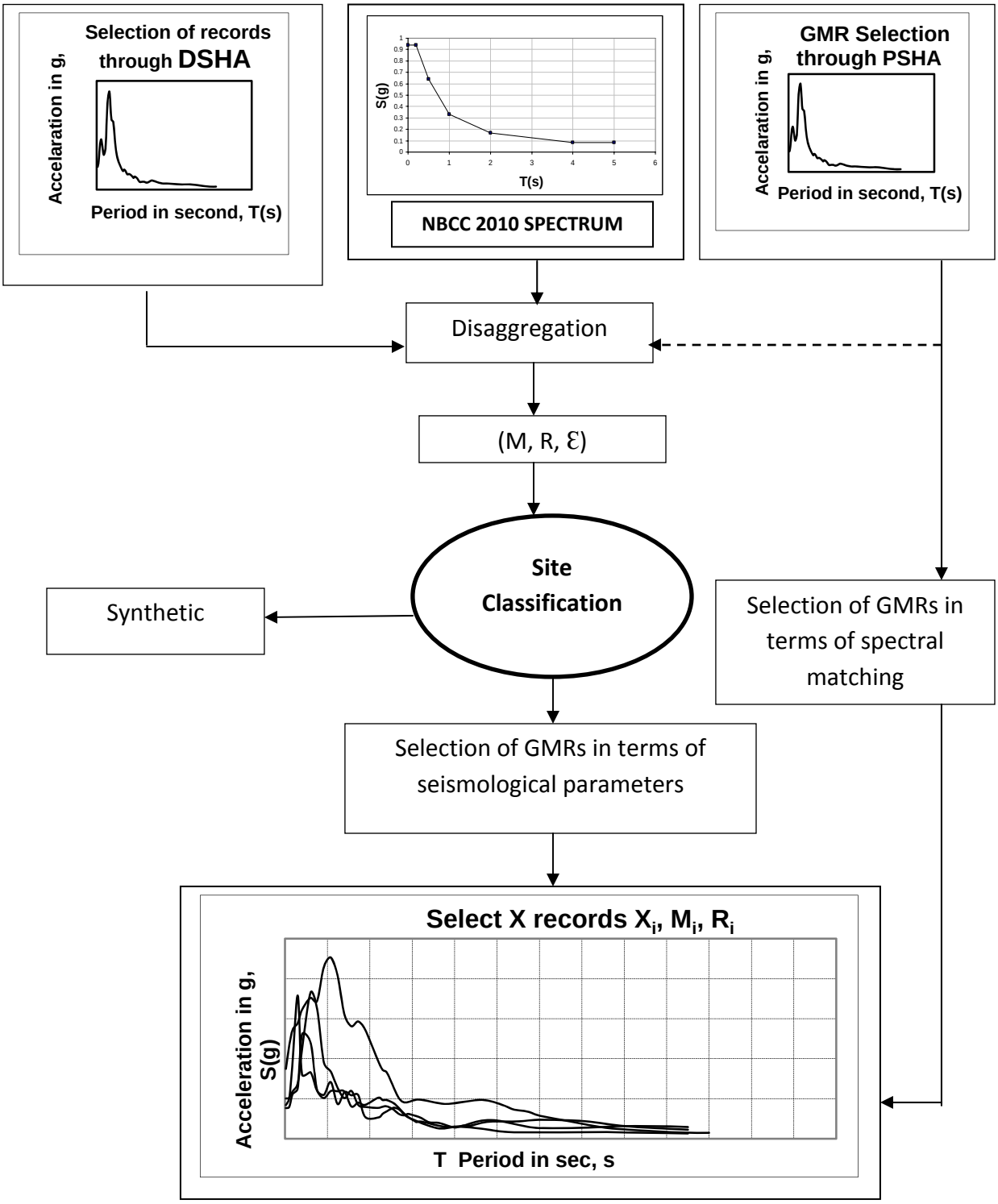

Figure 4.1: Available Selection procedures for strong motion records Bommer and Acevedo (2004)

The primary selection of records itself is usually carried out from the available data banks and are generally based on the engineering characteristics of an earthquake like magnitude and distance, strong–motion criteria, and site soil conditions. For a detailed study of seismicity on a particular area or for a structure of importance, a Seismic Hazard Analysis is required to be carried out. The hazard estimation, if carried out deterministically by assuming the design earthquake scenario in terms of magnitude, source to site distance, and the site-soil conditions, the process is referred to as *Deterministic Seismic Hazard Analysis* (DSHA). On the other hand, if the earthquake scenario is explicitly calculated by the method of any disaggregation techniques available, the process is referred to as *Probabilistic Seismic Hazard Analysis* (PSHA). In the DSHA approach, the strong motion parameters are estimated for the most severe ground motions at the specified site, considering the nature of the site soil geology, the distance from the site to the fault zone, and the data from the past earthquakes. The most important aspect of the DSHA process is to carefully estimate the "maximum credible or the "design scenario earthquake "based on the seismic zones and the seismo-tectonic and geological features of the source zone. As process is said to involve inherent ambiguities, it has a very low probability of occurrence, and in some cases, the hazard levels are found to be impractical to be used in the analysis for cost based economic feasibility studies. The PSHA process overcomes the limitations of DSHA in predicting the probability of occurrence. It is the most common method used for SHA originally developed by Cornell (1968). The probabilistic approach serves as an excellent method for risk management and in economic feasibility studies by taking account of the frequency or probability of exceedance of the earthquake against the design life of a structure or facility. PSHA gives

the cumulative seismicity of a particular site for a given period to estimate the strong motion parameters of an earthquake, the result of which is a site specific uniform hazard spectrum. The required engineering parameters of an earthquake i.e., Magnitude (M), Source to site distance (R) and ground motion deviation which are not available from the resulting hazard curves, are obtained by the process of disaggregation of the design earthquake scenarios. The method proposed by McGuire (1995) for disaggregation has been widely used. The selection process for the ground motion records, in general, can also be classified broadly under the following categories.

a. Selection based on Magnitude (M) and Distance (R)
b. Selection based on Site Soil Conditions
c. Selection based on Spectral Matching of Strong motion parameters
    - Evaluation of a/v (i.e., peak ground acceleration to velocity) ratio
    - Effect of duration of ground motion shaking

4.2.1 Selection based on Magnitude (M) & Distance (R)

It is the most commonly used parameter for initial ground motion selection, where the magnitude of the earthquake selected is recommended to have the same value or +/- 0.2 to that corresponding to the target spectrum. The magnitude of the earthquake is found to have considerable effect on the demand of the structure as it influences the duration and shape of the response spectrum strongly. Although there are many techniques available for altering the shape of the response spectrum, it is necessary to keep the shape of the response spectrum in close agreement to that of the target spectrum. For this reason, the magnitude of the earthquake selected is also an important parameter, which is usually

used in conjunction with the source to site distance from the fault zone to the site in consideration to form a pair of selection parameters in the initial search of records. However, the spectral shape is found to be less sensitive to distance (R) than to that of magnitude. A collection of ground motion records sorted with magnitude and source-distance (M, R) are usually referred to as a bin of records. In this methodology the variation between the record and scenario magnitudes is recommended to be closely spaced. Stewart et al. [2001] suggested a magnitude half-bin width of $\pm$0.25 M, while Bommer and Acevedo [2004] recommended $\pm$ 0.20 M. Therefore, while searching for real records, the search parameters for the magnitude is spaced closely, and widened for the distance range, if required.

Nevertheless, recent studies have questioned the effectiveness of (M,R) based selection method because of the deviating and unreliable results in structural response observed after direct use of earthquake record sets based on this particular criterion as input to non-linear dynamic analysis. The source to site distance derived from the earthquake scenarios has been proven to be an inadequate predictor of structural response. However, in spite of the noted shortcomings, the method is largely familiar and in use by structural engineers.

4.2.2 Selection based on Site Soil Conditions

One of the important parameters for selection of earthquake records is the soil profile at the site of the interest. The soil strata classification parameter generally refers to the top 30 m and is said to influence the amplitude and shape of the response spectra to a large extent. Boore (2004) has stated that soil strata much below 30 m also influences the

response spectra, the parameter is more often used in conjunction with the M, R selection criteria. In such a scenario, it is observed that the M, R, S selection criteria greatly reduces the number of records selected for a dynamic analysis; in which case, the selection of records from similar soil database is recommended.

4.2.3 Selection based on Spectral Matching of strong motion parameters

As recommended in most building codes, one of the most important criteria for a selected earthquake record is that it is a representative ground motion observed at a suitable source to site distance. This specification directly relates to the compatibility of the record to the target spectrum rather than the seismological criteria at the site specified. This situation has given rise to the selection based on spectral matching as a prominent method wherein selection of real accelerograms is obtained on the basis of degree of compatibility to the corresponding 'target' spectrum as provided in the the relevant building code or through a seismic hazard analysis. Ambraseys et al. [2004] proposed Eq. (4.1) as a means to verify spectral compatibility of a given record with the target spectrum for the European strong-motion databank.

$$\mathbf{D_{rms}} = \frac{\mathbf{1}}{\mathbf{N}} \sqrt{\sum_{\mathbf{i=1}}^{\mathbf{N}} \left(\frac{\mathbf{S\alpha_o(Ti)}}{\mathbf{PGAo}} - \frac{\mathbf{S\alpha_s(Ti)}}{\mathbf{PGAs}} \right)^{\mathbf{2}}} \tag{4.1}$$

In the above equation, N is the number of periods at which the spectral shape is specified $S\alpha_0(T_i)$ is the spectral acceleration of the record at period T_i, $S\alpha_s(T_i)$ is the target spectral acceleration at the same period, while PGA_0 and PGA_s are the peak ground acceleration of the record and the zero-period anchor point of the target spectrum, respectively. A

small value of D_{rms} indicates a close match between the spectral shape of the recorded motion and the target spectrum. In general, the value of D_{rms} depends on the size of the earthquake record databank and the number of records required. It is also dependent on the period range of interest that must be specified for spectral matching, with a shorter range being preferable to a longer one. Furthermore, the need to efficiently match the target spectrum over the longer period range, which is of primary interest in many structural engineering problems, led Beyer and Bommer [2007] to modify Eq. (4.1) by proposing a scale factor, a for each record that minimizes the root-mean-square difference D_{rms} between the scaled geometric mean spectrum of the real record and the target spectrum.

$$\boldsymbol{\delta_i = \sqrt{\frac{1}{N}\sum_{i=1}^{N}} \left(\frac{S\alpha_j(T_i) - S\alpha_{REF}(T_i)}{S\alpha_{REF}(T_i)}\right)^2} \tag{4.2}$$

In the equation 4.2 $S\alpha_j(T_i)$ represents the pseudo-acceleration ordinate of the real spectrum j at period Ti, $S\alpha_{REF}(T_i)$ represents the value of the spectral ordinate of the code spectrum at the same period, and N is the number of values used within a pre-defined range of periods. Another procedure for selection of earthquake records is the selection of real time histories whose spectral ordinates match to that of target spectrum for the period range considered in a way that scaling is not required (Idriss, 1993). Anderson and Naeim (1993) selected 120 records from a database with their plots of constant strength inelastic response spectra; these ground motions are suitable for engineering use and recommended for analysis purposes.

4.2.3.1 Evaluation of a/v ratio :

Based on seismotectonic features of a particular region, the ratio of the maximum acceleration to that of the maximum velocity has been noted to be a complimentary measure of the selection process. Tso et.al. [1992] and Sawada et.al. [1992] concluded that this parameter is related to the earthquake magnitude, distance from source, and the frequency contents of the accelerograms. They grouped the accelerograms based on the ratio of the peak acceleration (in *g*) to the peak velocity (in m/s) ratio (*a/v* ratio) into Low ($a/v \leq 0.8$), Intermediate ($0.8 < a/v \leq 1.20$) and High ($a/v > 1.20$).

4.2.3.2 Effect of duration of ground motion shaking

Strong motion duration is considered to be an additional and complimentary parameter in the selection of ground motion records. The duration of ground shaking mainly depends on the duration of rupture zone and the magnitude of the earthquake. Hannock and Bommer [2006] pointed out that a structure undergoing stiffness and/or strength degradation due to fatigue damage and absorbed hysteretic energy are more likely to undergo large damage due to a long duration of shaking. However ASCE Standards 04-98 (ASCE, 2000) recommends that duration of the ground motion should be representative of the design or scenario earthquake records.

The selection procedure and the methodology presented here allows the engineer to make a rational decision on using an appropriate earthquake record in time domain for the non-linear dynamic time-history analysis. The ground motion records are usually selected considering a few parameters and various other limiting factors like time, resources and available data.

4.3 Scaling of the selected GMRs

For time history analysis, a ground motion record is selected such that the record is compatible to the design spectrum. There are a number of methods available for scaling a ground motion record in order to obtain a record that would represent the seismicity of a location as expressed in the design response spectrum. The commonly used methods for scaling or deriving a design spectrum compatible ground motion records are listed below with a brief description.

4.3.1 PGA Scaling

In this scaling technique the input accelerogram is multiplied by a scalar quantity to match the peak ground acceleration as that of the site specific target spectrum. Fig 4.2 shows the Peak Ground acceleration of the input ground motion record and Fig 4.3 shows the Peak ground acceleration of the design spectrum, the scale factor is given by the following formula (Eq. 4.3).

$$\textbf{Scale Factor} = \frac{\mathbf{PGA_{ds}}}{\mathbf{PGA_{gmr}}} \qquad (4.3)$$

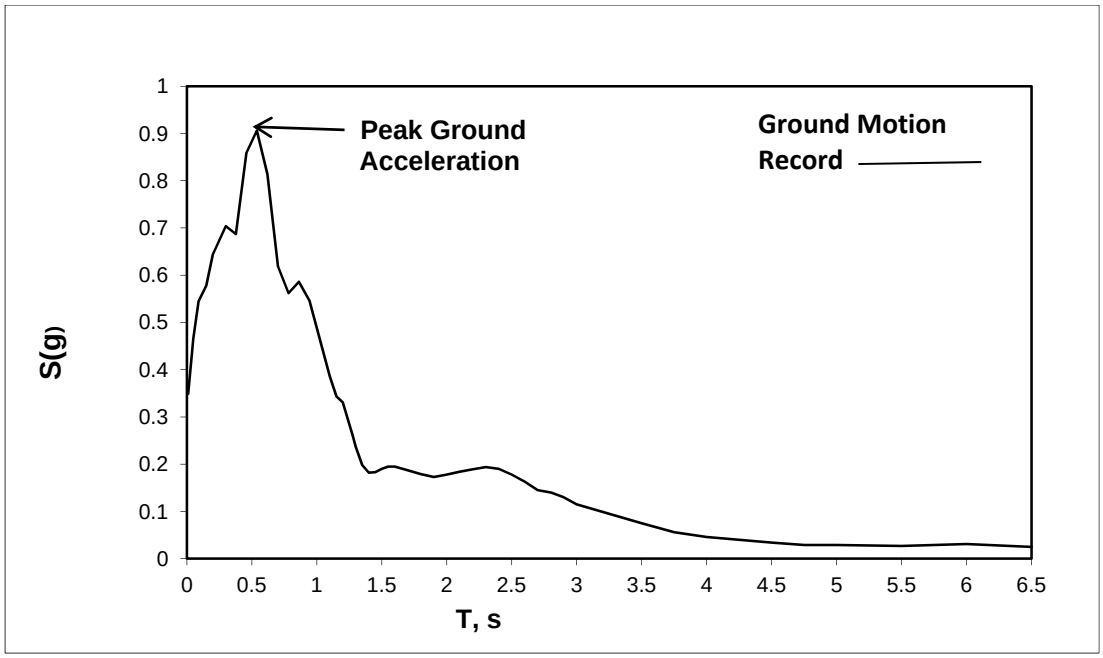

Fig 4.2. Peak Ground Acceleration in the selected GMR

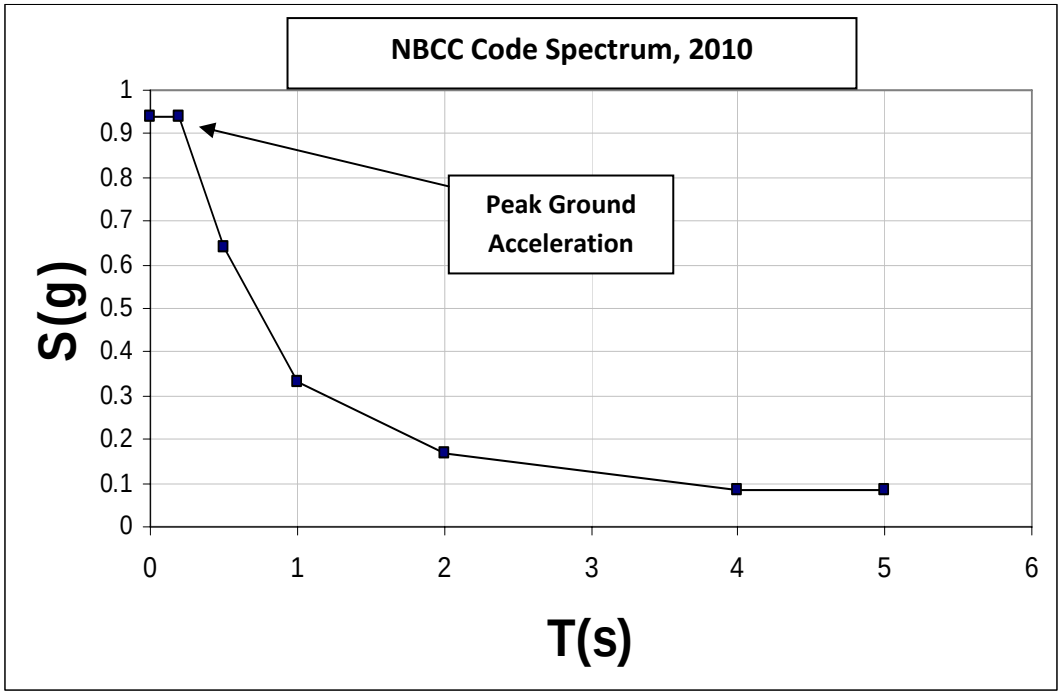

Fig.4.3 Peak Ground Acceleration from the NBCC Code Spectrum

4.3.2 Ordinate Scaling Method

In this scaling technique the input accelerogram is multiplied by a scalar quantity to match the spectral ordinate at the fundamental period of vibration of the structure as that of the target spectrum .Fig.4.4 shows the ordinate at T_1 of the structure on the input ground motion record and Fig .4.5 shows the ordinate at T_1 of the structure on the design spectrum, the scale factor is given by the formula (Eq. 4.4):

$$\textbf{Scale Factor} = \frac{\textbf{T1 Ordinate}_{\textbf{ds}}}{\textbf{T1 Ordinate}_{\textbf{gmr}}} \qquad (4.4)$$

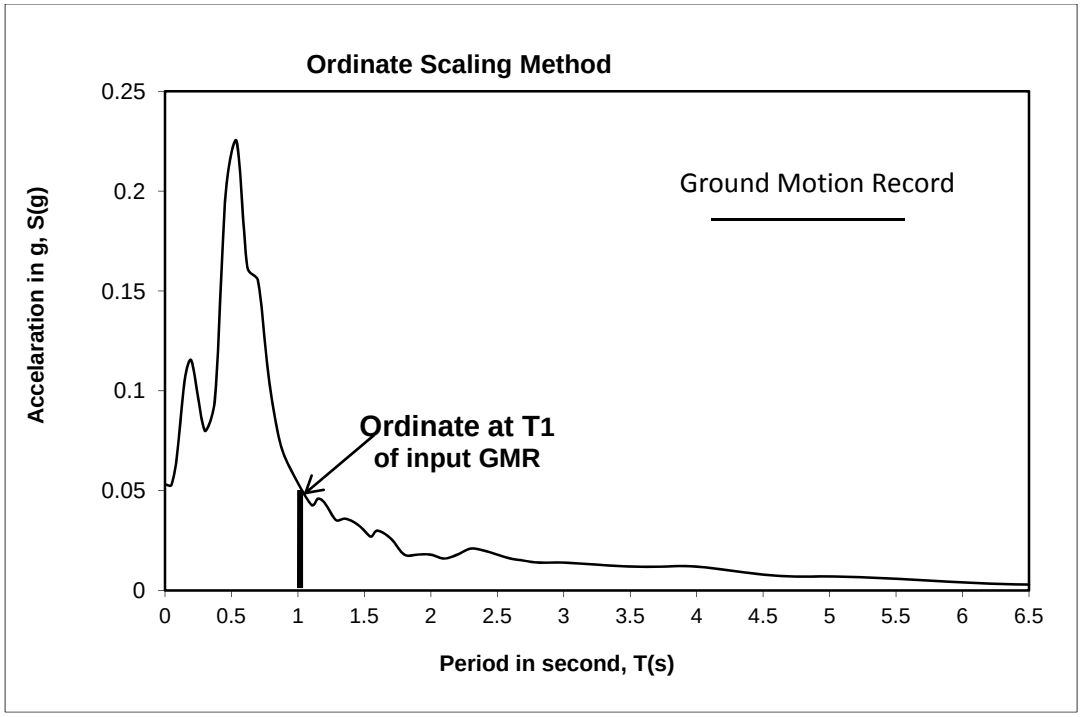

Fig 4.4. Ordinate at T_1 on the input GMR

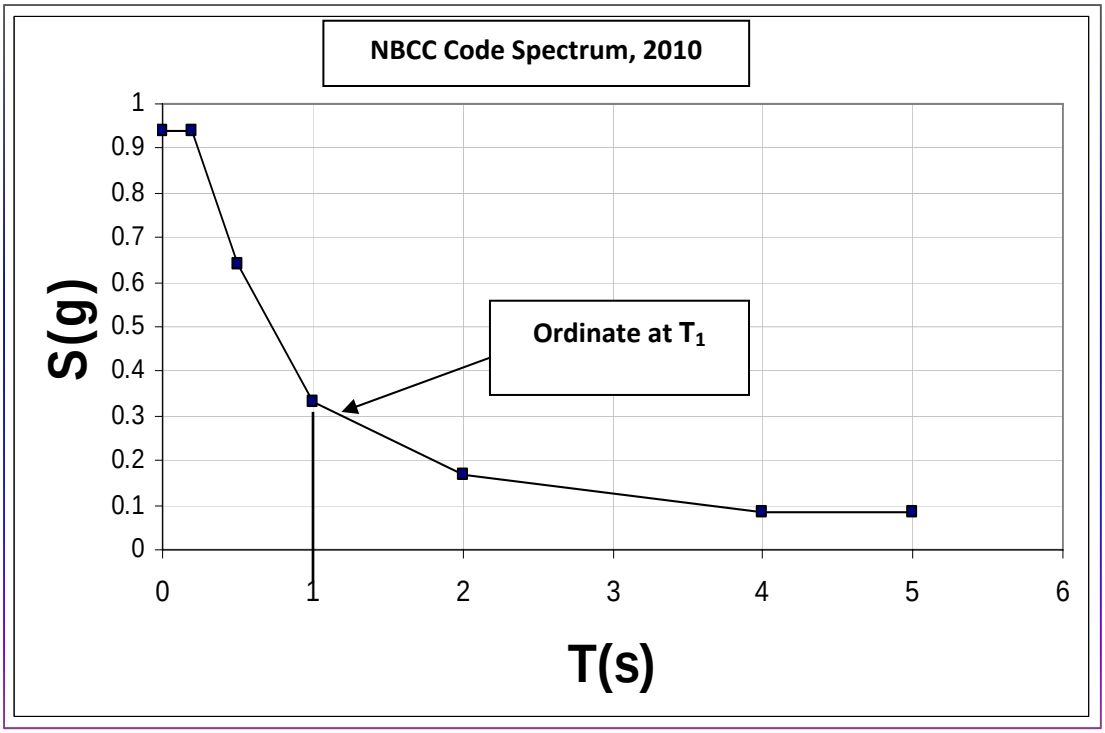

Fig 4.5. Ordinate at T_1 on the NBCC Code Spectrum

4.3.3 Least Square Method

This scaling technique was proposed by Somerville et al., (1997a, b), under this method the input accelerogram is multiplied by a scalar that minimizes the weighted sum of the errors (differences) between the accelerogram response spectrum and the target spectrum, the weights used are 0.3, 1.0, 2.0, 4.0 at the period corresponding to the first, second, third and fourth modes (i.e., T_1, T_2, T_3, T_4), respectively. Fig. 4.6 shows the co-ordinates of the least square method on the input ground motion record at 0.3s, 1s, 2s and 4s respectively and Fig .4.7 shows the the co-ordinates of the least square method on the design spectrum at 0.3s, 1s, 2s and 4s respectively

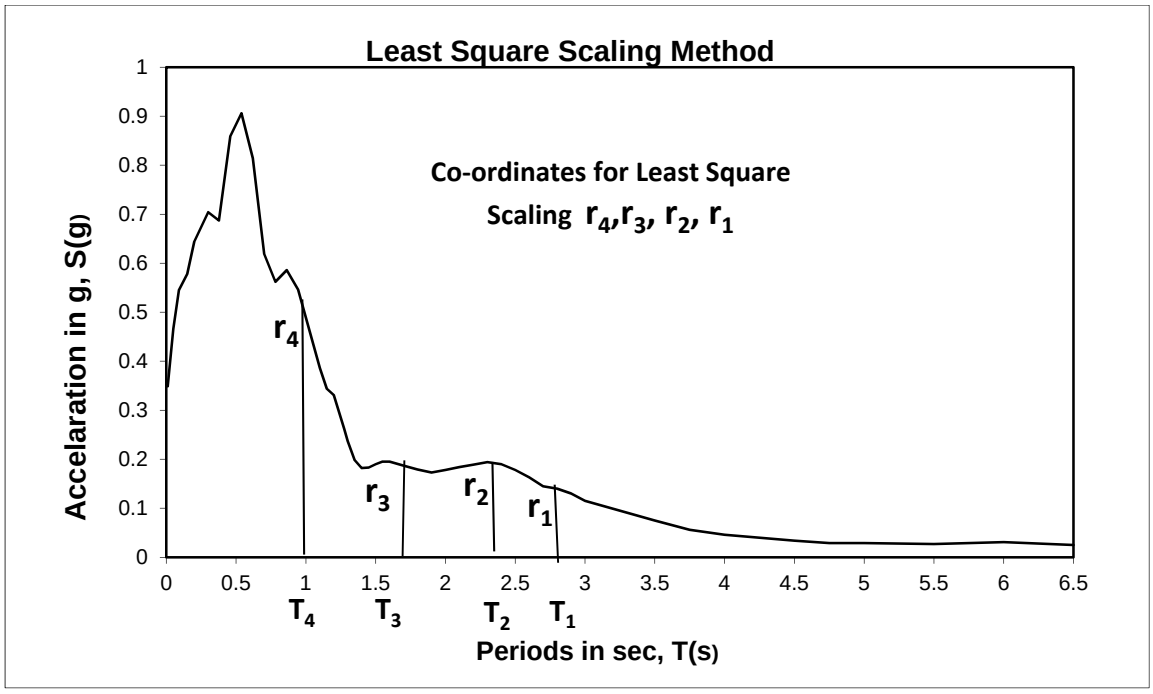

Fig 4.6.Least Square Scaling Ordinates on the input Ground Motion Record

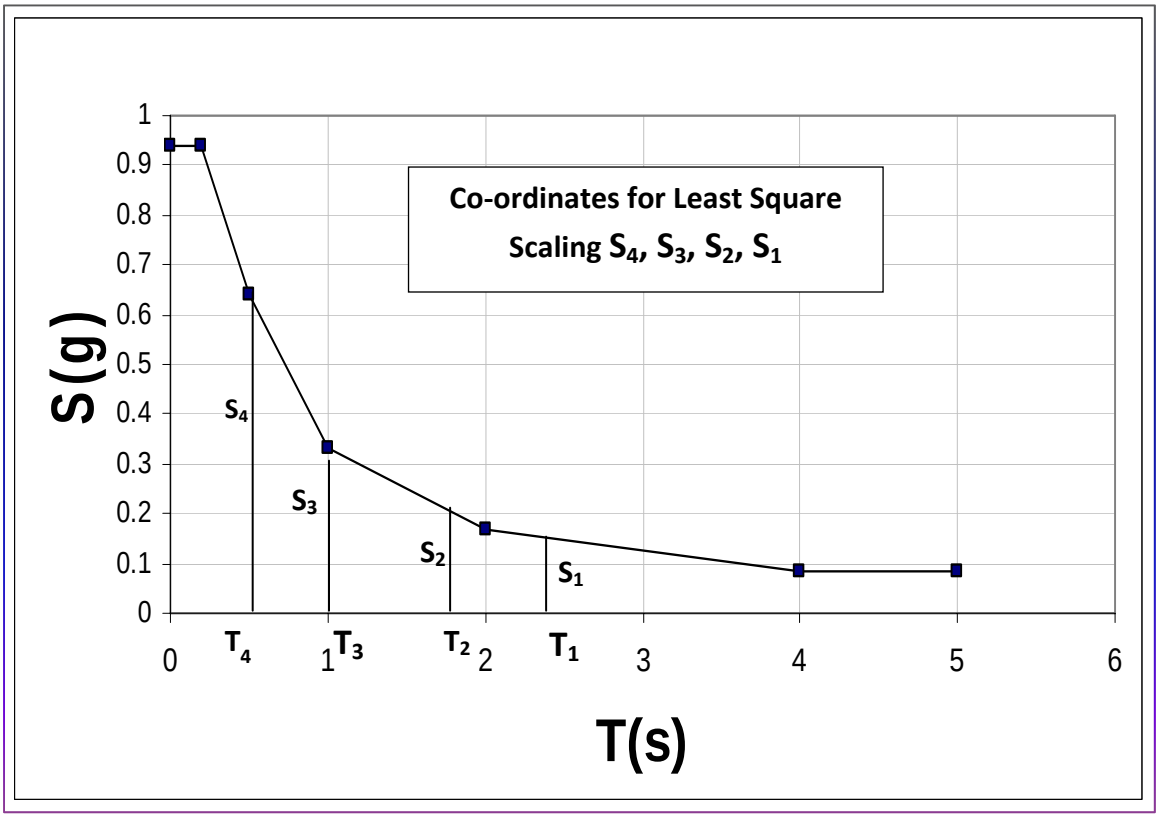

Fig 4.7 .Least Square Scaling Ordinates on the NBCC Spectrum

Scale factor in the Least-square scaling method is given by the following expression (Eq. 4.5):

$$\textbf{Scale Factor} = \frac{0.6S_1r_1+0.6\ S_2\ r_2+0.6S_3r_3+0.6S_4r_4}{0.6\ r_1^2+0.6\ r_2^2+0.6\ r_2^3+0.2r_2^4} \qquad (4.5)$$

4.3.4 Partial Area Method

In this scaling technique the area under the acceleration response spectrum between the second mode period, T_2 and 1.2 times the first mode period, T_1 be the same as that of the target spectrum (Naumoski et al., 2004). Fig .4.8 shows the area under the input GMR between T_2 and $1.2\ T_1$ and Fig.4.9 shows the area under the target spectrum between T_2 and $1.2\ T_1$. The scale factor is given by the following ratio (Eq. 4.6).

$$\textbf{Scale Factor} = \frac{\textbf{Area under Target Spectrum}}{\textbf{Area under input ground motion record}} \qquad (4.6)$$

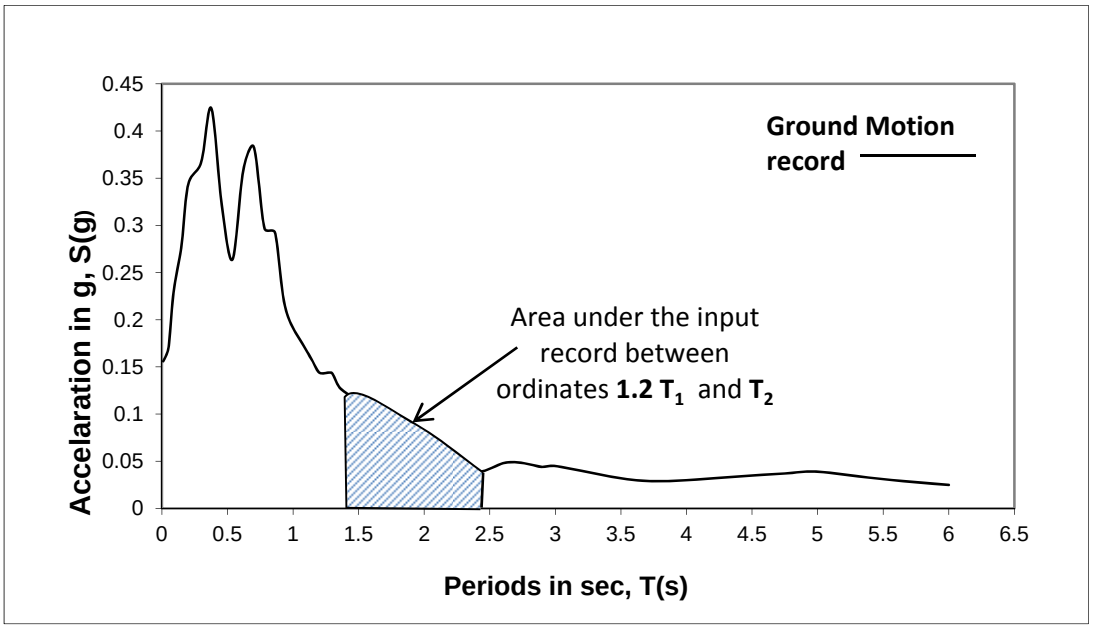

Fig 4.8 .Partial Area Scaling Ordinates on the input Ground Motion Record

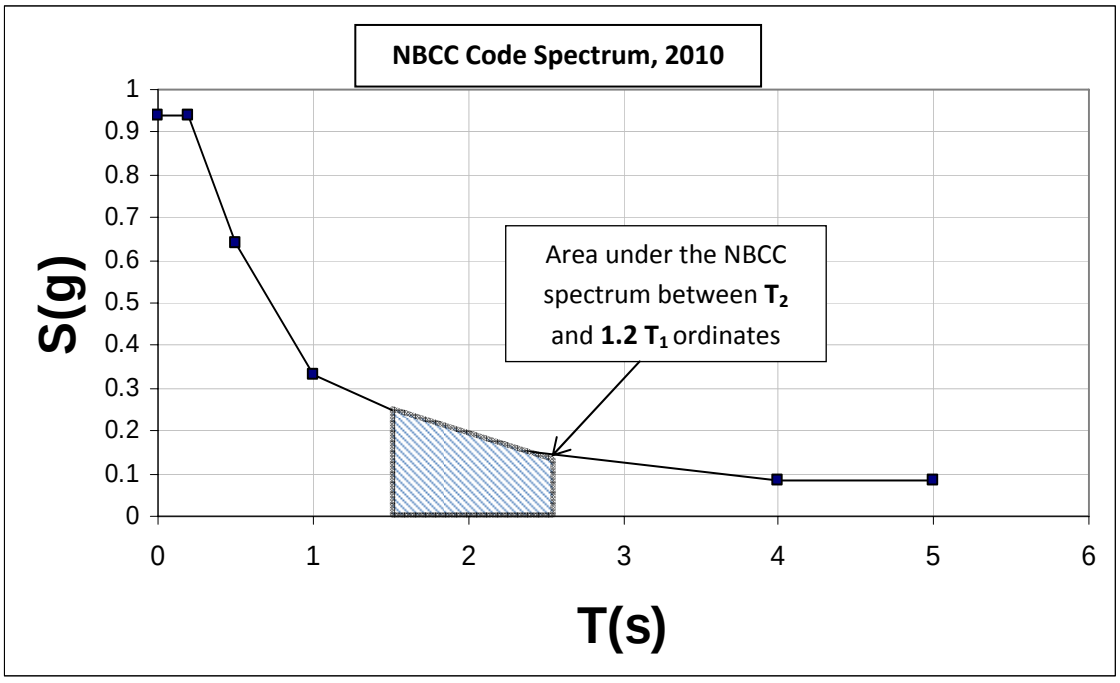

Fig.4.9 .Partial Area Scaling Ordinates on the NBCC Code Spectrum

4.3.5 PS_a Scaling Method

This scaling technique requires the area under input spectrum and target spectrum to be equal between the period range 0-2 s (Naumoski et al., 2004).

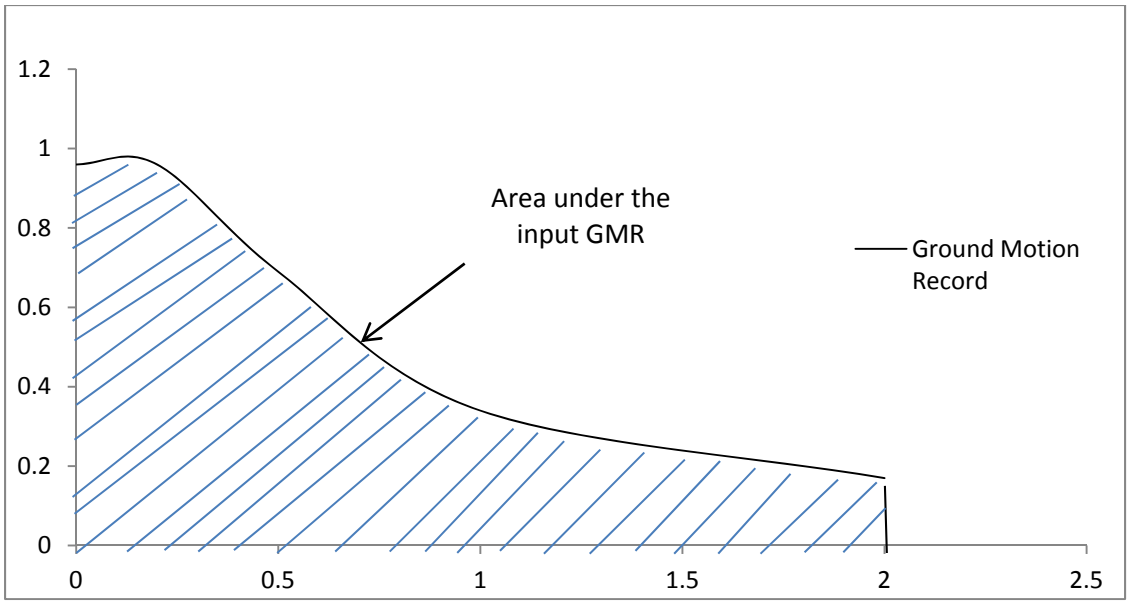

Fig 4.10 .PSa Scaling Ordinates on the input Ground Motion Record

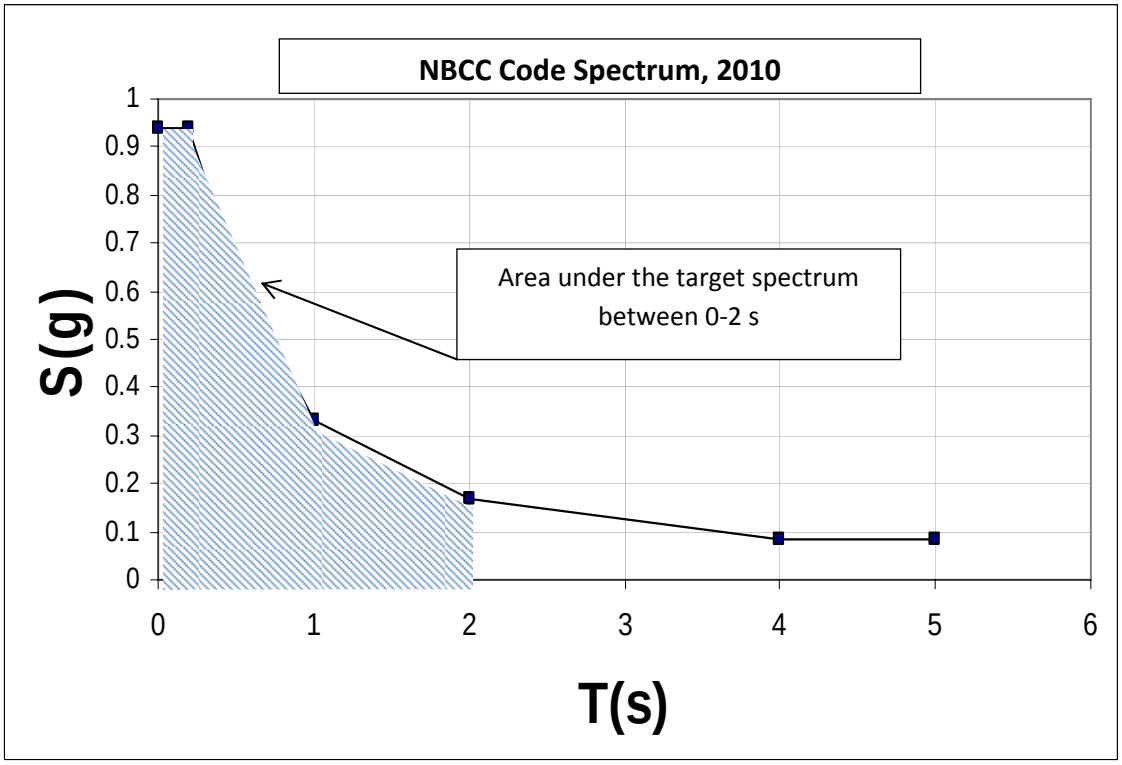

Fig 4.11 .PSa Scaling Ordinates on the NBCC Spectrum

Fig .4.8 shows the area under the input GMR between *0* and *2s* and Fig.4.9 shows the area under the target spectrum between *0* and *2 s*. The scale factor is given by the following expression (Eq. 4.6)

$$\textbf{Scale Factor} = \frac{\textbf{Area under Target Spectrum}}{\textbf{Area under input ground motion record}} \qquad (4.6)$$

4.3.6 ASCE-7 Scaling Method

This technique requires that the average value of spectral ordinates should not be smaller than those of the target spectra for the period range $0.2T_1$ to $1.5T_1$ where T is the fundamental vibration (i.e., same as T_1) of the structure.

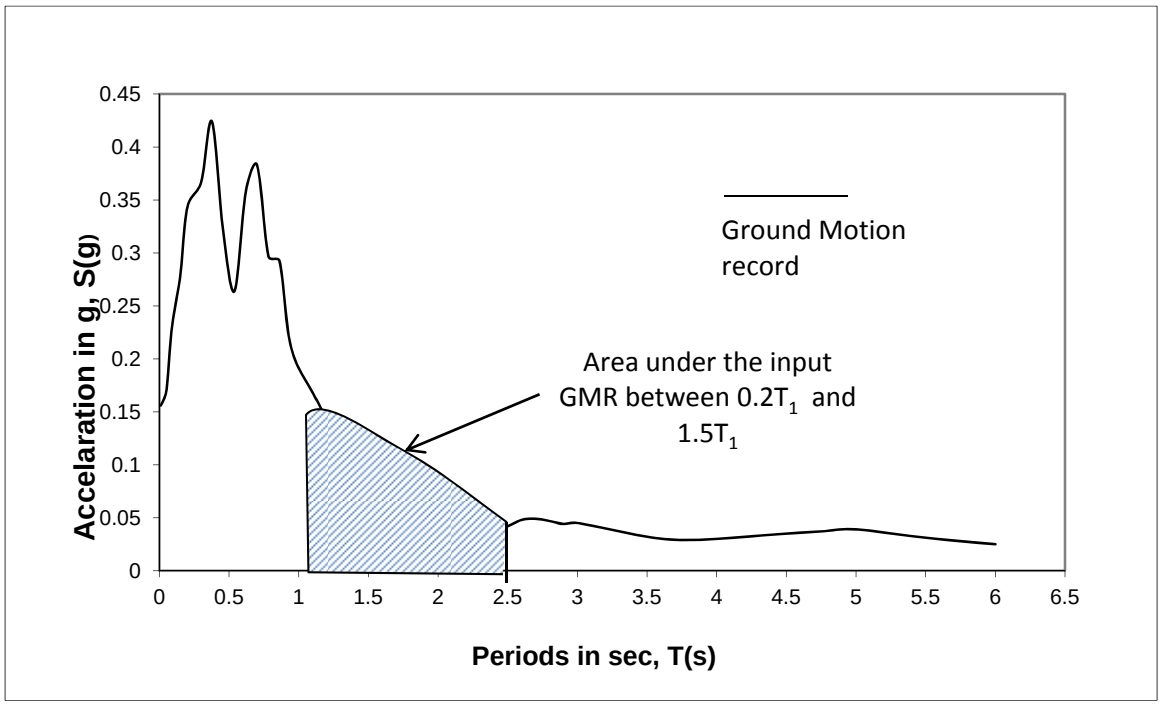

Fig 4.12 ASCE-7 Scaling Ordinates on the input Ground Motion Record

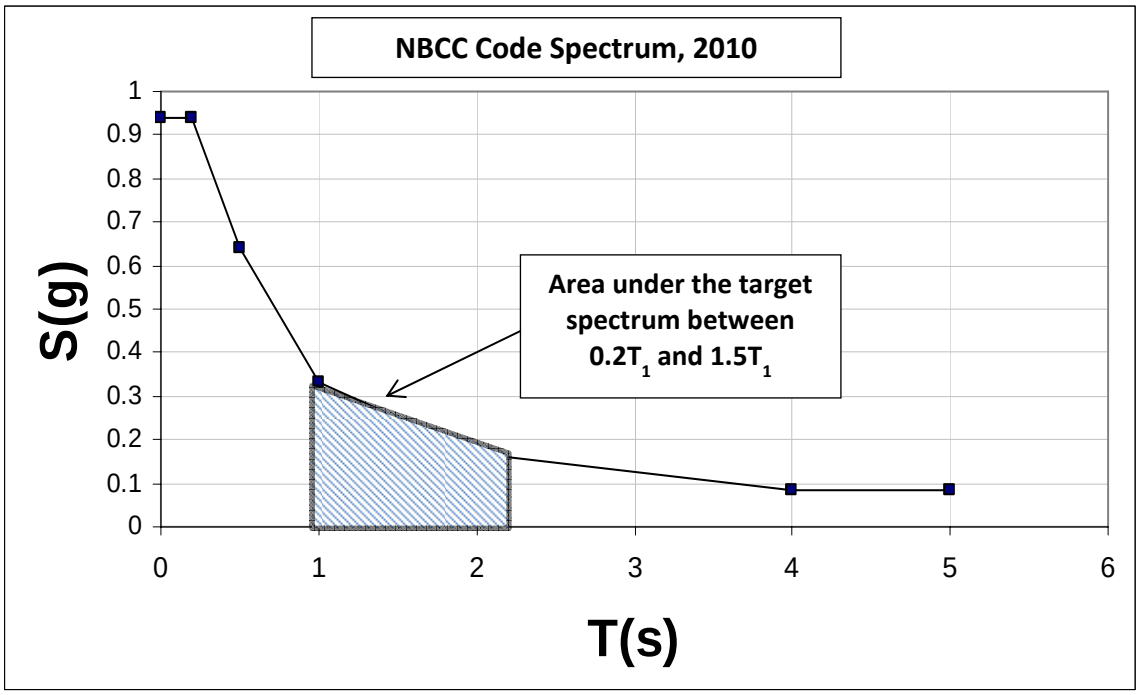

Fig 4.13 ASCE Scaling Ordinates on the NBCC Spectrum

Fig .4.12 shows the area under the input GMR between 0.2 T_1 and 1.5 T_1 and Fig.4.13 shows the area under the target spectrum between 0.2 T_1 and 1.5 T_1. The scale factor is given by the following expression (Eq. 4.7).

$$\textbf{Scale Factor} = \frac{\textbf{Area under Target Spectrum}}{\textbf{Area under input ground motion record}} \qquad (4.7)$$

4.3.7 Spectrum Matching Technique

In this method spectrum matching is done by modifying the frequency contents of the input accelerogram to match its response spectrum to the target spectrum. There are different software programs such as SeismoMatch (Abrahamson [1992] and Hancock et al. [2006]) or Synth (Naumoski et al. 2004) are available for matching matching the frequency of input spectrum to that of the target spectrum and generating the corresponding time history signal for the ground acceleration.

4.3.8 Spectrum-compatible artificial earthquake record

In this technique the input accelerogram which is pre matched with the site specific target spectrum are generated through simulation (e.g. Atkinson, 2009). Hence, these records are directly used as input accelerograms in time history analysis. Fig. 4.14 and Table 4.5 provides a brief description of artificial records used in scaling of the ground motion records to be used in time history analysis, the scale factor is not applicable in the case of artificial earthquake records as the records are spectrum compatible beforehand.

4.4 GMRs used in the present study

The scaling and matching techniques for the research has been carried out for 30 (thirty) ground motion records. Among these, eight records are synthesized and compatible to the seismic hazard spectrum for Vancouver, Canada developed by Atkinson, [Beresnev and Atkinson, 1998; Atkinson 2009], Fig.4.14 shows the 8 synthesized records from Atkinson of which 4 are short duration and 4 are long duration records (Bagchi 2001; Tremblay et al. 2001) and Table 4.1 represents the characteristics of the 8 synthesized ground motions and Figure 4.15 show their response spectra. In addition, twenty two real ground motion records obtained from the data base of Pacific Earthquake Engineering Research Center (PEER, 2006) have been selected by comparing the peak acceleration-peak velocity ratio of seismic motion (*a/v*) to be compatible with the seismicity of Vancouver, where *a/v* of a potential ground motion is expected to be close to 1 (Table 4.2). It is noted that the *a/v* ratio controls the spectral shape of the seismic motion. The response spectra of the ground motion records are shown in Figure 4.16.

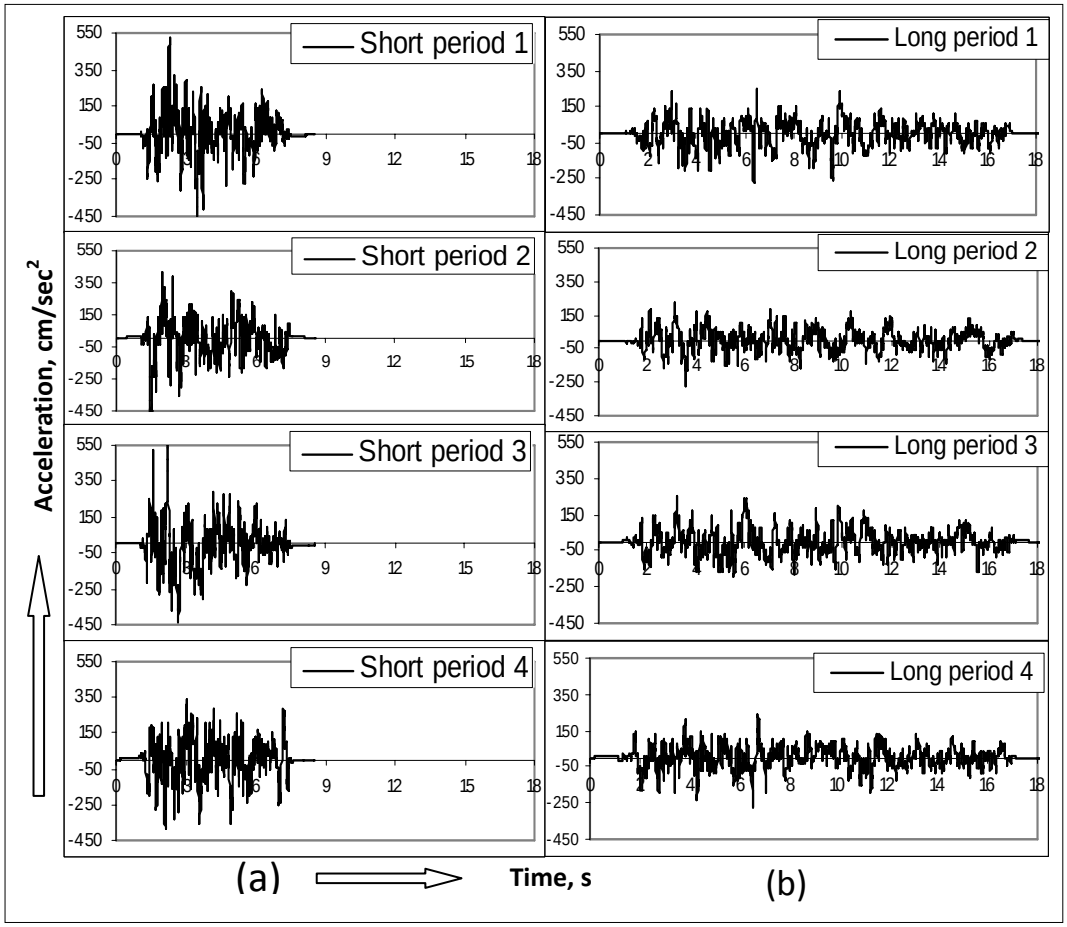

Figure 4.14: Time History of Atkinson's synthesized ground motions.
(a) Short period ground motions (b) Long period ground motions.

Table 4.1: Characteristics of Atkinson's Synthesized Ground Motion.

Record	LP1	LP2	LP3	LP4	SP1	SP2	SP3	SP4
Peak Acceleration (cm/sec^2)	266.2	279.4	248.6	271.7	523	527	567	380
Duration (s)	18.24	18.24	18.24	18.24	8.55	8.55	8.55	8.55

LP = Long Period, SP = Short Period

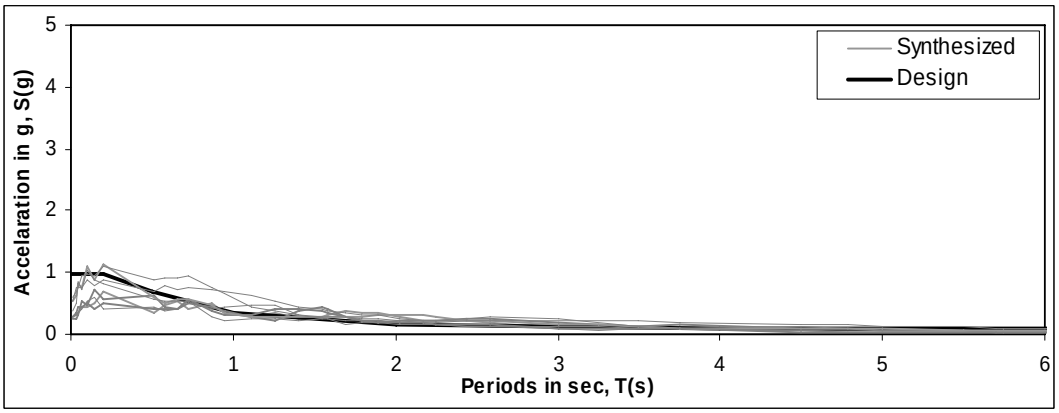

Figure 4.15: Spectra of selected Synthesized Ground Motion Records along with the NBCC 2005/2010 design spectrum

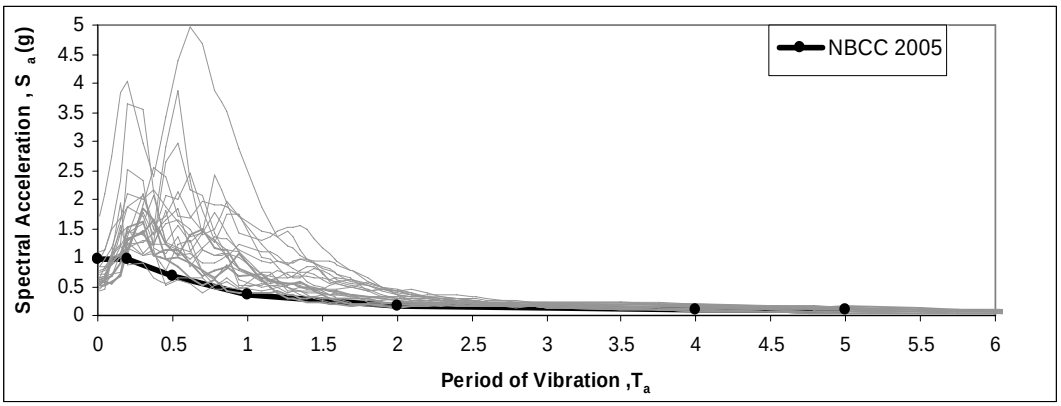

Figure 4.16: Spectra of selected Ground Motion Records along with the NBCC 2005/2010 design spectrum

Table 4.2: Summary of Real Ground Motion

Record No.	Location and year	PGA (*g*)	Peak Velocity (m/sec)	*a/v*
1	Imperial Valley (1940)	0.348	0.334	1.04
2	Kern Country (1952)	0.179	0.177	1.01
3	Kern Country(1952)	0.156	0.157	0.99
4	Borrego Country (1968)	0.046	0.042	1.09
5	San Fernando (1971)	0.150	0.149	1.01
6	San Fernando (1971)	0.211	0.211	1.00
7	San Fernando(1971)	0.165	0.166	0.99
8	San Fernando (1971)	0.180	0.205	0.88
9	San Fernando (1971)	0.199	0.167	1.19
10	Record No.S-882 Gazli USSR	0.07	0.07	1.00
11	Record No.S-634 Coalinga	0.078	0.068	1.15
12	Monte Negro-2 (1979)	0.171	0.194	0.88
13	Report Del Archivo: SUCH850919AL.T	0.105	0.112	0.94
14	Report del Archivo: VILE850919AT.T	0.123	0.105	1.17
15	Kobe, Japan (1995)	0.061	0.049	1.24
16	Kobe, Japan (1995)	0.694	0.758	0.92
17	Kobe, Japan (1995)	0.707	0.758	0.93
18	Kobe, Japan (1995)	0.144	0.150	0.96
19	Northridge, CA (1994)	0.469	0.571	0.82
20	Northridge, CA (1994)	0.510	0.493	1.03
21	Northridge, CA (1994)	0.088	0.072	1.22
22	Northridge, CA (1994)	0.080	0.082	0.98

As some of the scaling methods considered here utilize the modal periods of a structure, the first and second modal periods for all the building frames used here are reported in Table 4.7. The scale factors obtained using different methods are given in Tables 4.8 through 4.17. In these tables, the scale factors exceeding 5 have been identified and NA (Not Applicable) and the corresponding ground motion records are excluded from the analysis. A set of spectrum compatible records have also been generated by frequecncy-domain spectrum matching procedure using the Siesmo-match software. The spectra of these artificial records have been shown in Figure. 4.17.

Table 4.3: Modal periods of the building frames

SMRF	First period (T_1), s	Second period (T_2), s
5 storey	1.41	0.42
10 storey	2.53	0.82
15 storey	3.57	1.17
20 storey	4.79	1.58

Table 4.4: Scale Factors using PGA Method

Scaling Factor (SF) = S(g)NBCC/S(g)Field			
EQ Records	**S(g) Design Spec**	**S(g) GMR Spec**	**SF**
naver1	0.960	0.9060	**1.06**
naver2	0.960	0.5290	**1.81**
naver3	0.960	0.4240	**2.26**
naver6	0.960	0.5210	**1.84**
naver7	0.960	0.6110	**1.57**
naver8	0.960	0.7150	**1.34**
naver9	0.960	0.4870	**1.97**
naver10	0.960	0.7300	**1.32**
naver11	0.960	0.2070	**4.64**
naver12	0.960	0.2650	**3.62**
naver13	0.960	0.6430	**1.49**
naver14	0.960	0.3990	**2.41**
naver15	0.960	0.4230	**2.27**
kobejap1	0.960	0.2250	**4.27**
kobejap3	0.960	2.4860	**0.39**
kobejap4	0.960	1.0240	**0.94**
northdr1	0.960	2.3860	**0.40**
northdr2	0.960	1.2770	**0.75**
northdr3	0.960	1.4360	**0.67**
northdr4	0.960	0.2560	**3.75**

SF = Scale Factor; GMR = Ground Motion Record; Spec = Spectral Ordinate

Table 4.5: Scale Factors using Ordinate Method (5 and 10 storey)

5 Storey Building				10 Storey Building		
GMRs	**S(g) Design Spec**	**S(g) GMR Spec**	**SF**	**S(g) Design**	**S(g) Field**	**SF**
naver1	0.270	0.1822	**1.48**	0.1486	0.174	**0.86**
naver2	0.270	0.1252	**2.16**	0.1486	0.057	**2.60**
naver3	0.270	0.1218	**2.22**	0.1486	0.044	**3.40**
naver6	0.270	0.1184	**2.28**	0.1486	0.037	**4.03**
naver7	0.270	0.2652	**1.02**	0.1486	0.091	**1.63**
naver8	0.270	0.1227	**2.20**	0.1486	0.089	**1.67**
naver9	0.270	0.0793	**3.41**	0.1486	0.053	**2.80**
naver10	0.270	0.1187	**2.27**	0.1486	0.086	**1.73**
naver11	0.270	0.0400	**6.74**	0.1486	0.010	**14.23**
naver12	0.270	0.1044	**2.59**	0.1486	0.015	**10.10**
naver13	0.270	0.1370	**1.97**	0.1486	0.096	**1.55**
naver14	0.270	0.0747	**3.61**	0.1486	0.028	**5.23**
naver15	0.270	0.0730	**3.70**	0.1486	0.037	**4.03**
kobejap2	0.270	0.0897	**3.01**	NA	NA	**NA**
kobejap3	0.270	0.9191	**0.29**	0.1486	0.201	**0.74**
kobejap4	0.270	0.5113	**0.53**	0.1486	0.133	**1.11**
northdr1	0.270	0.5976	**0.45**	0.1486	0.155	**0.96**
northdr2	0.270	0.3954	**0.68**	0.1486	0.119	**1.24**
northdr3	0.270	0.5705	**0.47**	0.1486	0.171	**0.87**
northdr4	0.270	0.0900	**3.00**	NA	NA	**NA**

Table 4.6: Scale Factors using Ordinate Method (15 and 20 storey)

	15 Storey Building			20 Storey Building		
GMRs	**S(g) Design**	**S(g) Field**	**SF**	**S(g) Design**	**S(g) Field**	**SF**
naver1	0.1051	0.069604	**1.51**	0.088	0.029	**3.03**
naver2	0.1051	0.03558	**2.95**	0.088	0.26712	**0.33**
naver3	0.1051	0.031148	**3.37**	0.088	0.03724	**2.36**
naver6	0.1051	0.032284	**3.26**	0.088	0.02576	**3.42**
naver7	0.1051	0.039968	**2.63**	0.088	0.06704	**1.31**
naver8	0.1051	0.05542	**1.90**	0.088	0.05716	**1.54**
naver9	0.1051	0.068432	**1.54**	0.088	0.04416	**1.99**
naver10	0.1051	0.085308	**1.23**	0.088	0.04428	**1.99**
naver13	0.1051	0.050864	**2.07**	0.088	0.02552	**3.45**
naver15	0.1051	0.023716	**4.43**	0.088	0.02288	**3.85**
kobejap3	0.1051	0.111036	**0.95**	0.088	0.05204	**1.69**
kobejap4	0.1051	0.055864	**1.88**	0.088	0.02464	**3.57**
northdr1	0.1051	0.055012	**1.91**	0.088	0.02852	**3.09**
northdr2	0.1051	0.07016	**1.50**	0.088	0.0354	**2.49**
northdr3	0.1051	0.064876	**1.62**	0.088	0.047992	**1.83**

Table 4.7: Scale Factors using Least Square Method (5 and 10 storey)

	5 Storey Building			10 Storey Building		
GMRs	**S(g) Design Spec**	**S(g) GMR Spec**	**SF**	**S(g) Design Spec**	**S(g) GMR Spec**	**SF**
naver1	0.70318	0.75583	**0.93**	0.7467	0.79673	**0.94**
naver2	0.70318	0.3693	**1.90**	0.7467	0.35705	**2.09**
naver3	0.70318	0.35356	**1.99**	0.7467	0.34086	**2.19**
naver6	0.70318	0.2676	**2.63**	0.7467	0.26213	**2.85**
naver7	0.70318	0.4288	**1.64**	0.7467	0.49056	**1.52**
naver8	0.70318	0.2823	**2.49**	0.7467	0.33742	**2.21**
naver9	0.70318	0.345	**2.04**	0.7467	0.36318	**2.06**
naver10	0.70318	0.3557	**1.98**	0.7467	0.37429	**1.99**
naver11	0.70318	0.15198	**4.63**	0.7467	0.13767	**5.42**
naver12	0.70318	0.17096	**4.11**	0.7467	0.15627	**4.78**
naver13	0.70318	0.43135	**1.63**	0.7467	0.43225	**1.73**
naver14	0.70318	0.27939	**2.52**	0.7467	0.26642	**2.80**
naver15	0.70318	0.22938	**3.07**	0.7467	0.22119	**3.38**
kobejap2	0.70318	0.15849	**4.44**	0.7467	0.17206	**4.34**
kobejap3	0.70318	2.21181	**0.32**	0.7467	2.0103	**0.37**
kobejap4	0.70318	0.92385	**0.76**	0.7467	0.9252	**0.81**
northdr1	0.70318	1.55988	**0.45**	0.7467	1.42684	**0.52**
northdr2	0.70318	1.0694	**0.66**	0.7467	0.98174	**0.76**
northdr3	0.70318	1.32772	**0.53**	0.7467	1.26662	**0.59**
northdr4	0.70318	0.21299	**3.30**	0.7467	0.20523	**3.64**

Table 4.8: Scale Factors using Least Square Method (15 and 20 storey)

	15 Storey Building			**20 Storey Building**		
GMRs	**S(g) Design Spec**	**S(g) GMR Spec**	**SF**	**S(g) Design Spec**	**S(g) GMR Spec**	**SF**
naver1	0.75733	0.68733	**1.10**	0.80887	0.57974	**1.40**
naver2	0.75733	0.33997	**2.23**	0.80887	0.3048	**2.65**
naver3	0.75733	0.32565	**2.33**	0.80887	0.28554	**2.83**
naver6	0.75733	0.25759	**2.94**	0.80887	0.22759	**3.55**
naver7	0.75733	0.55776	**1.36**	0.80887	0.53254	**1.52**
naver8	0.75733	0.3782	**2.00**	0.80887	0.37404	**2.16**
naver9	0.75733	0.37347	**2.03**	0.80887	0.33529	**2.41**
naver10	0.75733	0.39561	**1.91**	0.80887	0.378	**2.14**
naver13	0.75733	0.38812	**1.95**	0.80887	0.35815	**2.26**
naver14	0.75733	0.21712	**3.49**	0.80887	0.17459	**4.63**
naver15	0.75733	0.19663	**3.85**	0.80887	0.18815	**4.30**
kobejap3	0.75733	1.74361	**0.43**	0.80887	1.33105	**0.61**
kobejap4	0.75733	0.85218	**0.89**	0.80887	0.70161	**1.15**
northdr1	0.75733	1.14477	**0.66**	0.80887	0.90938	**0.89**
northdr2	0.75733	0.86556	**0.87**	0.80887	0.67825	**1.19**
northdr3	0.75733	1.09215	**0.69**	0.80887	0.86771	**0.93**
northdr4	0.75733	0.18547	**4.08**	0.80887	0.16002	**5.05**

Table 4.9: Scale Factor using Partial Area Method (5 and 10 storey)

Records	PADS	PARS	**SF**	PADS	PARS	**SF**
naver1	0.5078	0.5801	**0.88**	0.5387	0.5041	**1.07**
naver2	0.5078	0.2693	**1.89**	0.5387	0.2349	**2.29**
naver3	0.5078	0.2672	**1.90**	0.5387	0.2094	**2.57**
naver6	0.5078	0.1965	**2.58**	0.5387	0.1661	**3.24**
naver7	0.5078	0.3181	**1.60**	0.5387	0.3234	**1.67**
naver8	0.5078	0.2168	**2.34**	0.5387	0.2266	**2.38**
naver9	0.5078	0.2588	**1.96**	0.5387	0.2201	**2.45**
naver10	0.5078	0.2344	**2.17**	0.5387	0.2263	**2.38**
naver11	0.5078	0.1284	**3.96**	NA	NA	**NA**
naver12	0.5078	0.1284	**3.95**	0.5387	0.1151	**4.68**
naver13	0.5078	0.3095	**1.64**	0.5387	0.2745	**1.96**
naver14	0.5078	0.2158	**2.35**	0.5387	0.1538	**3.50**
naver15	0.5078	0.1636	**3.10**	0.5387	0.1293	**4.17**
kobejap1	0.5078	0.1040	**4.88**	NA	NA	**NA**
kobejap2	0.5078	0.1194	**4.25**	0.5387	0.1222	**4.41**
kobejap3	0.5078	1.7074	**0.30**	0.5387	1.3367	**0.40**
kobejap4	0.5078	0.7027	**0.72**	0.5387	0.6765	**0.80**
northdr1	0.5078	1.2699	**0.40**	0.5387	0.9380	**0.57**
northdr2	0.5078	0.7828	**0.65**	0.5387	0.6336	**0.85**
northdr3	0.5078	1.0297	**0.49**	0.5387	0.8565	**0.63**
northdr4	0.5078	0.1625	**3.12**	0.5387	0.1371	**3.93**

PADS – Partial area under the design spectrum, PARS – Partial area under the record spectrum

Table 4.10: Scale Factor using Partial Area Method (15 and 20 storey)

GMRs	PADS	PARS	**SF**	PADS	PARS	**SF**
naver1	0.4818	0.4238	**1.14**	0.4312	0.3750	**1.15**
naver2	0.4818	0.2134	**2.26**	0.4312	0.2006	**2.15**
naver3	0.4818	0.1791	**2.69**	0.4312	0.1772	**2.43**
naver6	0.4818	0.1593	**3.02**	0.4312	0.1423	**3.03**
naver7	0.4818	0.3679	**1.31**	0.4312	0.3556	**1.21**
naver8	0.4818	0.2350	**2.05**	0.4312	0.2528	**1.71**
naver9	0.4818	0.2090	**2.30**	0.4312	0.2304	**1.87**
naver10	0.4818	0.2683	**1.80**	0.4312	0.2729	**1.58**
naver12	0.4818	0.0861	**5.59**	0.4312	0.0496	**8.69**
naver13	0.4818	0.2664	**1.81**	0.4312	0.2381	**1.81**
naver14	0.4818	0.1287	**3.74**	0.4312	0.1115	**3.87**
naver15	0.4818	0.1326	**3.63**	0.4312	0.1338	**3.22**
kobejap1	0.4818	0.1094	**4.40**	0.4312	0.0821	**5.25**
kobejap2	0.4818	0.1094	**4.40**	0.4312	0.0821	**5.25**
kobejap3	0.4818	0.9604	**0.50**	0.4312	0.6718	**0.64**
kobejap4	0.4818	0.5422	**0.89**	0.4312	0.3749	**1.15**
northdr1	0.4818	0.6592	**0.73**	0.4312	0.4237	**1.02**
northdr2	0.4818	0.5151	**0.94**	0.4312	0.4037	**1.07**
northdr3	0.4818	0.6114	**0.79**	0.4312	0.4650	**0.93**
northdr4	0.4818	0.1102	**4.37**	0.4312	0.0843	**5.11**

PADS – Partial area under the design spectrum, PARS – Partial area under the record spectrum

Table 4.11: Scale Factors using PS_a Scaling

GMRs	S(g) Design Spec	S(g) GMR Spec	SF
naver1	0.967	0.8909	**1.09**
naver2	0.967	0.4430	**2.18**
naver3	0.967	0.4212	**2.30**
naver6	0.967	0.3501	**2.76**
naver7	0.967	0.5512	**1.75**
naver8	0.967	0.3802	**2.54**
naver9	0.967	0.4190	**2.31**
naver10	0.967	0.4457	**2.17**
naver12	0.967	0.2155	**4.49**
naver13	0.967	0.5272	**1.83**
naver14	0.967	0.3135	**3.09**
naver15	0.967	0.2692	**3.59**
kobejap3	0.967	2.4648	**0.39**
kobejap4	0.967	1.1017	**0.88**
northdr1	0.967	1.7930	**0.54**
northdr2	0.967	1.3123	**0.74**
northdr3	0.967	1.5093	**0.64**
northdr4	0.967	0.2473	**3.91**

Table 4.12: Scale Factors using ASCE-7 method (5 and 10 storey)

	5 Storey Building			10 Storey Building		
GMRs	**S(g) Design Spec**	**S(g) GMR Spec**	**SF**	**S(g) Design Spec**	**S(g) GMR Spec**	**SF**
naver1	0.70318	0.75583	**0.93**	0.7467	0.79673	**0.94**
naver2	0.70318	0.3693	**1.90**	0.7467	0.35705	**2.09**
naver3	0.70318	0.35356	**1.99**	0.7467	0.34086	**2.19**
naver6	0.70318	0.2676	**2.63**	0.7467	0.26213	**2.85**
naver7	0.70318	0.4288	**1.64**	0.7467	0.49056	**1.52**
naver8	0.70318	0.2823	**2.49**	0.7467	0.33742	**2.21**
naver9	0.70318	0.345	**2.04**	0.7467	0.36318	**2.06**
naver10	0.70318	0.3557	**1.98**	0.7467	0.37429	**1.99**
naver13	0.70318	0.43135	**1.63**	0.7467	0.43225	**1.73**
naver14	0.70318	0.27939	**2.52**	0.7467	0.26642	**2.80**
naver15	0.70318	0.22938	**3.07**	0.7467	0.22119	**3.38**
kobejap2	0.70318	0.15849	**4.44**	0.7467	0.17206	**4.34**
kobejap3	0.70318	2.21181	**0.32**	0.7467	2.0103	**0.37**
kobejap4	0.70318	0.92385	**0.76**	0.7467	0.9252	**0.81**
northdr1	0.70318	1.55988	**0.45**	0.7467	1.42684	**0.52**
northdr2	0.70318	1.0694	**0.66**	0.7467	0.98174	**0.76**
northdr3	0.70318	1.32772	**0.53**	0.7467	1.26662	**0.59**
northdr4	0.70318	0.21299	**3.30**	0.7467	0.20523	**3.64**

Table 4.13: Scale Factors using ASCE-7 method (15 and 20 storey)

	15 Storey Building			**20 Storey Building**		
GMRs	**S(g) Design Spec**	**S(g) GMR Spec**	**SF**	**S(g) Design Spec**	**S(g) GMR Spec**	**SF**
naver1	0.75733	0.68733	**1.10**	0.80887	0.57974	**1.40**
naver2	0.75733	0.33997	**2.23**	0.80887	0.3048	**2.65**
naver3	0.75733	0.32565	**2.33**	0.80887	0.28554	**2.83**
naver6	0.75733	0.25759	**2.94**	0.80887	0.22759	**3.55**
naver7	0.75733	0.55776	**1.36**	0.80887	0.53254	**1.52**
naver8	0.75733	0.3782	**2.00**	0.80887	0.37404	**2.16**
naver9	0.75733	0.37347	**2.03**	0.80887	0.33529	**2.41**
naver10	0.75733	0.39561	**1.91**	0.80887	0.378	**2.14**
naver13	0.75733	0.38812	**1.95**	0.80887	0.35815	**2.26**
naver14	0.75733	0.21712	**3.49**	0.80887	0.17459	**4.63**
naver15	0.75733	0.19663	**3.85**	0.80887	0.18815	**4.30**
kobejap3	0.75733	1.74361	**0.43**	0.80887	1.33105	**0.61**
kobejap4	0.75733	0.85218	**0.89**	0.80887	0.70161	**1.15**
northdr1	0.75733	1.14477	**0.66**	0.80887	0.90938	**0.89**
northdr2	0.75733	0.86556	**0.87**	0.80887	0.67825	**1.19**
northdr3	0.75733	1.09215	**0.69**	0.80887	0.86771	**0.93**

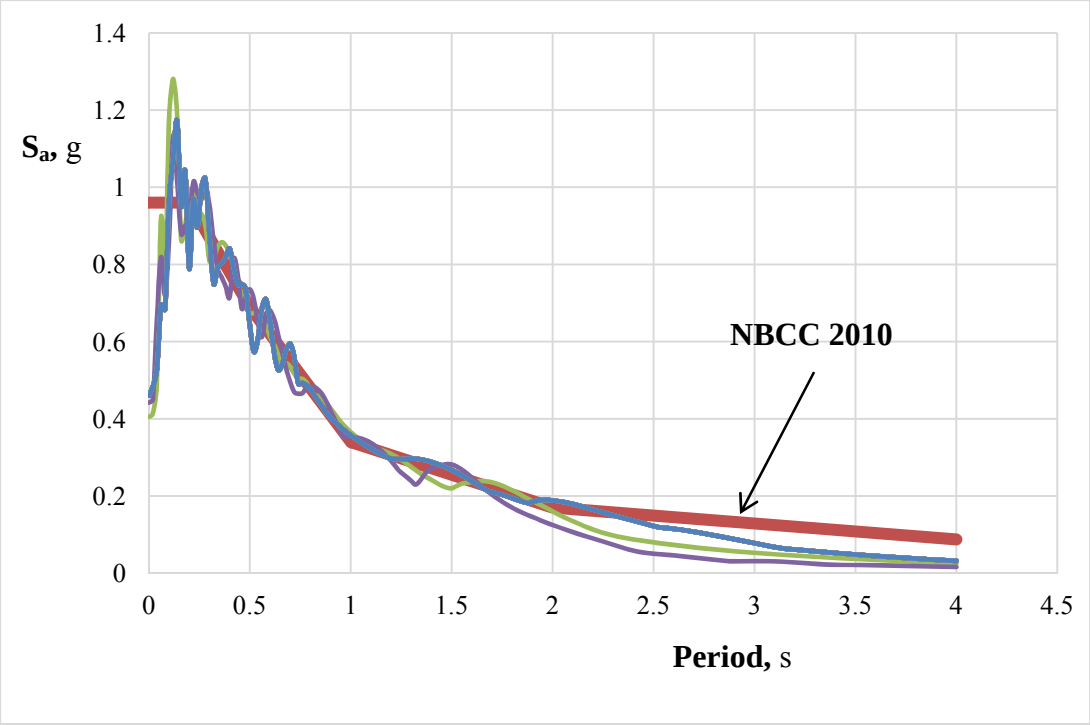

Fig 4.17 – Spectra of records matched with frequency matching with the Seismomatch software

4.5 Summary

This chapter provides a brief description of the more commonly known procedures for selecting earthquake ground motion records to use in the nonlinear dynamic time history analysis along with the familiar engineering parameters through which selection can be done through classification. The chapter also describes on how to implement different methods of scaling of GMR with explanatory sketches. The history of selecting earthquake records and the uncertainties one may across while selecting a suite of records for time history analysis is discussed. Further, the scale factors for each of the scaling methods have been tabulated.

Chapter 5

Static Pushover Analysis

5.1 Introduction

Static pushover analysis is a nonlinear analysis procedure in which structural deformations due to incrementally increased lateral forces are determined. Static lateral loads are applied using predetermined load magnitudes that represent approximately the relative inertia forces generated at the specific site. Strength displacement, deformation demands in the structure can be calculated at global, storey, and element levels through the pushover analysis. The pushover analysis is implemented in recent seismic guidelines for retrofitting of existing building structures [FEMA 273 (1997), ATC-40 (1996)]. Pushover analysis has been shown to provide a reliable and consistent estimate of the deformation response for structures that respond to hazards primarily in the first mode. The biggest advantage however, lies in its ability to provide information regarding yielding sequence and capacity of a structure. The DRAIN-2DX software has been used for analysis of plane two dimensional models of the frames. The pushover analysis has been performed using inverted triangular load distribution patterns for all frames. The base shears considered are the normalized base shear (Herrera et al 2003) and the base shear coefficient is defined as the ratio of the seismic base shear (V) to the weight (W) tributary to the frame of the building. Using the results from the pushover analysis a plot of base shear vs. roof displacement called the pushover curve (Akbas et al. 2003) is obtained. From the pushover curve one can estimate the capacity of the building and also trace the different stages of deformation like beam and column yielding.

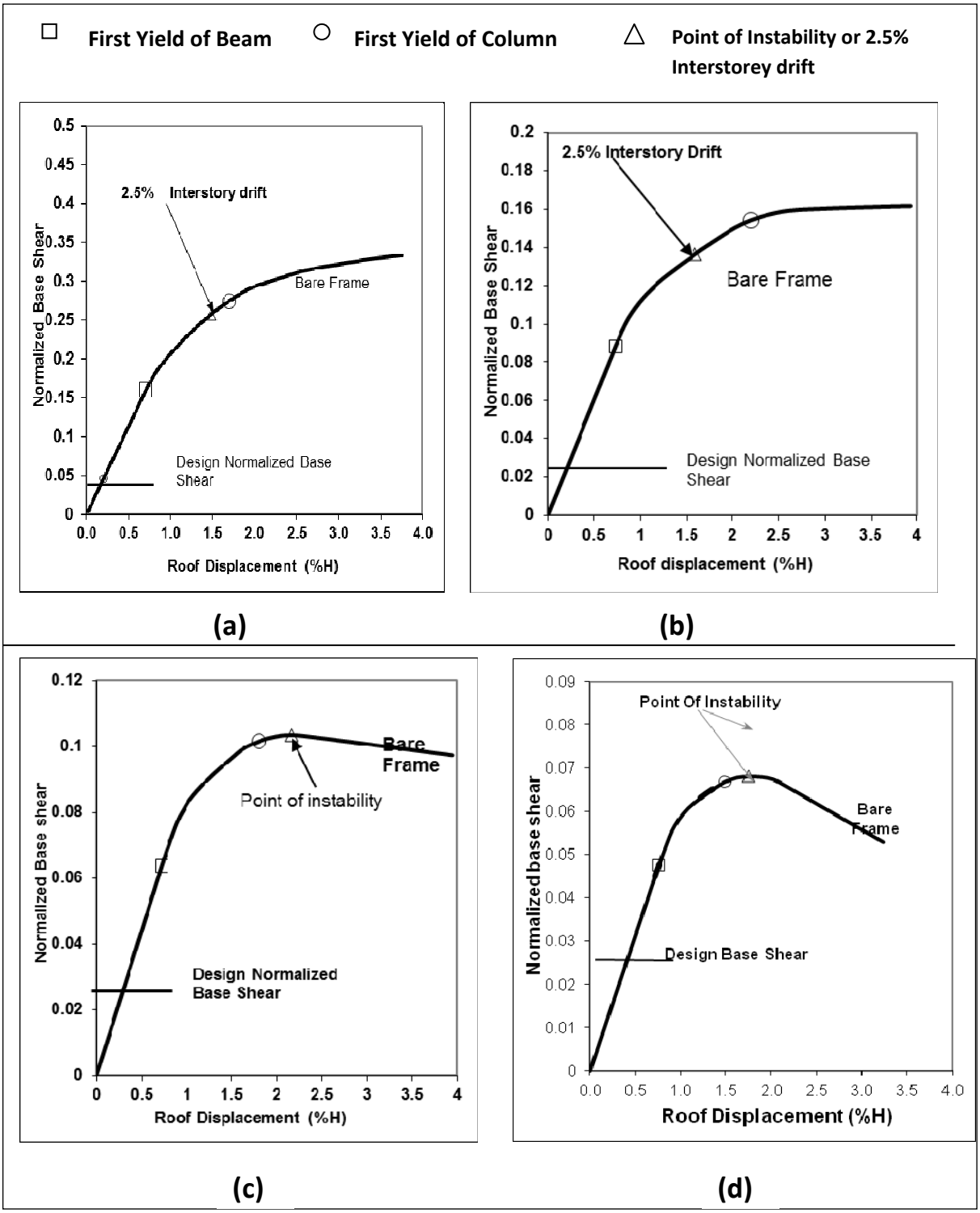

Figure 5.1 Pushover Curves for (a) 5 Storey SMRF (b) 10 Storey SMRF (c) 15 Storey SMRF (d) 20 Storey SMRF

The pushover graphs of different frames are shown in Figure 5.1. On the graph the point of first yielding of beam and column is shown along with the point of instability of the Steel Moment Resisting Frame.

The pushover analysis has been carried out by considering 5% strain hardening, P-Δ effect is considered in the analysis to account for large deformations and the second order effect. The point of instability has been marked on the pushover curve to indicate the point where the structure fails and the slope of the pushover graph tends to shift in the downward direction. In SMRFs that are found to be fail beyond the 2.5% interstorey drift, the point corresponding to 2.5% interstorey drift is marked on the graph as the point of failure. The capacity of the frames is calculated from the pushover graph by estimating the yield displacement due to seismic load. In the analysis the gravity load (D+0.5L) is applied corresponding to lateral load. The pushover curve for the 5, 10, 15, 20 storey frames are shown in the Figure 5.1.

The normalized design base shear of 5, 10, 15 and 20 storey buildings are found to be 0.042, 0.0253, 0.0255 and 0.0264. The numbering sequence of beam and column is shown in the Figure 3.1. The first yielding in the 5 storey frame starts from the beam no. 6 at a normalized base shear of 0.159, the first yielding of the column starts at the normalized base shear of 0.273 in column no.6 for bare frame. Plastic hinge formation in the 10 storey building occurs first at beam no.12 for normalized base shear of 0.0886 similarly the first yielding in a column occurs at normalized base shear of 0.154. In the 15 storey building the first yielding of beam occurs at normalized base shear 0.064 at beam no.19. and the column yielding occurs at a normalized base shear of 0.10 at column no.31. In the 20 storey frame building the first beam yielding occurs at the normalized base shear of 0.048 in beam no.23 and at 0.066 in column no.41. The summary of base shear and the displacements at the first beam and column yielding are given in Table 5.1.

The available capacity and the deformation demand are also calculated in the pushover analysis. The base shear, lateral roof displacement and the interstorey drifts at the point of instability are also determined as percentage of total height of building from the pushover analysis and presented. In the pushover analysis it has also been observed that the formation of plastic hinges occur in the beams first, and in the columns they occur at the lower storey, which satisfies the requirements of the capacity based seismic design.

Table 5.1 Base Shear Coefficient at the first beam and first column yielding

	First Beam Yielding		Fist Column Yielding	
SMRF Level	Base Shear Coefficient	Beam Index	Base Shear Coefficient	Column Index
5 Storey	0.159	No. 6	0.273	No. 6
10 Storey	0.0886	No.12	0.154	No. 11
15 Storey	0.064	No.19	0.074	No. 31
20 Storey	0.048	No.23	0.066	No. 41

The pushover curves presented in Figure 5.1 are idealized as bilinear curves to obtain the yield points of the building frames. The corresponding yield displacements and normalized base shear are given in Table 5.2. Table 5.3 shows the values of the base shear coefficient and corresponding roof displacement at failure.

Table 5.2 Design base shear and yield points of the SMRFs.

SMRF	Design base shear, KN	Normalized base shear at yield F_y/W	Yield displacement, D_y, in $\%H$
5 storey	178.8	0.22	0.75
10 storey	306.2	0.12	0.90
15 storey	366.4	0.09	1.00
20 storey	401.0	0.063	0.90

H=Height of the building.

Table 5.3 Displacement at failure (i.e., point of instability or 2.5% drift) of the frames.

SMRF	Normalized Base Shear, F_u/W	Roof Displacement, D_u in $\%H$	Interstorey Drift, d_u in $\%h$
5 Storey	0.275	1.495	2.50
10 Storey	0.145	1.690	2.50
15 Storey	0.105	2.095	2.42
20 Storey	0.065	1.750	2.35

H = height of the building, h= storey height

The roof displacement from the pushover analysis has also been observed for the parameter-Maximum (Mean (M) + Standard deviation (SD)) interstorey drift obtained from the time history analysis presented in the next chapter. Table 5.4 shows the values of roof displacement are used to compare the dynamic analysis and the static analysis.

Table 5.4: Roof displacement (% H) at Maximum M+SD of interstorey drift.

SMRF	Roof displacement (% H) (Dynamic)	Roof displacement (% H) (Pushover, at failure)
5 Storey	1.183	1.495
10 Storey	1.220	1.690
15 Storey	1.144	2.095
20 Storey	1.483	1.750

M=Mean value, SD=Standard deviation.

5.2 Performance estimation based on the Pushover Analysis

5.2.1 Capacity Demand Diagram Method

The concept of capacity spectrum method proposed by Freeman *et al.* (1975) was later developed and proposed by Chopra and Goel (1999) called as Capacity Demand Diagram method. This method involves transforming a multiple degrees of freedom (MDOF) system into an equivalent single degree of freedom (SDOF) system using a suitable factor which is determined based on the deformed modal shape, Φ. The first modal deformation shape has been used here as the deformed shape of the structure to develop the capacity diagram. The masses and the modal displacements from the first mode, Φ are tabulated for 20, 15, 10, and 5 storey frames as follows (Tables 5.5 through 5.8, respectively).

Table 5.5 Base shear distribution in 20 storey SMRF

Storey	**Height hi(m)**	**Weight (Wi, KN)**	**hiWi (KNm)**	**F (KN)**	**Mass (m)**	**Phi Φ**
20	74.20	590.87	43842.55	113.59	60.23	1.00
19	70.55	758.00	53476.86	28.20	77.27	0.99
18	66.90	758.00	50710.17	26.74	77.27	0.97
17	63.25	758.00	47943.47	25.28	77.27	0.95
16	59.60	758.00	45176.77	23.82	77.27	0.92
15	55.95	758.82	42456.15	22.39	77.35	0.89
14	52.30	759.65	39729.52	20.95	77.44	0.85
13	48.65	759.65	36956.81	19.49	77.44	0.81
12	45.00	759.65	34184.10	18.02	77.44	0.76
11	41.35	759.65	31411.39	16.56	77.44	0.71
10	37.70	762.37	28741.30	15.15	77.71	0.66
9	34.05	765.09	26051.34	13.74	77.99	0.60
8	30.40	765.09	23258.76	12.26	77.99	0.53
7	26.75	765.09	20466.18	10.79	77.99	0.47
6	23.10	765.09	17673.60	9.32	77.99	0.40
5	19.45	767.13	14920.71	7.87	78.20	0.33
4	15.80	769.17	12152.93	6.41	78.41	0.26
3	12.15	769.17	9345.45	4.93	78.41	0.19
2	8.50	769.17	6537.97	3.45	78.41	0.12
1	4.85	786.73	3815.62	2.01	80.20	0.06
Sum		**15104.39**	**588851.63**	**400.96**	**1539.69**	

Table 5.6 Base shear distribution in 15 storey SMRF

Storey	**Height hi(m)**	**Weight (Wi, KN)**	**hiWi (KNm)**	**F (KN)**	**Mass (m)**	**Phi Φ**
15	55.95	742.96	41568.74	83.20	75.73	1
14	52.3	759.51	39722.11	36.89	77.42	0.934763
13	48.65	759.51	36949.92	34.31	77.42	0.869526
12	45	759.51	34177.72	31.74	77.42	0.80429
11	41.35	759.51	31405.53	29.16	77.42	0.739053
10	37.7	761.40	28704.85	26.65	77.61	0.673816
9	34.05	763.30	25990.33	24.13	77.81	0.608579
8	30.4	763.30	23204.29	21.55	77.81	0.543342
7	26.75	763.30	20418.24	18.96	77.81	0.478105
6	23.1	763. 30	17632.20	16.37	77.81	0.412869
5	19.45	766.23	14903.29	13.84	78.11	0.347632
4	15.8	769.17	12152.93	11.28	78.41	0.282395
3	12.15	769.17	9345.45	8.68	78.41	0.217158
2	8.5	769.17	6537.97	6.07	78.41	0.151921
1	4.85	784.81	3806.32	3.53	80.00	0.086685
Sum		**11454.14**	**346519.90**	**366.38**	**1167.60**	

Table 5.7 Base shear distribution in 10 storey SMRF

Storey	Height hi(m)	Weight (Wi, KN)	hiWi (KNm)	F (KN)	Mass (m)	Phi Φ
10	37.7	727.54	27428.19	75.73	74.16	1
9	34.05	747.03	25436.33	44.53	76.15	0.903183
8	30.4	747.03	22709.67	39.75	76.15	0.806366
7	26.75	747.03	19983.02	34.98	76.15	0.709549
6	23.1	747.03	17256.36	30.21	76.15	0.612732
5	19.45	755.53	14695.01	25.72	77.02	0.515915
4	15.8	764.03	12071.61	21.13	77.88	0.419098
3	12.15	764.03	9282.92	16.25	77.88	0.322281
2	8.5	764.03	6494.22	11.37	77.88	0.225464
1	4.85	764.71	3708.83	6.49	77.95	0.128647
Sum		**7527.97**	**159066.20**	**306.16**	**767.38**	

Table 5.8 Base shear distribution in 5 storey SMRF

Storey	Height hi(m)	Weight (Wi, KN)	hiWi (KNm)	F (KN)	Mass (m)	Phi Φ
5	19.45	583.95	11357.81	55.28	59.53	1
4	15.8	747.22	11806.05	47.21	76.17	0.812339
3	12.15	747.22	9078.71	36.31	76.17	0.624679
2	8.5	747.22	6351.36	25.40	76.17	0.437018
1	4.85	754.66	3660.08	14.64	76.93	0.249357
Total		**3580.26**	**42254.01**	**178.83**	**364.96**	

To transform MDOF to a SDOF system, the transformation factor Γ is applied and given by the below formulae (Chopra and Goel, 1999)

$$m^* = \sum m_i \Phi_i \quad \text{.....5.1}$$

$$\Gamma = \frac{m^*}{\sum m_i \Phi_i^2} \quad \text{..... 5.2}$$

where m_i is the mass of ith storey, m^* is the mass of the equivalent single-degree-of –freedom system, Φ_i is the assumed displacement at the ith storey and Γ is the transformation factor applied to transform the multi-degree-of-freedom system to the corresponding SDOF system. The transformation factor and the mass m^* for the different frames are tabulated below

Table 5.9 - Values of Γ and m^* of SMRF

SMRF	$\boldsymbol{\Gamma}$	$\boldsymbol{m^*}$
20 Storey	1.306	950.0
15 Storey	1.454	631.3
10 Storey	1.432	430.1
5 Storey	1.394	221.5

The pushover analysis has been done according to code by applying an inverted triangular force distribution in which the total equivalent earthquake force has been considered. The hazard spectra considered if taken from NBCC 2010 and has been used as design spectra to determine demand diagram The pushover curve from the MDOF system is idealized in a bilinear form, which is then converted to the capacity curve of the equivalent SDOF system by dividing the roof displacement at yield by the transformation factor, Γ, and the yield base shear by the equivalent mass, *m**. Based on the data provided in Tables 5.2, 5.3 and 5.9, the yield and ultimate base shear and displacement values of the equivalent SDOF system for each building are computed and presented in A-D (Acceleration-Displacement) format in Table 5.10.

Table 5.10 - Yield and ultimate base shear and displacement values of the equivalent SDOF systems in A-D format using the CDD method

SMRF	S_{ay}^*, g	D_y^*, mm	S_{au}^*, g	D_u^*, mm	Ductility (μ)
20 Storey	0.102	499	0.105	970	1.94
15 Storey	0.166	498	0.194	1046	2.10
10 Storey	0.214	455	0.259	854	1.88
5 Storey	0.363	390	0.453	779	2.00

The hazard spectra conceived in NBCC (2010) has been further used to determine the demand curve in A-D format, given by the following equation

$$D = \frac{\mu}{R_y}\left(\frac{T_n}{2\pi}\right)^2 A \quad \text{(Fajfar 2000)} \qquad \ldots\ldots\ldots\ldots\ldots\ldots\ldots\ldots\ 5.6$$

Where D is the roof displacement, μ is the ductility, R_y ductility reduction factor, T_n is the period of vibration and A is the spectral acceleration. For Krawinkler and Nasser proposed R_y-μ-T_n relation the following Equations are used.

$$R_y = \left[C(\mu - 1) + 1\right]^{1/C} \quad \text{(Chopra and Goel 1999)} \ldots\ldots\ldots\ldots\ldots\ldots\ 5.7$$

R_y ductility reduction factor, μ is the ductility capacity and C is a constant as described in the Equation 5.8.

$$C(T_n, \alpha) = \frac{T_n^a}{1 + T_n^a} + \frac{b}{T_n} \quad \text{(Chopra and Goel 1999)} \ldots\ldots\ldots\ldots\ldots\ 5.8$$

where b and α are constant of the material property, T_n is the period of vibration in sec.

A number of R-μ-T relations are readily available in the literature given by, Newmark and Hall (1982); Krawinkler and Nassar (1992); Vidic et al. (1994); and Miranda and Bertero (1994). Figure 10 shows the demand spectra constructed using different R-μ-T for the four different building frames and it is noted to produce similar demand spectra.

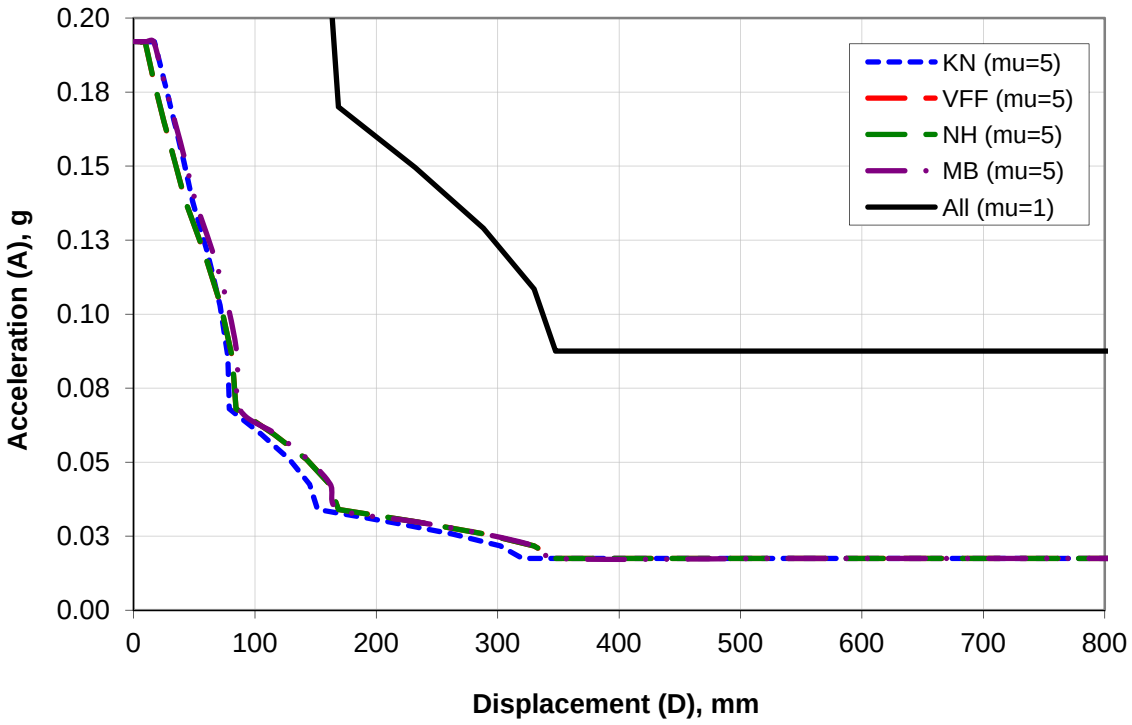

Figure 5.2. Seismic demand curves using different R-μ-T relations (KN = Krawinkler and Naser (1992);VFF = Vidic *et al.* (1994); and NH = Newmark and Hall (1982))

For the application of the CDD method, the Capacity Curve (CC) of the equivalent SDOF system of a building frame is plotted using the data given Table 5.10 and overlaid with the Demand Curves (DC) generated using Equation 5.8 or other methods as shown in Figure 5.2. The Capacity-Demand diagrams developed for different building frames are shown in Figure 5.3 through 5.6.

Figure 5.3 shows the capacity-demand diagram of the SDOF system diagram for the twenty-storey building where the capacity curve CC1 is overlaid with the demand curve for different values of ductility μ (mu). From the intersection of capacity diagram and the elastic demand diagram as indicated by Point 1 in Figure 5.3, the displacement demand to the SDOF system is found to be 450 mm. For the corresponding MDOF system, the displacement demand is estimated to be (450*1·306) or 588 mm (0·79% of the building height). Assuming an average

ratio of storey drift to roof drift to be 1·6 as suggested by Gupta and Krawinkler (2000), the maximum interstorey drift demand can be estimated to be 1·27%, which is somewhat lower than the mean interstorey drift obtained from the dynamic time history analysis (about 1·6 to 1·7% depending on the method of scaling). Considering the Vision 2000 Committee prescribed level of performance (SEAOC, 1995), the CDD method indicates the achievement of the LS (Life Safety) performance of the structure, which is consistent with the dynamic analysis presented earlier.

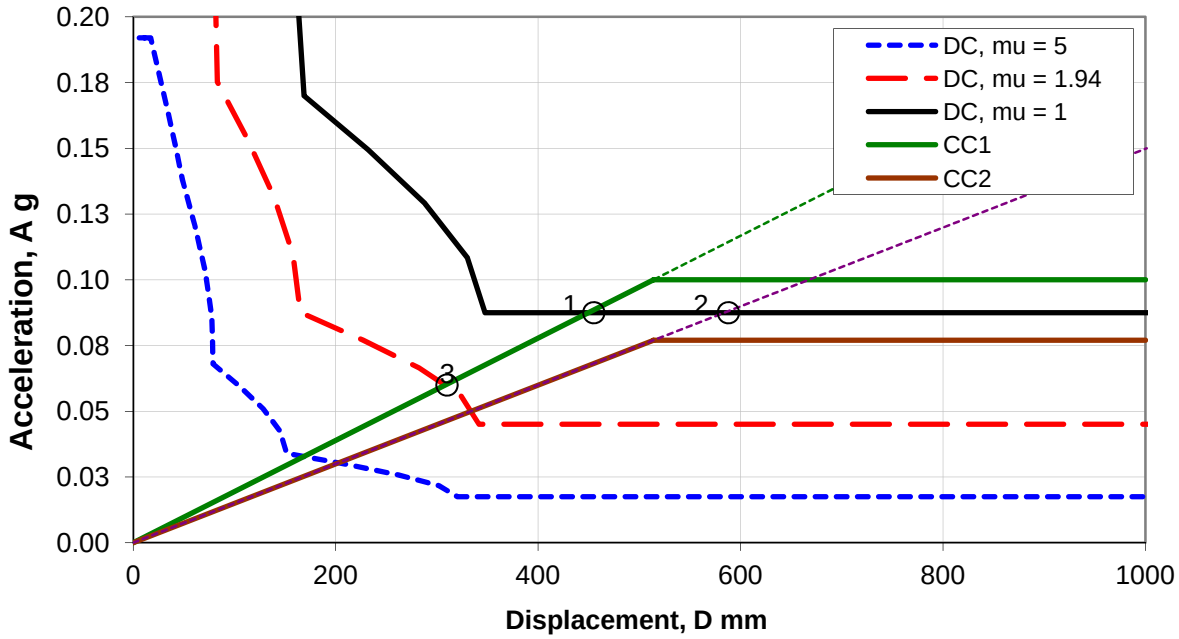

Figure 5.3. Application of the CDD, N2 and DBSD methods (20 storey building)

For the 15, 10 and 5 storey buildings the CDD plots are shown in Figures 5.4, 5.5 and 5.6, respectively. From the intersection of the capacity curve CC1 and the elastic demand curve (DC-mu=1) as indicated by Point 1 in each of the above figures, the SDOF demand and the corresponding MDOF demand for each building have been obtained the same ways as described above in the context of the twenty storey building. The results have been summarized in Table

5.11 which indicates that the estimated interstorey drift demand in each building is within 2.5% as required by NBCC 2010.

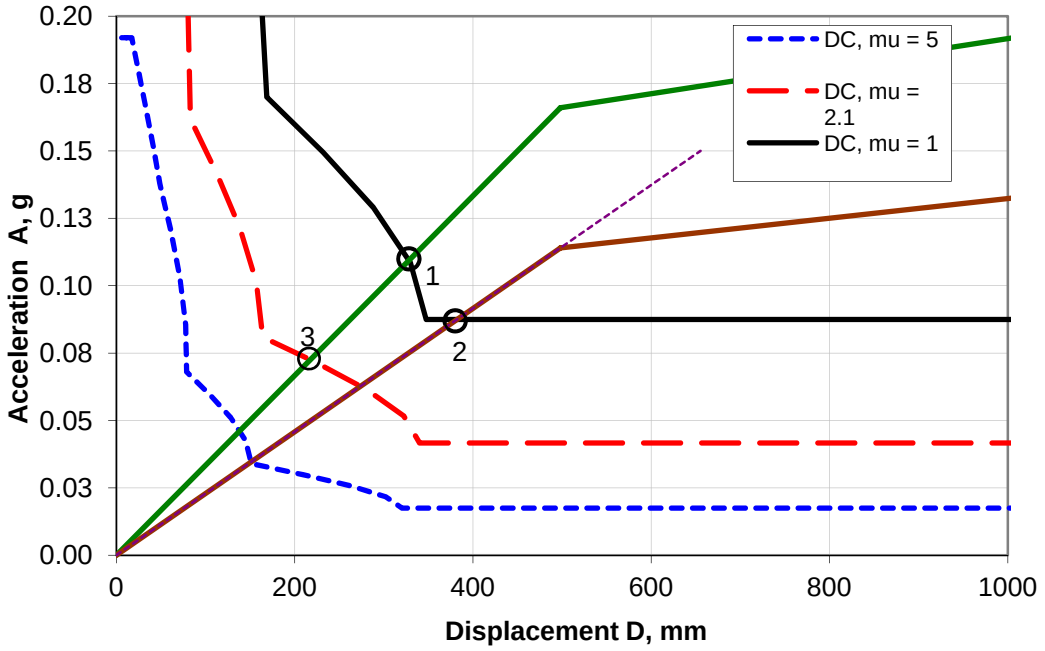

Figure 5.4 Application of the CDD, N2 and DBSD methods (15 storey building)

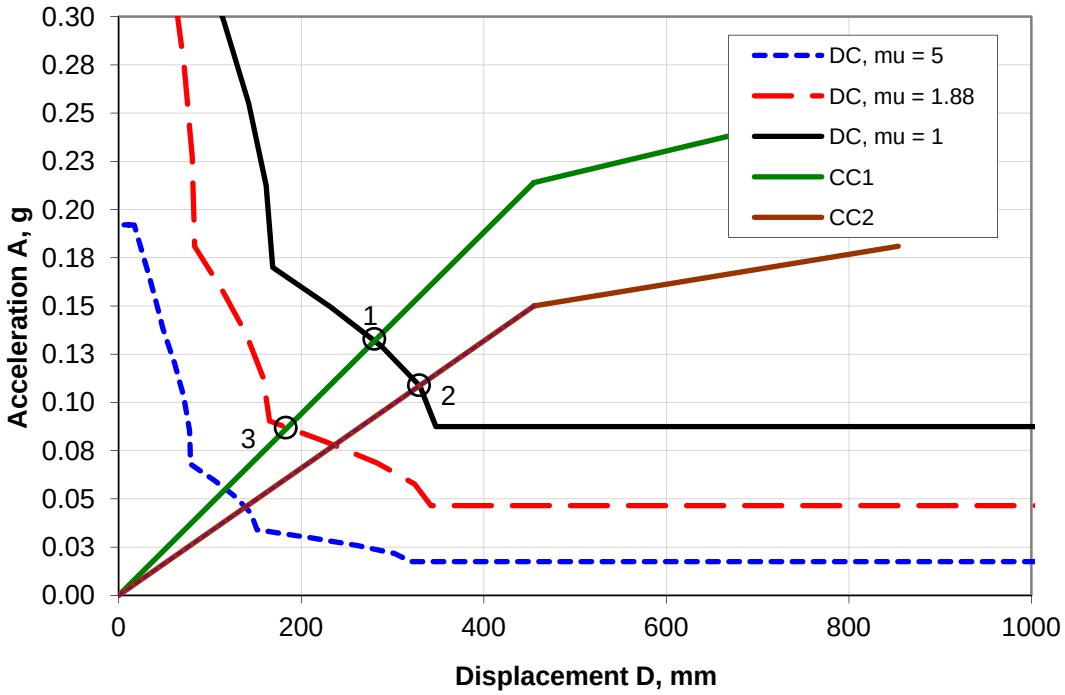

Figure 5.5 Application of the CDD, N2 and DBSD methods (10 storey building)

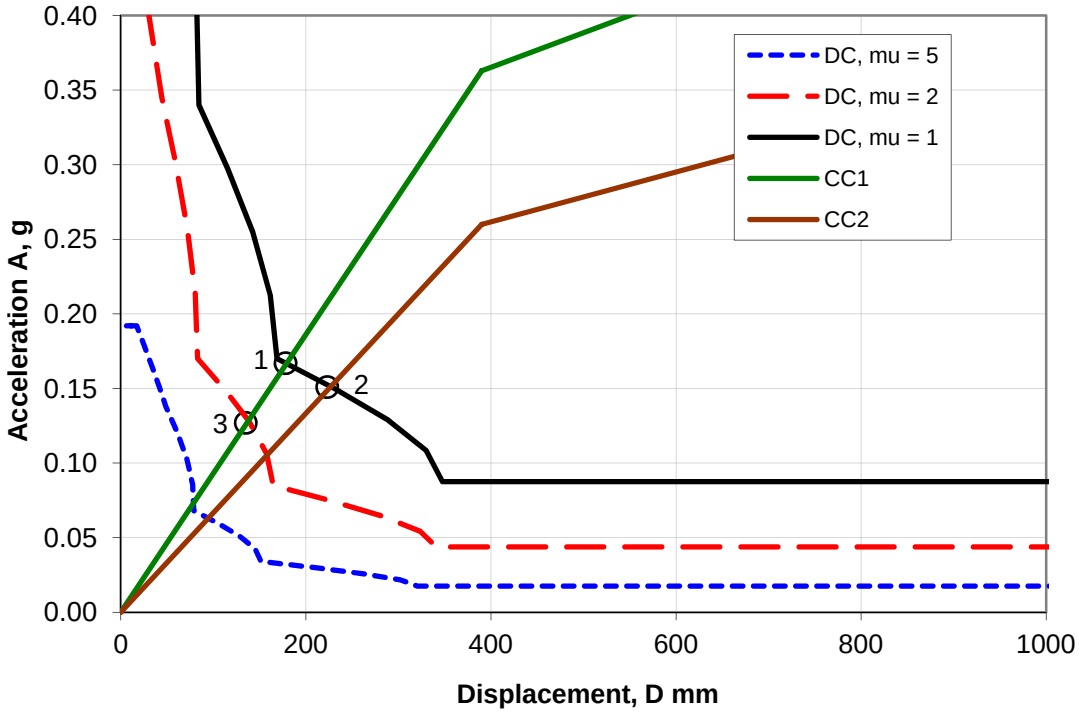

Figure 5.6. Application of the CDD, N2 and DBSD methods (5 storey building)

Table 5.11 - The SDOF and MDOF demand using the CDD method

SMRF	SDOF Displacement, mm	MDOF Displacement, mm	Roof Drift, %H	Estimated Interstorey Drift, %h
20 Storey	450	588	0.79	1.27
15 Storey	328	477	0.85	1.36
10 Storey	280	401	1.06	1.70
5 Storey	178	248	1.28	2.04

5.2.2 N2 Method

The N2 method was proposed by Fajfar (2000) which is known to be an extension of the capacity-demand diagram method. The capacity diagram is constructed the same way as described in the earlier section, however, in this method the yield base shear is divided by the factor $m^*\Gamma$, instead of m^*. The elastic period, T^* of the idealized bilinear system is given by the equation (5) (Fajfar, 2000).

$$T^* = 2\pi\sqrt{\frac{m^* D_y^*}{F_y}} \quad \text{(Fajfar, 2000)} \ldots\ldots\ldots\ldots\ldots\ldots\ldots\ldots\ldots\ldots\ldots\ldots$$

Based on the above description, the yield and ultimate shear, and the elastic period of the equivalent SDOF structures have calculated and shown in Table 5.12.

Table 5.12 - Yield and ultimate base shear in acceleration format and the elastic period of the equivalent SDOF using the N2 method

SMRF	S_{ay}^*, g	S_{au}^*, g	T^*, s
20 Storey	0.078	0.081	4.51
15 Storey	0.114	0.134	3.47
10 Storey	0.150	0.181	2.92
5 Storey	0.260	0.325	2.08

The capacity curve for the equivalent SDOF system using the N2 method has been shown by CC2 in Figure 5.3. The acceleration at the yield point (S_{ay}) is determined to be 0·078 *g*. As the capacity curve CC2 does not intersect the elastic demand curve, the intersection of the line following the slope of the capacity curve with the demand curve as indicated by Point 2 in Figure 5.3, is considered for estimating the elastic acceleration (S_{ae}), which is found to be 0·088 *g*. The

corresponding elastic displacement (S_{de}) is found to be 590 mm. The ductility reduction factor for the structure is given by ($R_\mu = S_{ae} / S_{ay}$) which equals to 1·14. The elastic period of system (T^* = 4·51 s as shown in Table 5.11) is greater than the critical period, Tc = 0·2 s which further supports the ductility value of R_μ = 1·14. In the case of $T^* > Tc$, the elastic displacement and the inelastic displacement is considered equal, i.e. $S_a = S_{ae}$ (Fajfar, 2000). Therefore, the inelastic displacement demand of SDOF system is 590 mm. Hence, the inelastic displacement demand of the MDOF system is (590*1·306) or 771 mm (1·04% of building height), and the ultimate displacement of the building is about 874 mm (1·18% of building height). The ductility demand of the structure determined here is less than the ductility capacity of 1·94 as indicated in Table 5.10. Therefore, the system has adequate ductility and the design is said to be satisfactory.

For the 15, 10 and 5 storey buildings the N2 Capacity curves are shown and CC2 in Figures 5.4, 5.5 and 5.6, respectively. From the intersection of the capacity curve CC2 and the elastic demand curve (DC-mu=1) as indicated by Point 2, the elastic acceleration and the corresponding displacements are determined. In each of the above figures (Figs. 5.4-5.6), the capacity curve CC2 intersects the elastic demand curve before the yield point is reached. Therefore, the ductility reduction factor R_μ in these cases is considered to be 1. Also, the elastic period in each case is larger than the critical period of 0.2 s as in the case of the twenty storey building. In that case, the inelastic demand is assumed to be the same as the elastic demand as recommended in Fajfar (2000). A summary of the SDOF and MDOF demands is given in Table 5.13. The ductility demand of the structures determined here is less than their ductility capacities as indicated in Table 5.10. Therefore, the systems are deemed to have adequate ductility and the design is considered satisfactory.

Table 5.13 - The SDOF and MDOF demand using the N2 method

SMRF	SDOF Displacement, mm	MDOF Displacement, mm	Roof Drift, %H	R_μ
20 Storey	590	771	1.04	1.14
15 Storey	380	553	0.99	1.0
10 Storey	329	471	1.25	1.0
5 Storey	223	311	1.60	1.0

5.2.3 DBSD Method

This method is proposed by Humar and Ghorbanie-Asl (2005). The preliminary target roof displacement is checked against the following limits

a. Maximum roof displacement permissible as per code provisions
b. Roof displacement magnitude at the P-Δ instability limit in pushover analysis.
c. Roof displacement at which the element's ductility demand exceeds its ductility strength.

The design of the structure is done normally by computing the base shear of the multi-degree-of-freedom (MDOF) system and is then transformed to SDOF by using a modification factor.

The steps followed in this design method are as follows:

- Step-I. Compute the ductility strength (μ) from the initial yield displacement and the ultimate displacement. If the ductility capacity recommended by the code is lower than the calculated one than the code permitted, design is OK.
- Step-II. Compute the ultimate displacement of SDOF *(δ_u)*.
- Step-III. Construct the inelastic spectrum for ductility of μ along with the acceleration-displacement *(A-D)* of the spectrum using Equations 5.6 to 5.8.
- **Step-IV.** Determine the inelastic acceleration from the A-D spectrum for equivalent ultimate displacement *(δ_u)* and compute the design base shear from the inelastic acceleration obtained from the A-D spectrum. The design base shear is obtained using Equation 5.9 (Humar and Ghorbaine-Asl., 2005).

$$V = \frac{A_y m^*}{R_0} \quad \ldots\ldots\ldots\ldots\ldots\ldots \qquad 5.9$$

Wherein m^* is the mass of equivalent SDOF system given by dividing the mass of multi-degree-of-freedom system by a modification factor Γ as given by Equation 5.2, R_0 is the over strength related force reduction factor taken as 1·5 for the steel moment resisting frame according to NBCC (2010); and *Ay* is the spectral acceleration.

- **Step-V.** Design the structure for the base shear calculated in Step-IV using the procedure provided in the code (i.e., NBCC 2010).

- **Step-VI.** Perform the Static Pushover analysis on the designed structure to obtain a refined value of the yield and ultimate displacements. Repeat Steps I to V until the design base shear is acceptable.

The preliminary design of the building frames has been initially carried using the NBCC 2010 code based procedure, and the pushover curves are plotted for the buildings (Figure 5.1). The design base shear for each building computed as per code procedures is given in Table 5.2 .The yield and ultimate displacements provided in Table 5.2 and 5.3, respectively. The ductility capacity of each building as given in Table 5.10 are found to be lower than the code permitted ductility for a fully ductile moment resisting frame which is 5. Hence the computed ductility capacity as given in Table 5.10 is used in the design. The transformation factor Γ for each building is provided in Table 5.9 which is utilized for calculating the yield (d_y) and ultimate displacements (d_u) of the SDOF systems as listed in Table 5.10. The inelastic demand curve for the obtained for the corresponding ductility for each building as shown in Figures 5.3 through 5.6, in which the intersection of the inelastic demand curve and the capacity curve CC1 at Point 3 indicates the inelastic demand acceleration (A) and corresponding displacement demand. The revised design base shear is obtained using Equation 5.9 and listed in Table 5.14.

Table 5.14 - Estimation of the design base shear using the DBSD method

SMRF	A_y, g	m^*, t	V_y, KN	V_d, KN
20 Storey	0.060	950.0	372.8	401.0
15 Storey	0.073	631.3	301.4	366.4
10 Storey	0.087	430.1	244.7	306.2
5 Storey	0.127	221.5	183.9	178.8

It is found from Table 5.14 that the base shear estimated using the DBSD method is lower than that used in the equivalent static load-based design and hence the code-based static design procedure is satisfactory, yet conservative, in all cases except the five storey building. In the case

of the five storey building, V_y as determined from the DBSD method is less than 3% higher than the original design base shear V_d, and thus the original design is still satisfactory.

5.2.4 Yield Point Spectra Method (Aschheim, 2004)

Yield point Spectra (YPS) method is a direct and simplified method of Capacity Spectrum method, it is found to be useful when the performance objectives are specified in terms of ductility and peak displacement of structure, in such a scenario this method can be easily used to predict the performance of the structure. In this method a graphical procedure is followed to evaluate the performance of the structure which is a plot of base shear verses yield displacement. The yield point is constituted by the yield strength (F_y) and yield displacement (D_y). The following Equations (Eq. 5.10 and 5.11) are used to determine the yield point spectra.

$$D_y = \mu\left(\frac{T}{2\pi}\right)^2 S_a \quad \text{(Aschheim 2004)} \quad \ldots\ldots\ldots\ldots\ldots\ldots\ldots\ldots\ldots\ldots 5.10$$

$$S_a = \frac{S_{ae}}{R_\mu} \quad \text{(Fajfar 2000)} \quad \ldots\ldots\ldots\ldots\ldots\ldots\ldots\ldots\ldots\ldots\ldots\ldots\ldots\ldots\ldots 5.11$$

Wherein S_a is the inelastic spectral acceleration, S_{ae} is the elastic spectral acceleration, μ is the ductility capacity of the structure, R_μ is the ductility reduction coefficient, T is the period of vibration and D_y is the yield displacement. In the above equations the R-μ-T relationship proposed by Miranda and Bertero (1994) has been used. Equation 5.12 is applied to compute the value of R_μ.

$$R_\mu = \mu + (1-\mu)\exp\left(\frac{-16T}{\mu}\right) \quad \ldots\ldots\ldots 5.12$$

In the above equation μ is the ductility capacity of the structure, R_μ is the ductility reduction coefficient, T is the period of vibration.

YPS method can also be used to obtain the vibration properties for the target displacement and the ductility demands whereas other PBSD methods can only be used to determine the displacement properties from the given vibration data.

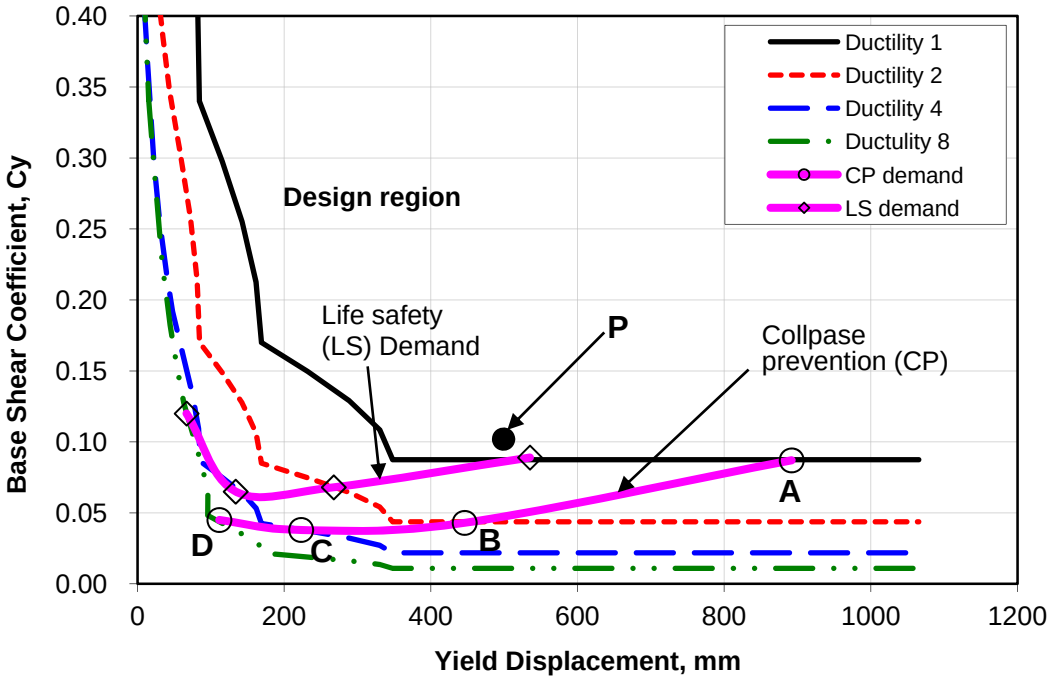

Fig 5.7 Yield point spectrum of NBCC 2010 response spectrum for Vancouver (20 storey building)

Figure 5.7 shows the application of the YPS procedure to the 20-storey building frame. The seismic hazard spectra for Vancouver as provided in NBCC (2010) are applied to obtain the yield point spectra for different values of ductility in (Figure 5.7). In order to predict the performance of the structure using the yield point spectra, the following two performance objectives are considered: (a) Collapse Prevention as per Vision 2000 Committee (SEAOC, 1995) recommendation and NBCC (2010) requirement of 2·5% interstorey drift and (b) Life

Safety objective based on Vision 2000 Committee's (SEAOC, 1995) recommendation of 1·5% interstorey drift. Correspondingly, the CP level of performance indicated by the performance demand curve ABCD in Figure 5.7 has been plotted. Gupta and Krawinkler (2000) stated that the storey drift to roof drift ratio for low to medium rise building varies between 1·2- 2·0. Considering the average value of 1·60, the roof displacement corresponding to an interstorey drift of 2·5% is computed to be 1159 mm, Under the first modal displacement vector the transformation factor for SDOF is 1·306. Hence, the maximum roof displacement of the SDOF structure is worked out as 1159/1·306 or 887 mm. therefore Point A in the graph corresponds to an elastic yield displacement of 887 mm, point B on the YPS represents a ductility of value 2 and yield displacement of 887/2 or 444 mm, point C on the YPS represents a ductility 4 and an yield displacement of 887/4 or 222 mm, and point D corresponds to a yield displacement of 887/8 111 mm with ductility factor of 8. Similarly, the LS performance demand curve is constructed in the similar fashion (Figure 5.7) to represent a interstorey drift of 1·5% which corresponds to a roof displacement of 535 mm. The base shear coefficient and roof displacement at yield for the equivalent SDOF systems are found to be 0·102 and 499 mm, respectively, as represented by the point P in Figure 5.7. As point P lies above both LS and CP levels of performance demand curve, the design satisfies both of these levels of performance objectives.

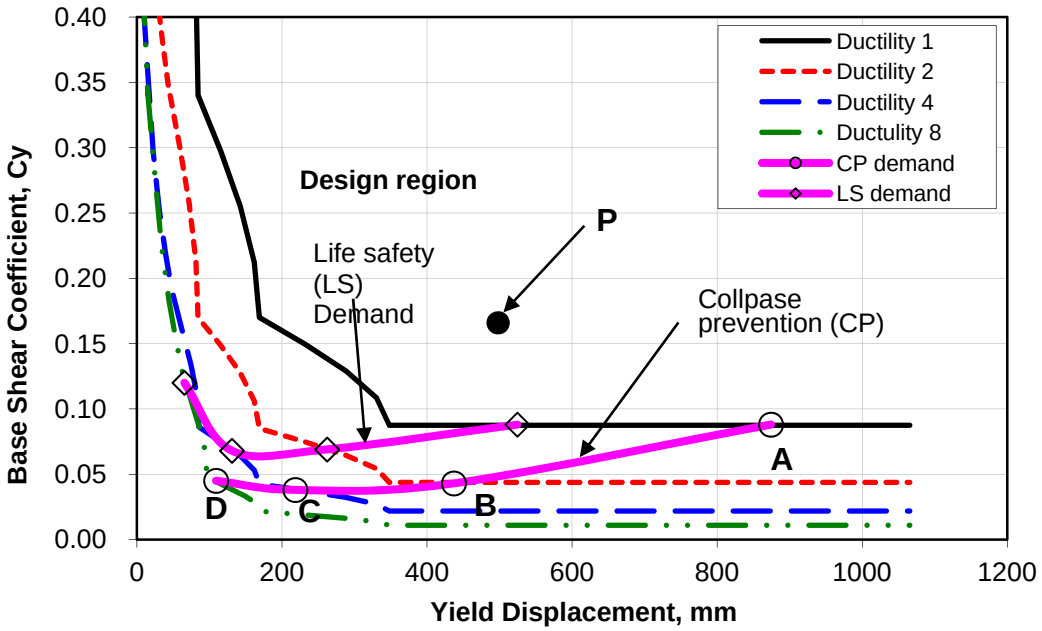

Fig 5.8 Yield point spectrum of NBCC 2010 response spectrum for Vancouver (15 storey building)

Figure 5.8 shows the plot of YPS for the 15 storey building in which the Collapse Prevention curve and the Life safety demand curves have been further plotted for the corresponding displacement values of 874 mm and 525 mm, respectively. As before, Point P indicating the yield capacity lies above both LS and CP levels of performance demand curve.

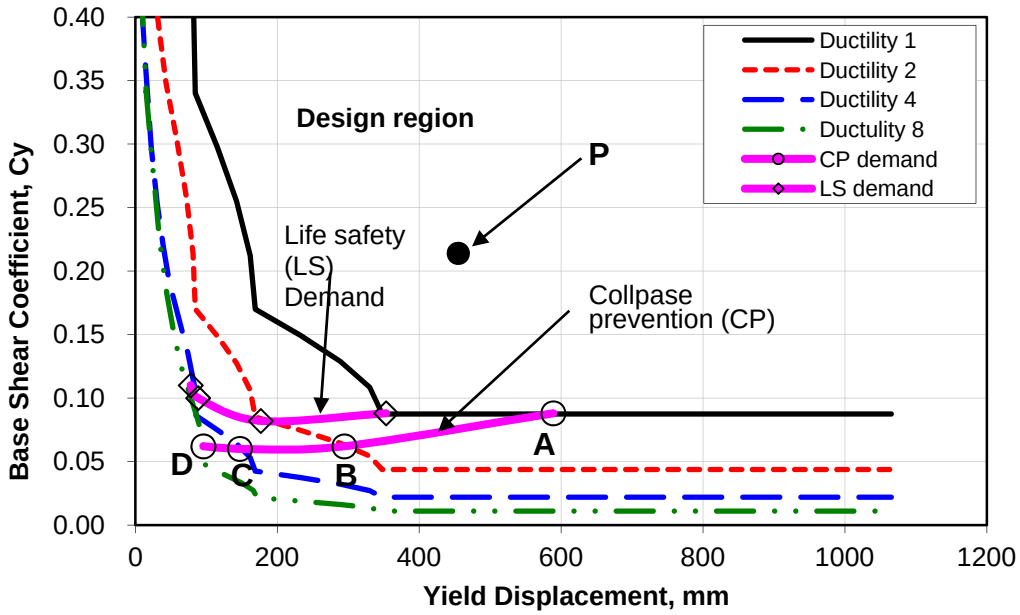

Fig 5.9 Yield point spectrum of NBCC 2010 response spectrum for Vancouver (10 storey building)

Figure 5.9 shows the plot of YPS for the 10 storey building in which the collapse prevention curve and the Life safety demand curve have been plotted for the corresponding displacement values of 589 mm and 353 mm, respectively. In this case, Point P indicating the yield capacity lies well above both LS and CP levels of performance demand curve.

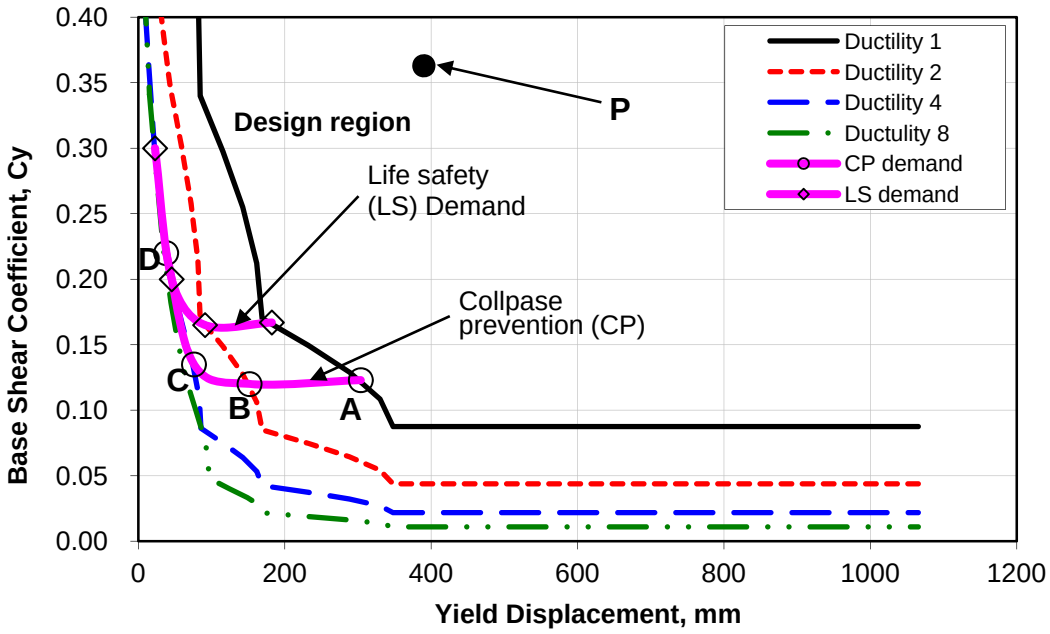

Fig 5.10 Yield point spectrum of NBCC 2005 response spectrum for Vancouver (5 storey building)

Figure 5.10 shows the plot of YPS for the 5 storey building in which the yield point spectra for the collapse prevention curve and the Life safety demand curves have been plotted for the corresponding displacement values of 304 mm and 182 mm, respectively. Here the yield capacity point (Point P) lies high above the CP and LS demand curves indicating a conservative design.

5.3 Summary

The static pushover analysis performed and the corresponding capacity curves have been obtained and interpreted with commonly known performance-based design methods. It is noted that all the methods are considered here confirm that the existing design based on the code procedure is adequate and many a times it is conservative. The pushover curves are also compared to the results obtained from the Time history analysis to determine the performance

achievements of the buildings. The pushover curves indicate that buildings fail to achieve the desired ductility in case of a real life scenario. Among different PBSD methods considered here to test the adequacy of the code-based design of the buildings for achieving different levels of performance, only the BDSD method is found to provide a direct estimation of modified forces to be used the refinement of the design. The other methods are helpful in comparing the displacement demand to capacity for a given level of performance objective. While there differences in the ways how the existing PBSD methods such as those considered here work, there is one common aspect in them, that is, they all require an MDOF structure to be converted to an equivalent SDOF structure by using a transformation technique. Also, they produce consistent results for buildings considered here.

Chapter 6

Non-linear Time-history Analysis

6.1 History

The basic performance objective of a designed structure under structural engineering practice was widely accepted as to provide adequate life-safety while keeping the construction cost economical. However, structures designed for critical facilities, like nuclear plants, manufacturing units and major business operations for which an interruption in operation or damage to the facility might result in severe socio-economic problems impacting the society at large. Hence, the present practice demands that engineered structures conform to a predictable performance in accordance to pre-defined performance objectives. It is also necessary to perform a cost-benefit-risk assessment considering the seismic hazards, resulting in controlling the earthquake-related investment for the structure during the design life span.

Traditionally, the seismic design codes recommends the design of a structure based on limits on stresses and member forces calculated from prescribed levels of applied lateral shear forces. Further, the performance objectives are in these codes are not clearly stated except to provide for life safety (strength and ductility) and damage control (serviceability drift limits). However, recent earthquakes such as the 1994 Northridge and 1995 Hanshin– Awaji (Kobe) earthquakes were noted to cause high level of

damage to structures, resulting in economic loss due to loss of use, public services line disruption, and cost of structural repair works were unexpectedly high.

It is noted that in the current code design procedures, there are uncertainties involved concerning the seismic demand and seismic capacity of the structure. Structural failures observed after the 1994 Northridge and 1995 Kobe earthquakes have exposed the weakness of the prevalent design and construction procedures notably in steel moment frames and pressed the need for new approaches for evaluation of building performance and design.

In the Performance-Based Seismic Design (PBSD) philosophy the design criteria are expressed in terms of achieving the stated performance levels corresponding to the stated levels of seismic hazard. In the design process, attempts must be made to address the core issue of the large uncertainty inherent in defining seismic demands and improving performance in the evaluation and design process.

6.2 Non-linear Time History Analysis

Non-linear Time History Analysis, often referred to as Non-linear Dynamic analysis is considered to be the most suitable method to estimate deformation and forces in an structure subjected to seismic ground excitation (Ghobarah, 2001). For the analysis to be reliable and credible, it is necessary to ensure that a) appropriate site-specific ground motion with specified hazard level are selected with confidence; b) the structural model is representative and realistic; c) analysis procedures and interpretation tools are reliable;

and d) identification of modes and sequence of element and component failure are predictable .

The main objective of dynamic analysis is to estimate the roof displacement and the interstorey drift of the building subjected to the seismic hazard. Dynamic analysis provided information on flexural yielding, and change of the pattern in strength and stiffness distribution of the structure. The maximum ductility and the deflection in the individual member can be determined through the results of a dynamic analysis. It also allows for considering the P-delta effect in the structure caused due to gravity loading on the lateral displacement. The DRAIN -2DX software has been employed to carry out the dynamic analysis for the considered 30 earthquake records. The discussion and analysis of the results in the following section are classified broadly into three categories a) Scaled GMR records b) Spectrum compatible GMR records c) Atkinson's artificial earthquake records .

6.3 Discussion of Interstorey drift results

6.3.1 PGA Scaling method

The interstorey drift graphs of the 5, 10, 15 and 20 storey frames have been plotted from the results of the Non-linear time history analysis for the selected GMRs scaled using the PGA scaling method.

Table 6.1 : PGA Scaling method - Summary of Interstorey drift for Real ground motion

SMRF	Interstorey Drifts (%hs) of SMRF			
	GMRs scaled by Peak Ground Acceleration method			
	Max. of Mean		Max. of (Mean+SD)	
	+	-	+	-
5 Storey	1.244185	-0.64124	1.607446	-0.81725
10 Storey	0.881252	-0.49075	1.176595	-0.71509
15 Storey	0.673171	-0.33707	0.94335	-0.46054
20 Storey	0.673202	-0.33178	0.832117	-0.42891

SD = Standard Deviation, h_s = Storey height.

Table 6.1 gives the values of mean, Sum of mean and the Standard deviation values of the interstorey drifts from the PGA Scaling method .

The Ground motion record NAVER2 is found to have the drift close to the positive mean value in the 5 storey frame, in the 10 storey frame NORTHRIDGE1 is found to have the drift close to the positive mean value, in the 15 storey frame the drift close to the positive mean value is obtained by scaling the record NAVER15, finally in the 20 storey frame NORTHRIDGE 4 ground motion record produces the modest drift in the building. Figure 6.1 shows the Interstorey drift graphs from the time history analysis of GMRs scaled using PGA method for the 5 storey SMRF and the 10 storey SMRF, Figure 6.2 shows the Interstorey drift graphs from the time history analysis of GMRs scaled using PGA method for the 15 storey SMRF and the 20 storey SMRF

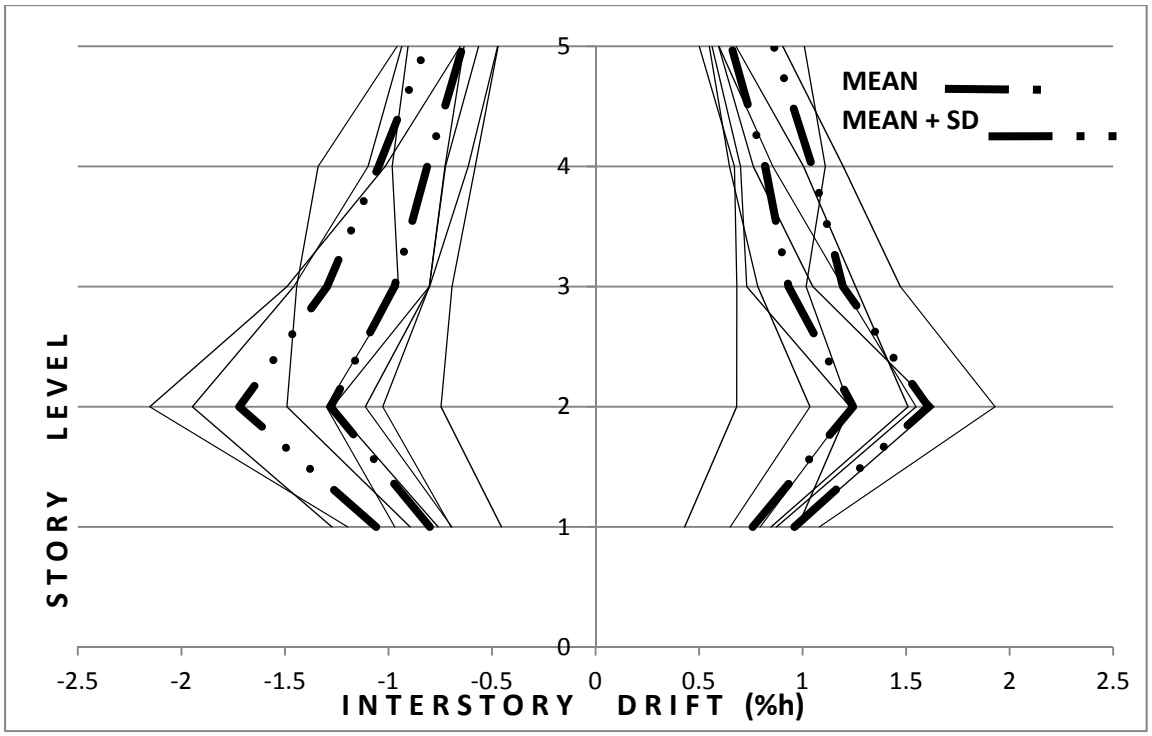

(a)

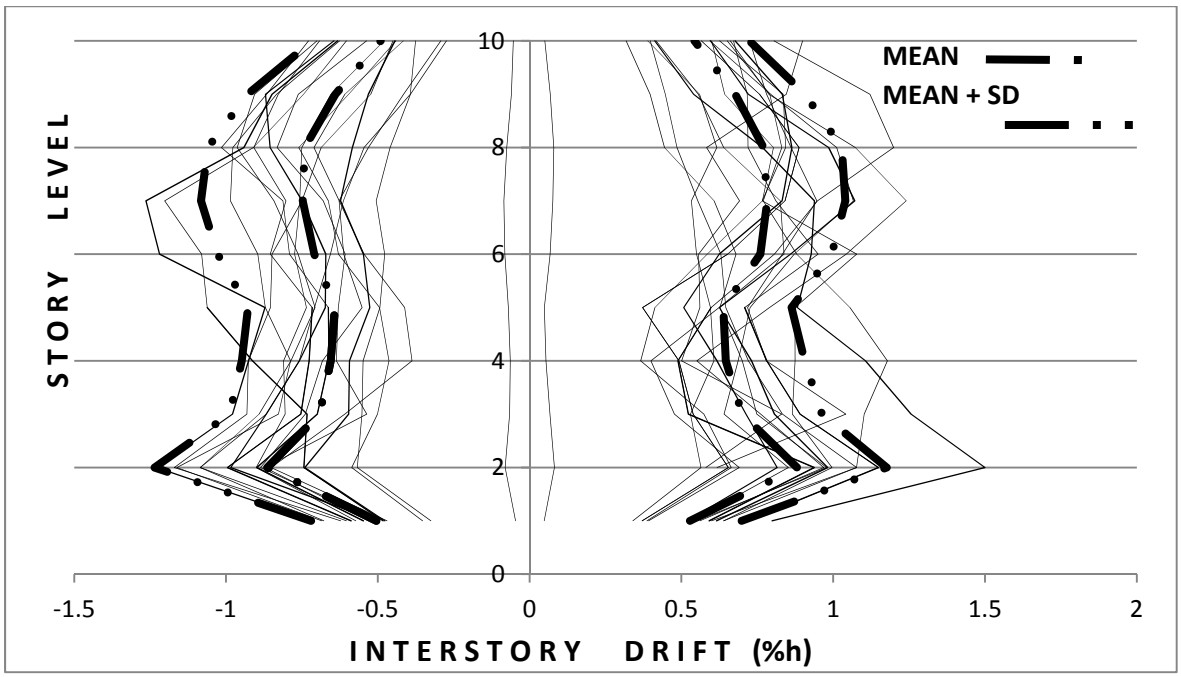

(b)

Figure 6.1 : Interstorey drift graphs from RHA of GMRs scaled using PGA method

(a) 5 storey SMRF (b) 10 storey SMRF

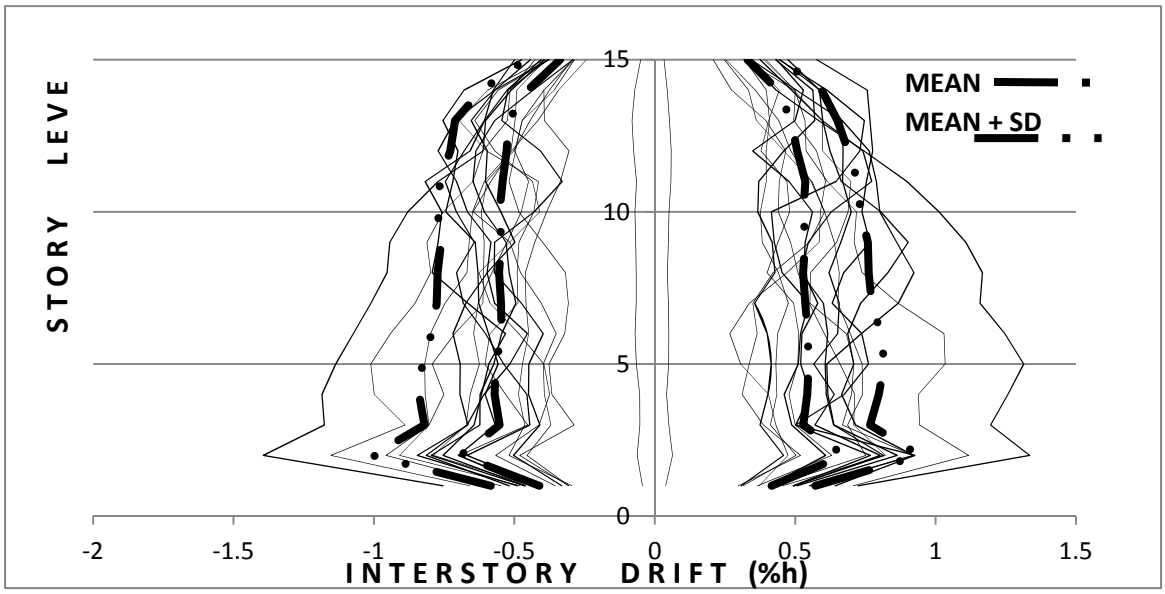

(a)

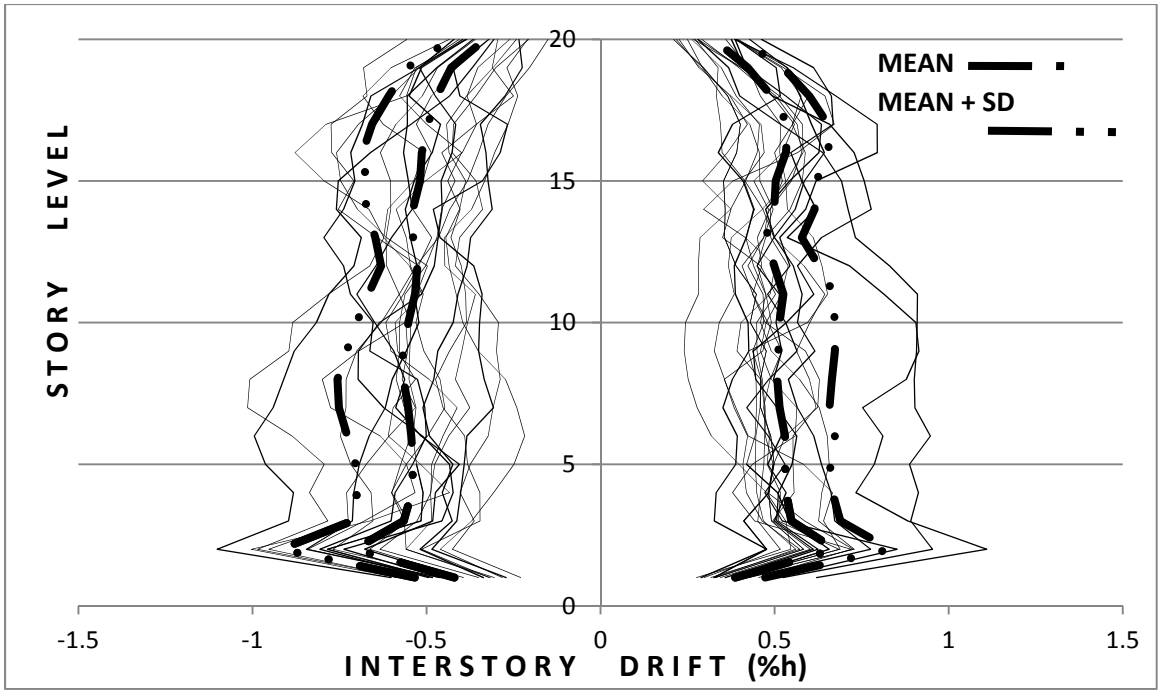

(b)

Figure 6.2: Interstorey drift graphs from RHA of GMRs scaled using PGA method
(a) 15 storey SMRF (b) 20 storey SMRF

Table 6.2: Base Shear (KN) from PGA scaling method

EQ Records	5 Storey	10 Storey	15 Storey	20 Storey
naver1	165	203	278	415
naver2	165	158	283	421
naver3	150	178	301	430
naver6	152	169	300	467
naver7	164	177	288	470
naver8	168	171	274	422
naver9	163	165	295	428
naver10	159	173	283	435
naver11	163	193	290	414
naver12	158	191	277	429
naver13	153	199	291	403
naver14	162	178	287	411
naver15	161	184	274	389
kobejap1	169	178	271	404
kobejap3	155	189	286	425
kobejap4	161	200	272	395
northdr1	164	179	269	400
northdr2	168	184	279	405
northdr3	178	187	288	411
northdr4	175	198	305	389

Table 6.2 gives the base shear values in the 5, 10, 15 and 20 storey buildings after the ground motions are scaled to the design spectrum using the PGA scaling method .

6.3.2 PS_a Scaling method

The interstorey drift graphs of the 5, 10, 15 and 20 storey frames have been plotted from the results of the Non-linear time history analysis obtained after the selected GMR for the time history analysis is scaled using the P**S$_a$**A scaling method .

Table 6.3: PS_a Scaling Method - Summary of Interstorey Drift for Real Ground Motion

SMRF	Interstorey Drifts (%hs) of SMRF			
	GMRs scaled by PSa scaling method			
	Max. of Mean		Max. of (Mean+SD)	
	+	-	+	-
5 Storey	1.483261	-0.76901	1.737574	-0.90917
10 Storey	1.125759	-0.61232	1.383671	-0.78159
15 Storey	0.862494	-0.4247	1.14435	-0.54325
20 Storey	0.839577	-0.38752	1.064295	-0.47288

SD = Standard Deviation, h_s = Storey height.

Table 6.3 gives the values of mean , Sum of mean and the Standard deviation values of the interstorey drifts from the PGA Scaling method .The Ground motion record NAVER3 is found to have the drift close to the positive mean value in the 5 storey frame, in the 10 storey frame NAVER15 is found to have the drift close to the positive mean value, in the 15 storey frame the drift close to the positive mean value is obtained by scaling the record NAVER15, finally in the 20 storey fame NAVER6 ground motion record produces the modest drift in the building. Figure 6.3 represents the Interstorey drift graphs from the time history analysis of GMRs scaled using PS_a method for the 5 storey SMRF and the 10 storey SMRF, Figure 6.4 represents the Interstorey drift graphs from the time history analysis of GMRs scaled using PS_a method for the 15 storey SMRF and the 20 storey SMRF.

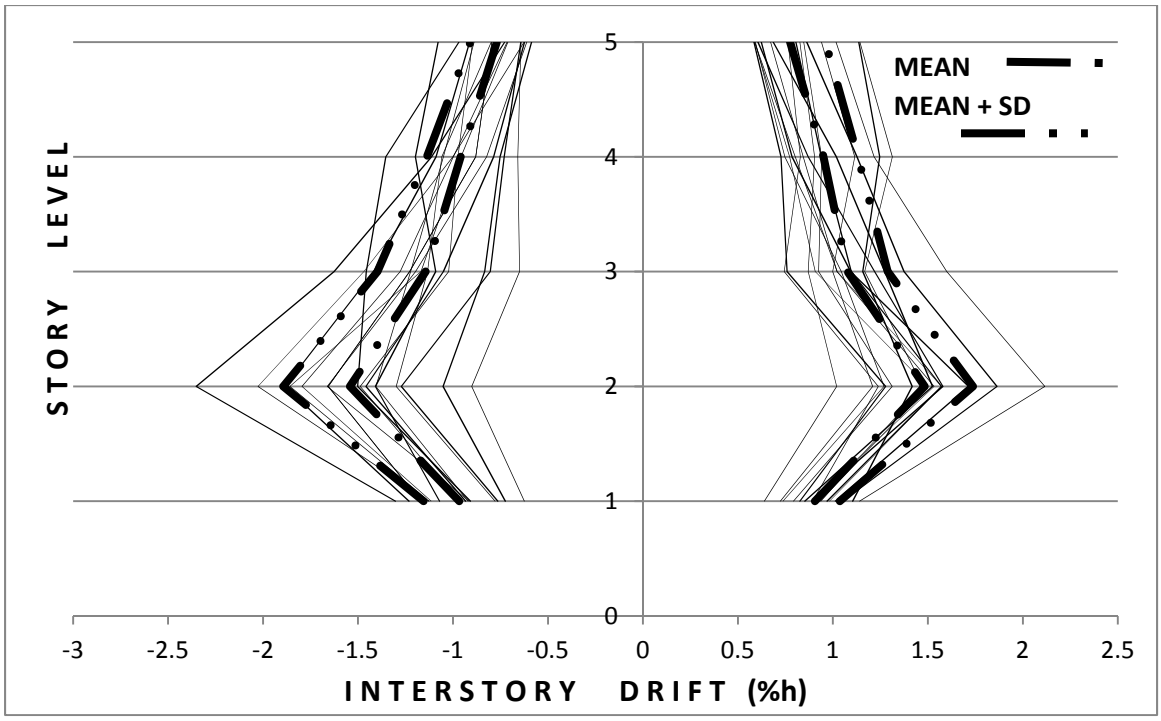

(a)

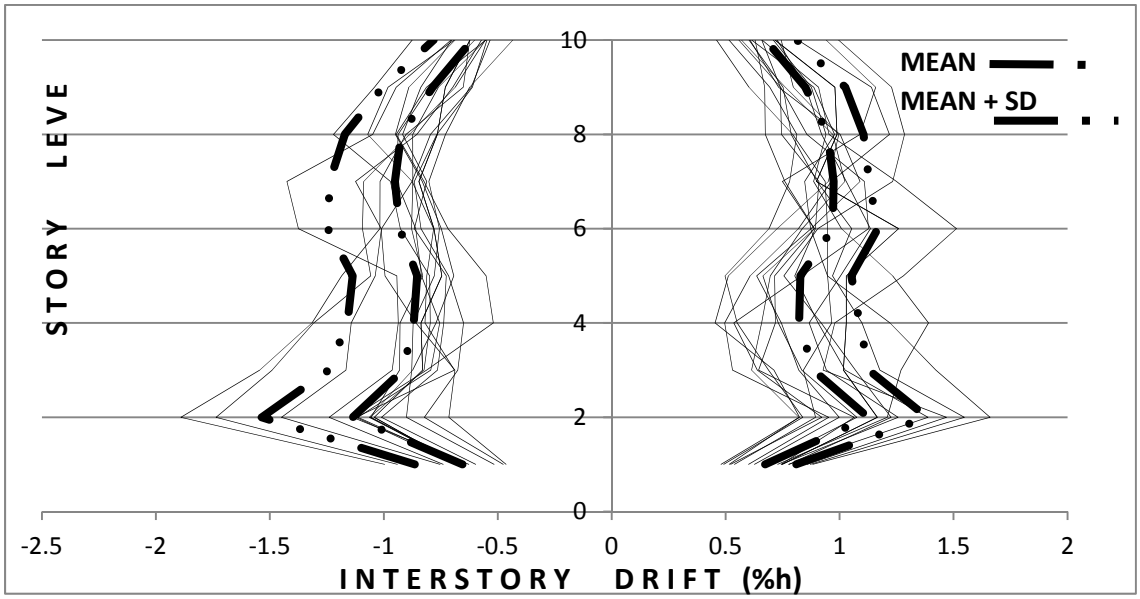

(b)

Figure 6.3: Interstorey drift graphs from RHA of GMRs scaled using PS_a method
(a) 5 storey SMRF (b) 10 storey SMRF

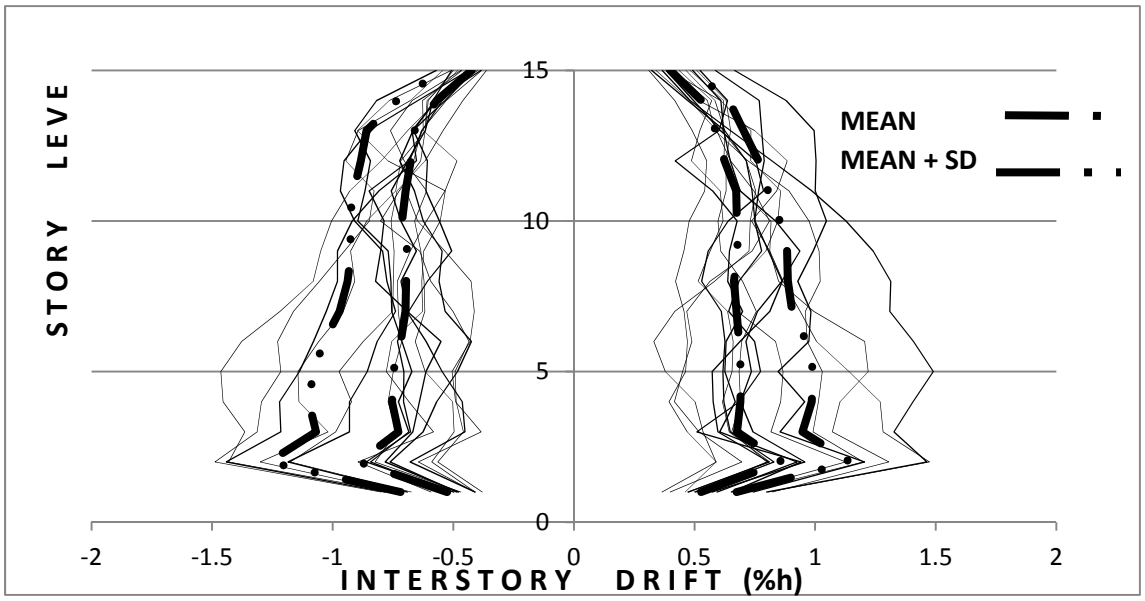

(a)

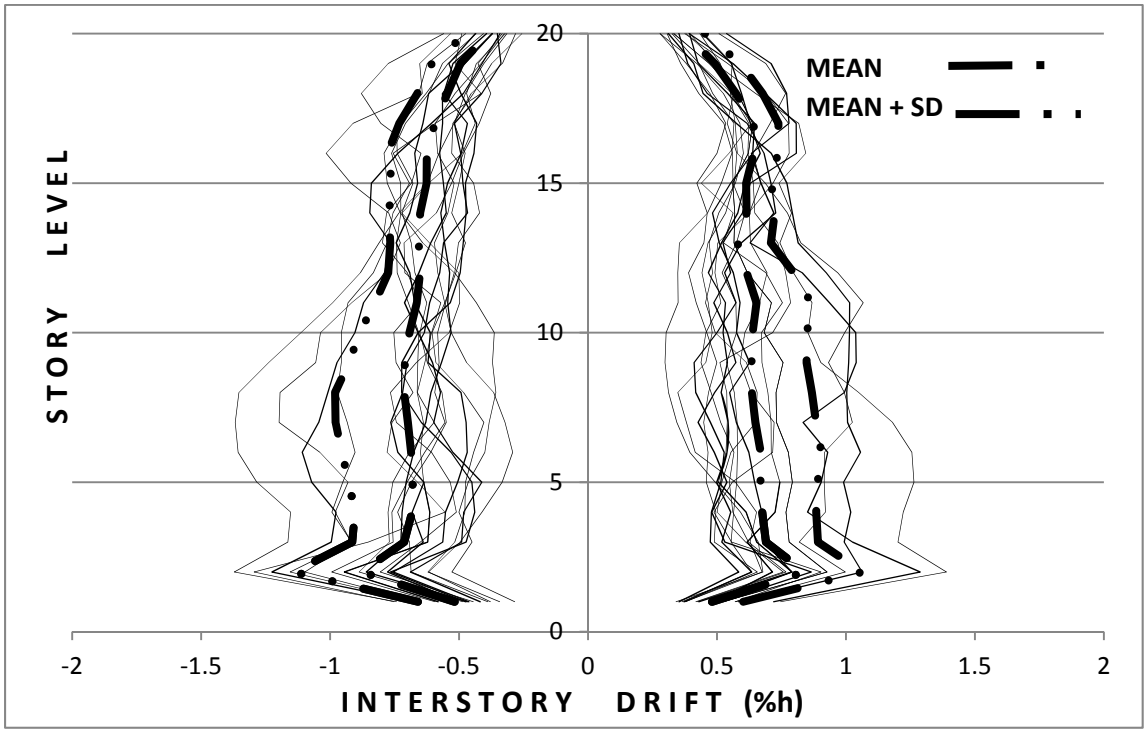

(b)

Figure 6.4: Interstorey drift graphs from RHA of GMRs scaled using PS_a method
(a) 15 storey SMRF (b) 20 storey SMRF

Table 6.4 : Base Shear (KN) from PSa scaling method

GMRs	5 Storey	10 Storey	15 Storey	20 Storey
naver1	135	189	275	386
naver2	145	181	283	402
naver3	162	184	302	412
naver6	125	215	282	395
naver7	127	182	276	394
naver8	124	173	283	406
naver9	133	177	291	393
naver10	136	183	301	404
naver12	152	174	311	415
naver13	143	181	288	418
naver14	137	173	294	422
naver15	144	175	297	385
kobejap3	150	196	305	400
kobejap4	147	191	310	397
northdr1	132	200	313	420
northdr2	134	204	316	396
northdr3	136	210	322	411
northdr4	144	203	330	423

Table 6.4 gives the base shear values in the 5, 10, 15 and 20 storey buildings after the ground motions are scaled to the design spectrum using the PS_a scaling method .

6.3.3 Ordinate Scaling method

The interstorey drift graphs of the 5, 10, 15 and 20 storey frames have been plotted from the results of the Non-linear time history analysis for the selected GMR scaled using the Ordinate scaling method .

Table 6.5 – Ordinate Scaling Method - Summary of Interstorey Drift for Real Ground Motion

SMRF	Interstorey Drifts (%hs) of SMRF			
	GMRs scaled by Ordinate scaling method			
	Max. of Mean		Max. of (Mean+SD)	
	+	-	+	-
5 Storey	1.367361	-0.71707	1.511227	-0.89374
10 Storey	1.302523	-0.69476	1.714063	-1.00643
15 Storey	1.408986	-0.62363	1.867248	-0.89513
20 Storey	1.099769	-0.59848	1.592114	-1.01768

SD = Standard Deviation, h_s = Storey height.

Table 6.5 gives the values of mean, Sum of mean and the Standard deviation values of the interstorey drifts from the Ordinate Scaling method. The Ground motion record NAVER6 is found to have the drift close to the positive mean value in the 5 storey frame, in the 10 storey frame NAVER9 is found to have the drift close to the positive mean value, in the 15 storey frame the drift close to the mean value is obtained by scaling the record NAVER6 , finally in the 20 storey fame NAVER13 ground motion record produces the modest drift in the building . Figure 6.5 represents the Interstorey drift graphs from the time history analysis of GMRs scaled using the ordinate method for the 5 storey SMRF and the 10 storey SMRF, Figure 6.6 represents the Interstorey drift graphs from the time history analysis of GMRs scaled using Ordinate method for the 15 storey SMRF and the 20 storey SMRF.

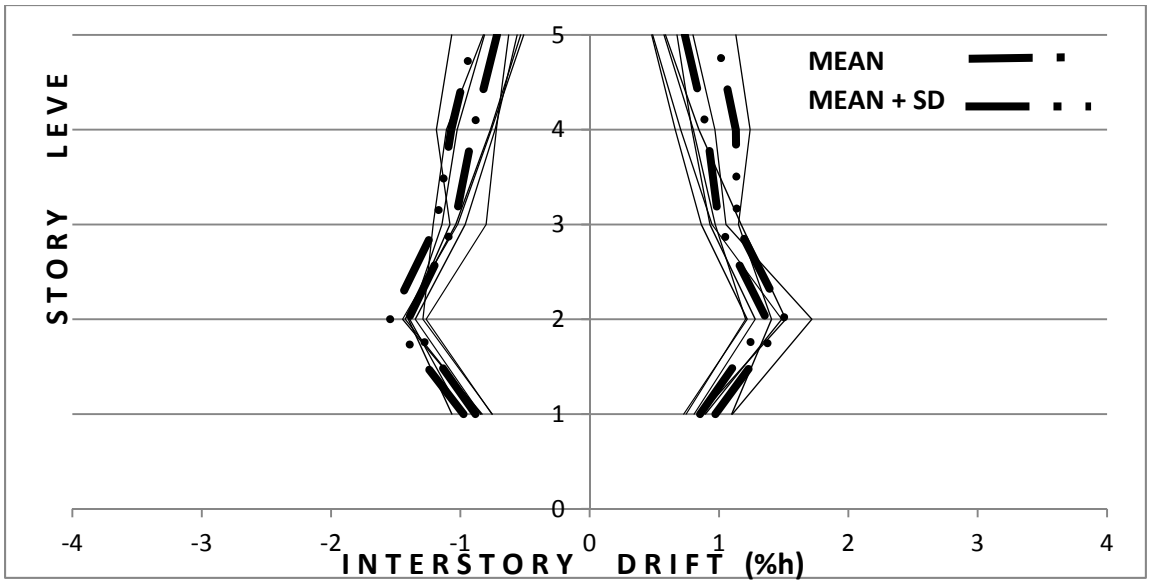

(a)

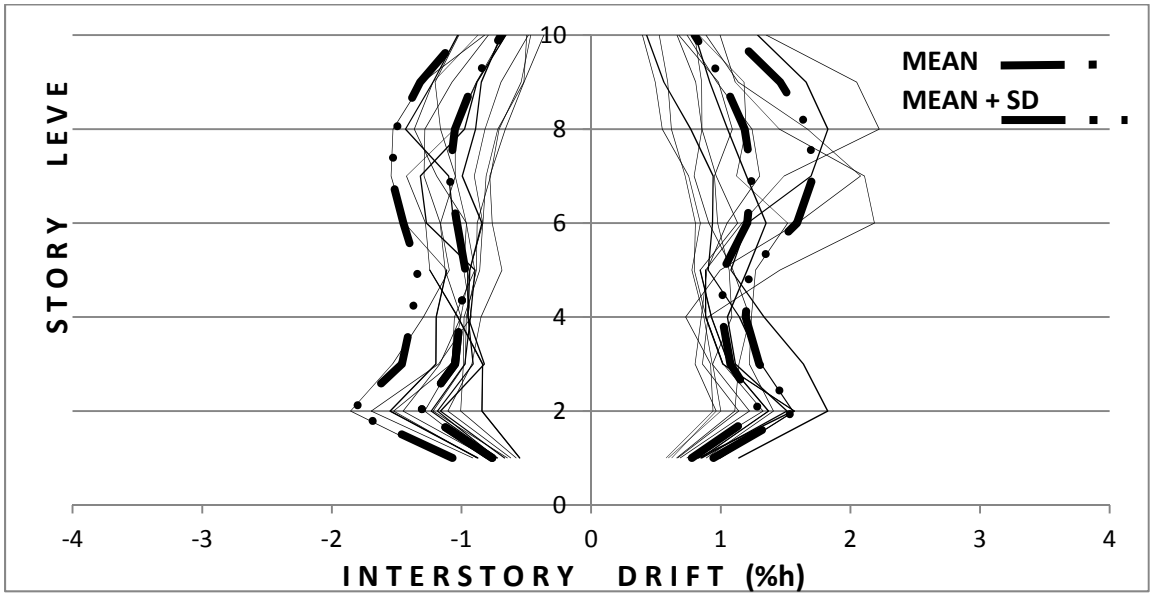

(b)

Figure 6.5: Interstorey drift graphs from RHA of GMRs scaled using Ordinate method (a) 5 storey SMRF (b) 10 storey SMRF

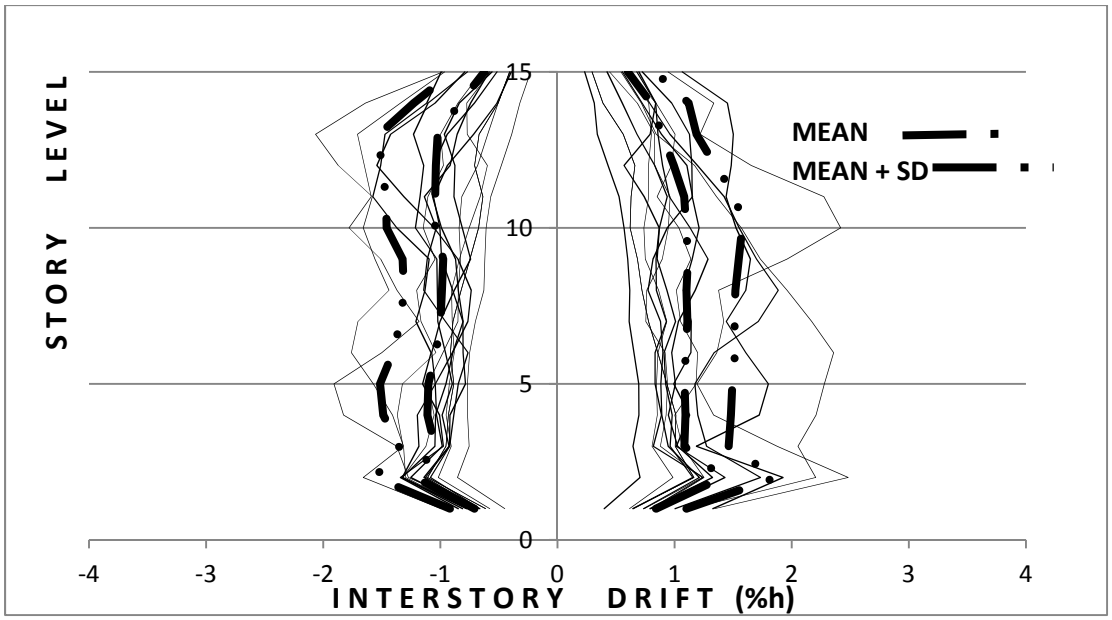

(a)

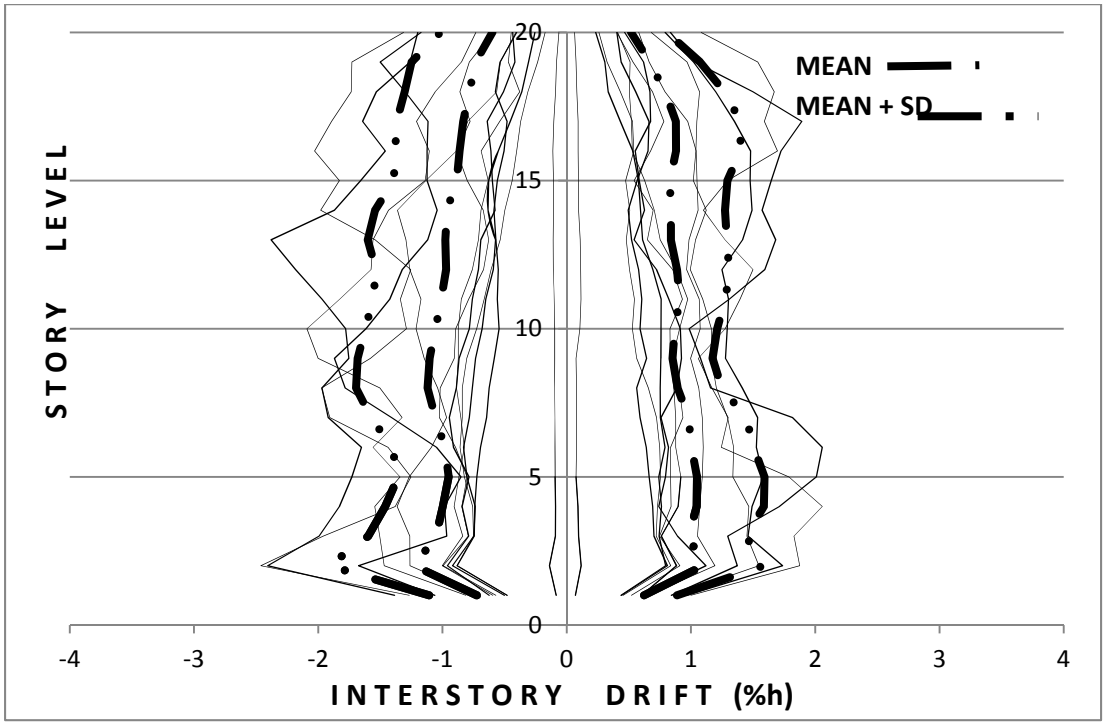

(b)

Figure 6.6: Interstorey drift graphs from RHA of GMRs scaled using Ordinate method (a) 15 storey SMRF (b) 20 storey SMRF

Table 6.6: Base Shear (KN) from Ordinate scaling method

GMR	5 Storey	10 Storey	15 Storey	20 Storey
naver1	123	220	278	381
naver2	144	197	294	421
naver3	150	221	284	407
naver6	143	189	293	402
naver7	132	186	297	401
naver8	134	194	286	423
naver9	145	203	299	443
naver10	157	207	315	410
naver11	153	208	322	402
naver12	151	192	283	395
naver13	148	183	285	386
naver14	154	185	288	379
naver15	169	191	287	388
kobejap2	172	177	274	412
kobejap3	175	184	283	414
kobejap4	173	179	286	411
northdr1	144	193	277	398
northdr2	146	192	287	396
northdr3	158	178	285	392
northdr4	149	186	281	390

Table 6.6 gives the base shear values in the 5, 10, 15 and 20 storey buildings after the ground motions are scaled to the design spectrum using the Ordinate scaling method .

6.3.4 Partial area scaling method

The interstorey drift graphs of the 5, 10, 15 and 20 storey frames have been plotted from the results of the Non-linear time history analysis for the selected GMR scaled using the Partial area scaling method .

Table 6.7 – Partial Area Scaling Method -Summary of Interstorey Drift for Real Ground Motion

SMRF	Interstorey Drifts (%hs) of SMRF			
	GMRs scaled by Partial area scaling method			
	Max. of Mean		Max. of (Mean+SD)	
	+	-	+	-
5 Storey	1.26888	-0.65818	1.58834	-0.81005
10 Storey	1.153488	-0.62655	1.396499	-0.80613
15 Storey	0.922696	-0.43006	1.232704	-0.59044
20 Storey	0.838254	-0.39392	1.15148	-0.55283

SD = Standard Deviation, h_s = Storey height.

Table 6.7 gives the values of mean , Sum of mean and the Standard deviation values of the interstorey drifts from the Partial area Scaling method .The Ground motion record KOBJAP1 is found to have the drift close to the positive mean value in the 5 storey frame, in the 10 storey frame NAVER10 is found to have the drift close to the positive mean value, in the 15 storey frame the drift close to the positive mean value is obtained by scaling the record NAVER15, finally in the 20 storey fame NAVER14 ground motion record produces the modest drift in the building . Figure 6.7 represents the Interstorey drift graphs from the time history analysis of GMRs scaled using Partial area method for the 5 storey SMRF and the 10 storey SMRF, Figure 6.8 represents the Interstorey drift graphs from the time history analysis of GMRs scaled using the Partial area method for the 15 storey SMRF and the 20 storey SMRF

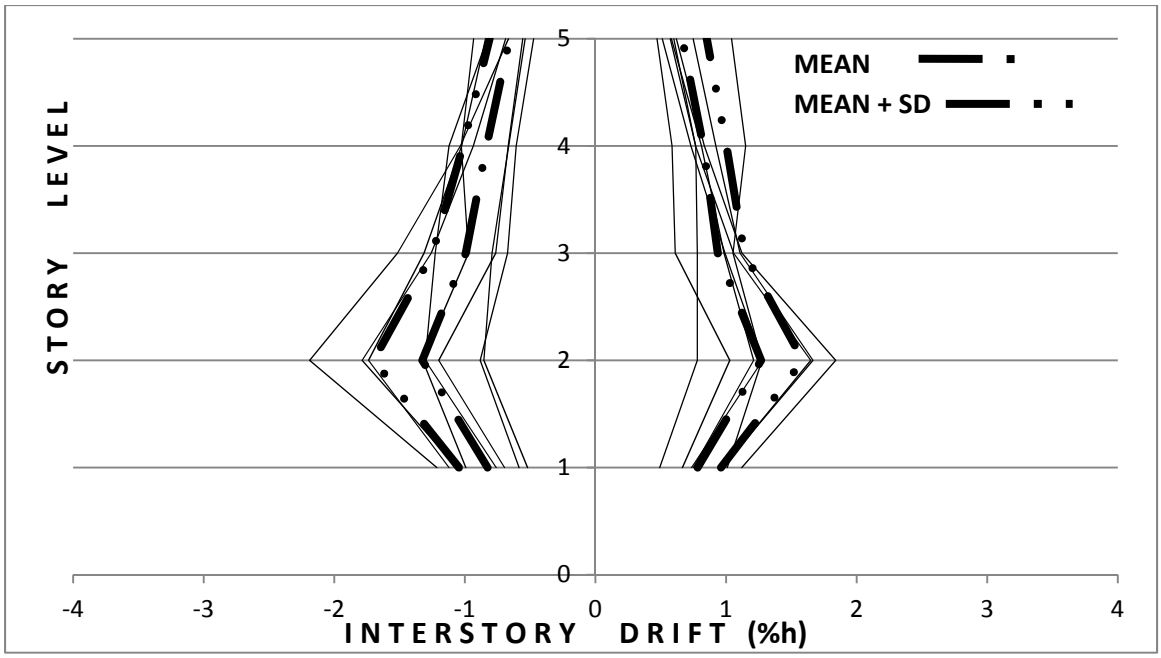

(a)

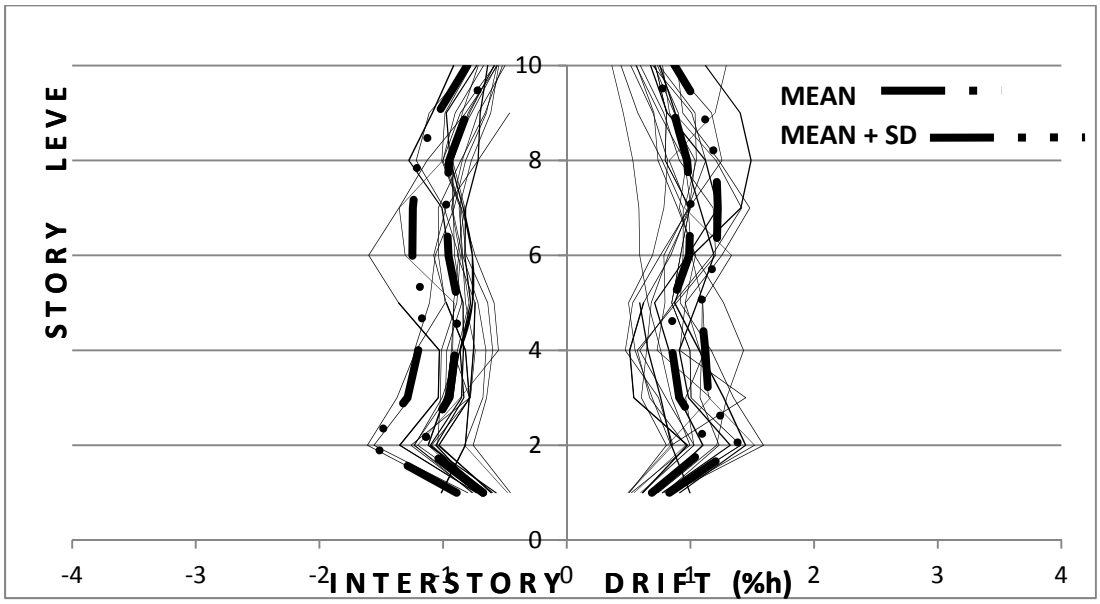

(b)

Figure 6.7: Interstorey drift graphs from RHA of GMRs scaled using Partial area scaling

(a) 5 storey SMRF (b) 10 storey SMRF

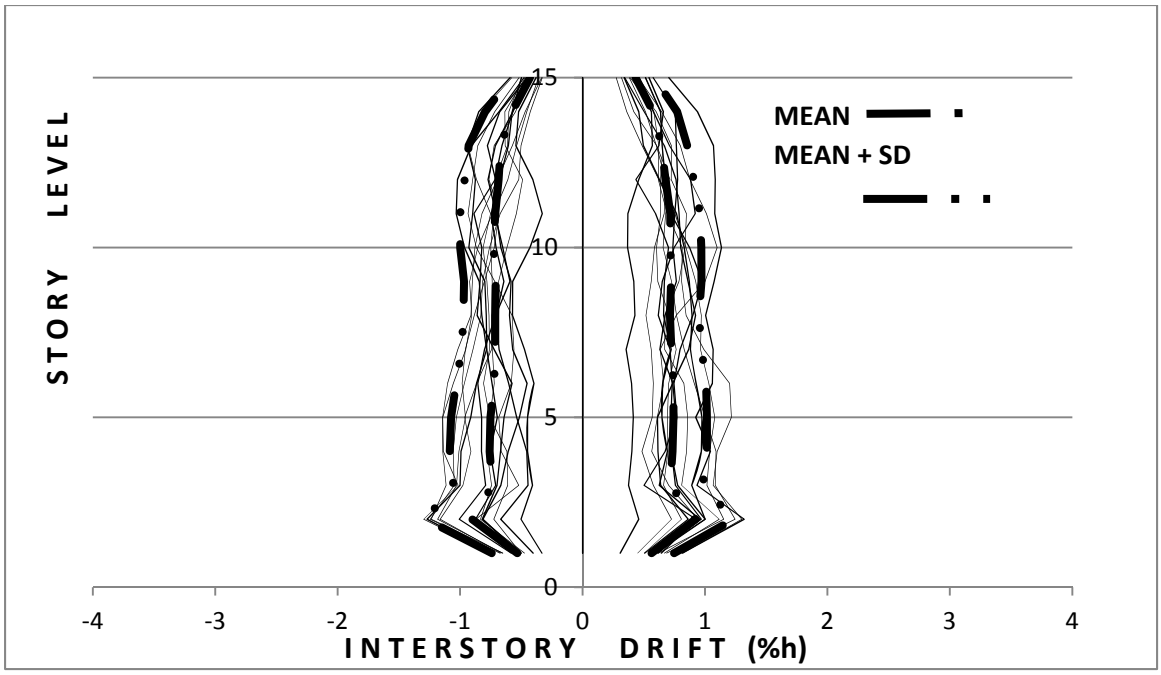

(a)

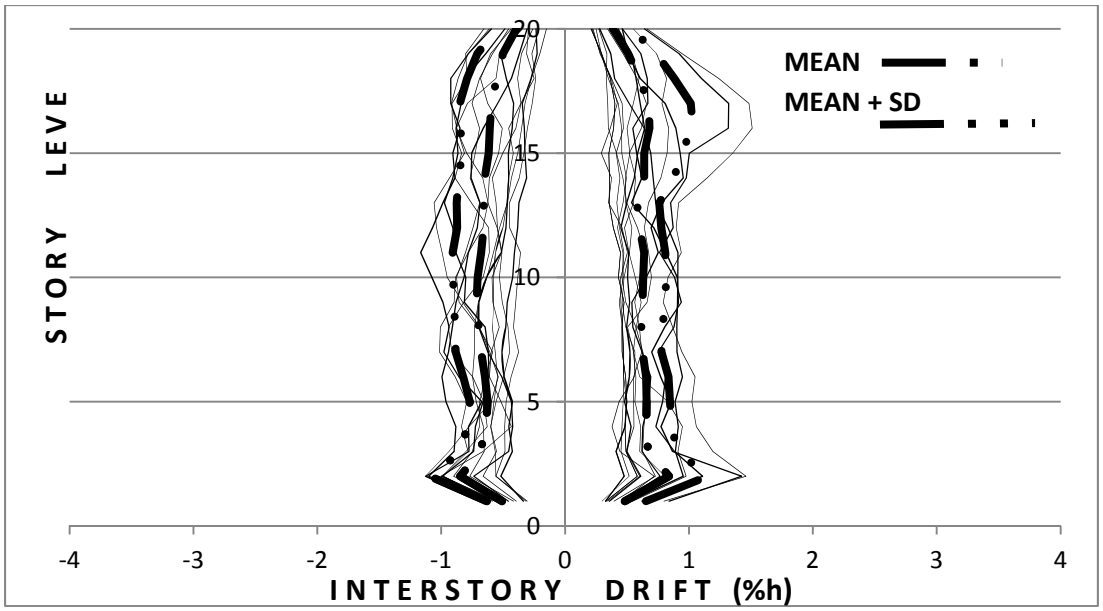

(b)

Figure 6.8: Interstorey drift graphs from RHA of GMRs scaled using Partial area scaling (a) 15 storey SMRF (b) 20 storey SMRF

Table 6.8: Base Shear (KN) from Partial area scaling method

GMRs	5 Storey	10 Storey	15 Storey	20 Storey
naver1	132	178	335	511
naver2	143	192	351	527
naver3	122	193	356	524
naver6	151	194	354	519
naver7	138	188	344	531
naver8	135	185	340	528
naver9	148	187	342	532
naver10	147	179	311	541
naver11	139	178	329	550
naver12	147	185	336	550
naver13	143	186	327	525
naver14	156	180	331	529
naver15	141	204	324	526
kobejap1	158	183	334	536
kobejap2	156	182	353	538
kobejap3	153	188	348	542
kobejap4	151	189	342	547
northdr1	148	213	352	552
northdr2	139	214	353	551
northdr3	143	197	357	522
northdr4	139	186	362	520

Table 6.8 gives the base shear values in the 5, 10, 15 and 20 storey buildings after the ground motions are scaled to the design spectrum using the Partial area scaling method .

6.3.5 ASCE 2007 scaling method

The interstorey drift graphs of the 5, 10, 15 and 20 storey frames have been plotted from the results of the Non-linear time history analysis for the selected GMR scaled using the ASCE 2007 scaling method .

Table 6.9 –ASCE 2007 Scaling Method- Summary of Interstorey Drift for Real Ground Motion

SMRF	Interstorey Drifts (%hs) of SMRF			
	GMRs scaled by ASCE 2007 scaling method			
	Max. of Mean		Max. of (Mean+SD)	
	+	-	+	-
5 Storey	1.22	-0.68	1.83	-0.81
10 Storey	1.08	-0.57	1.30	-0.73
15 Storey	0.89	-0.43	1.07	-0.57
20 Storey	1.00	-0.50	1.18	-0.64

SD = Standard Deviation, h_s = Storey height.

Table 6.9 gives the values of mean, Sum of mean and the Standard deviation values of the interstorey drifts from the ASCE 2007 Scaling method .The Ground motion record NAVER10 is found to have the drift close to the positive mean value in the 5 storey frame, in the 10 storey frame NAVER15 is found to have the drift close to the mean value, in the 15 storey frame the drift close to the mean value is obtained by scaling the record NAVER14, finally in the 20 storey fame NAVER13 ground motion record produces the modest drift in the building . Figure 6.9 represents the Interstorey drift graphs from the time history analysis of GMRs scaled using ASCE 2007 method for the 5 storey SMRF and the 10 storey SMRF, Figure 6.10 represents the Interstorey drift graphs from the time history analysis of GMRs scaled using the ASCE 2007 method for the 15 storey SMRF and the 20 storey SMRF

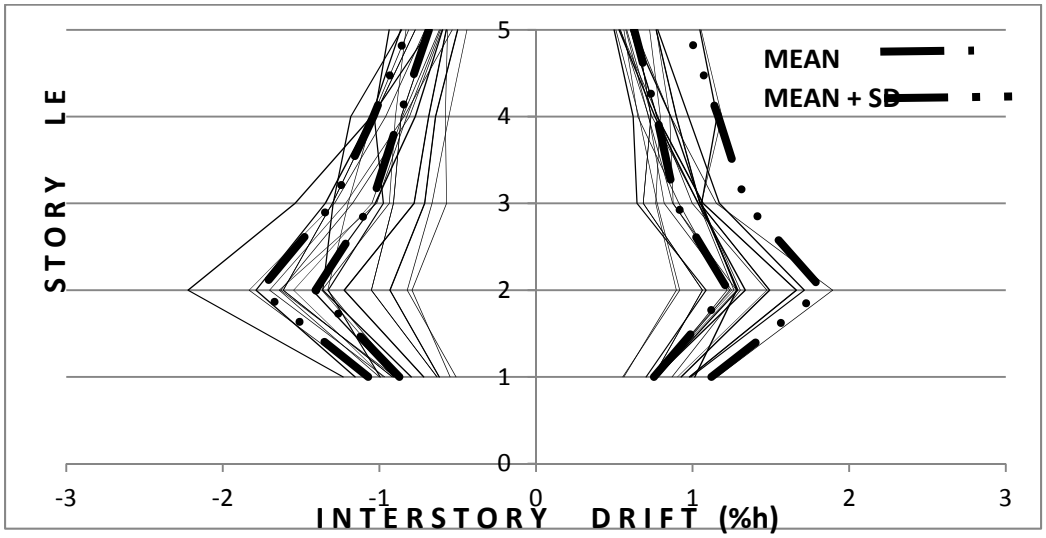

(a)

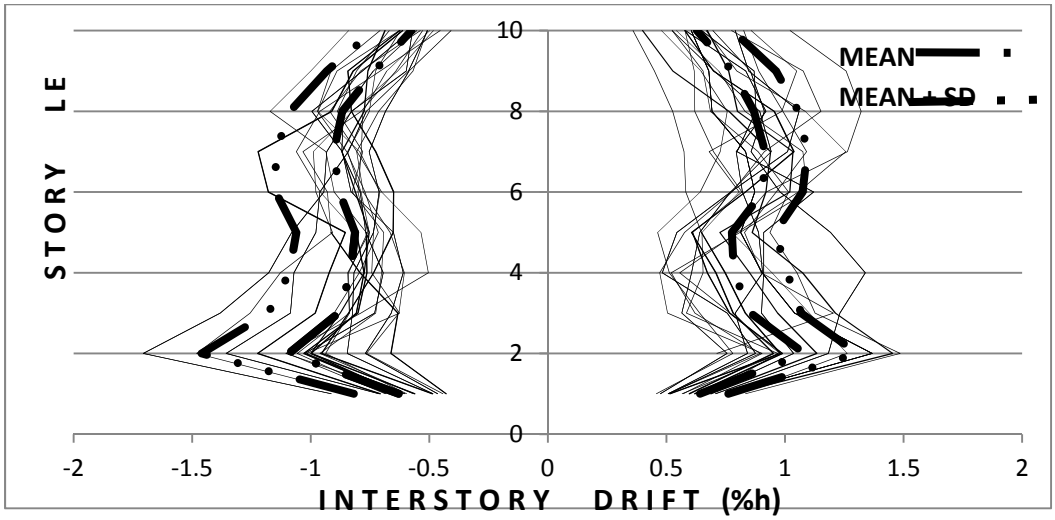

(b)

Figure 6.9: Interstorey drift graphs from RHA of GMRs scaled using ASCE 2007 scaling (a) 5 storey SMRF (b) 10 storey SMRF

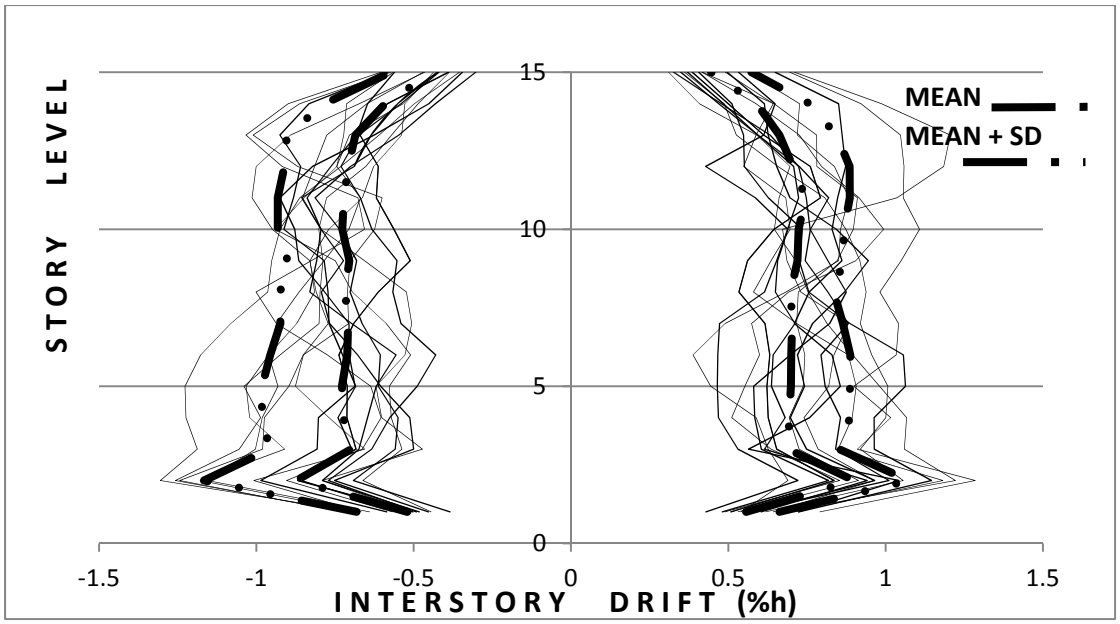

(a)

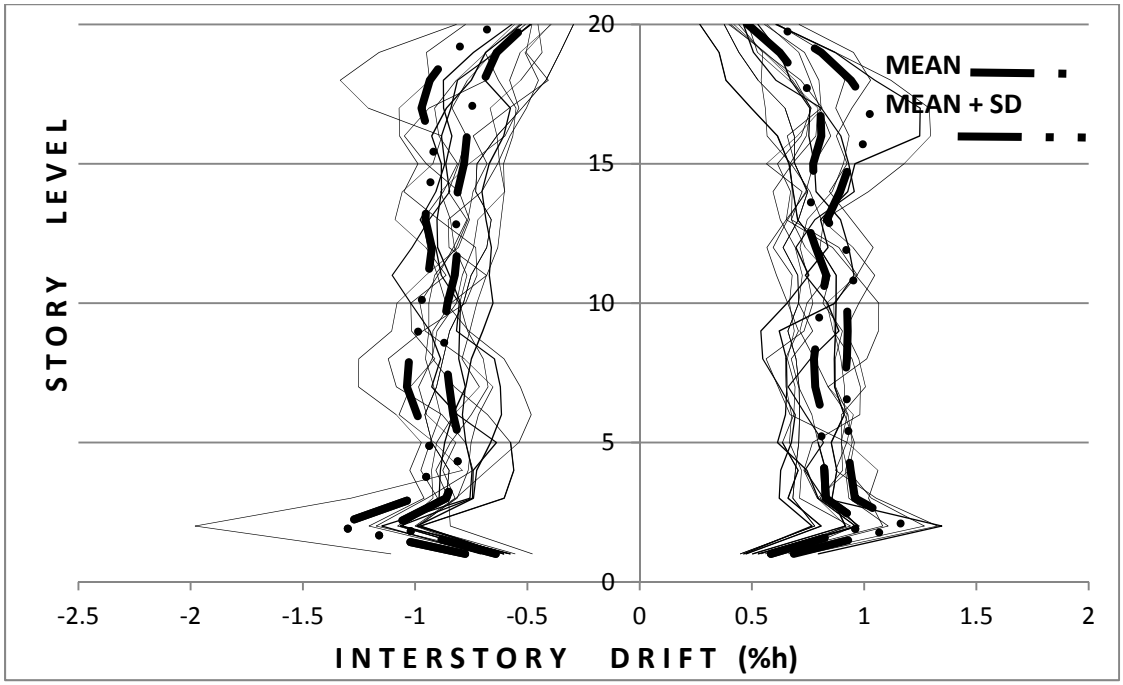

(b)

Figure 6.10: Interstorey drift graphs from RHA of GMRs scaled using ASCE 2007 scaling (a) 15 storey SMRF (b) 20 storey SMRF

Table 6.10: Base Shear (KN) from ASCE 2007 scaling method

GMRs	5 Storey	10 Storey	15 Storey	20 Storey
naver1	223	264	334	512
naver2	218	273	346	523
naver3	219	268	342	526
naver6	226	272	348	533
naver7	236	281	346	519
naver8	238	279	352	523
naver9	246	266	357	527
naver10	241	262	353	533
naver13	239	271	348	531
naver14	247	275	332	535
naver15	255	273	337	538
kobejap3	210	283	339	545
kobejap4	249	282	352	555
northdr1	256	274	354	523
northdr2	254	276	351	535
northdr3	255	278	357	547

Table 6.10 gives the base shear values in the 5, 10, 15 and 20 storey buildings after the ground motions are scaled to the design spectrum using the ASCE 2007 scaling method .

6.3.6 Least Square scaling method

The interstorey drift graphs of the 5, 10, 15 and 20 storey frames have been plotted from the results of the Non-linear time history analysis for the selected GMR scaled using the Least square scaling method .

Table 6.11 - Summary of Interstorey Drift for Real Ground Motion from Least Square Scaling Method

SMRF	Interstorey Drifts (%hs) of SMRF			
	GMRs scaled by Least Square scaling method			
	Max. of Mean		Max. of (Mean+SD)	
	+	-	+	-
5 Storey	1.06	-0.60	1.86	-0.91
10 Storey	1.10	-0.62	1.49	-0.89
15 Storey	0.81	-0.36	1.46	-0.55
20 Storey	0.54	-0.25	1.02	-0.46

SD = Standard Deviation, h_s = Storey height.

Table 6.11 gives the values of mean , Sum of mean and the Standard deviation values of the interstorey drifts from the Least Square Scaling method .The Ground motion record NAVER10 is found to have the drift close to the mean value in the 5 storey frame, in the 10 storey frame NRD2 is found to have the drift close to the mean value, in the 15 storey frame the drift close to the mean value is obtained by scaling the record NAVER8, finally in the 20 storey fame NRD2 ground motion record produces the modest drift in the building. Figure 6.11 represents the Interstorey drift graphs from the time history analysis of GMRs scaled using Least square method for the 5 storey SMRF and the 10 storey SMRF, Figure 6.12 represents the Interstorey drift graphs from the time history analysis of GMRs scaled using the Least square method for the 15 storey SMRF and the 20 storey SMRF

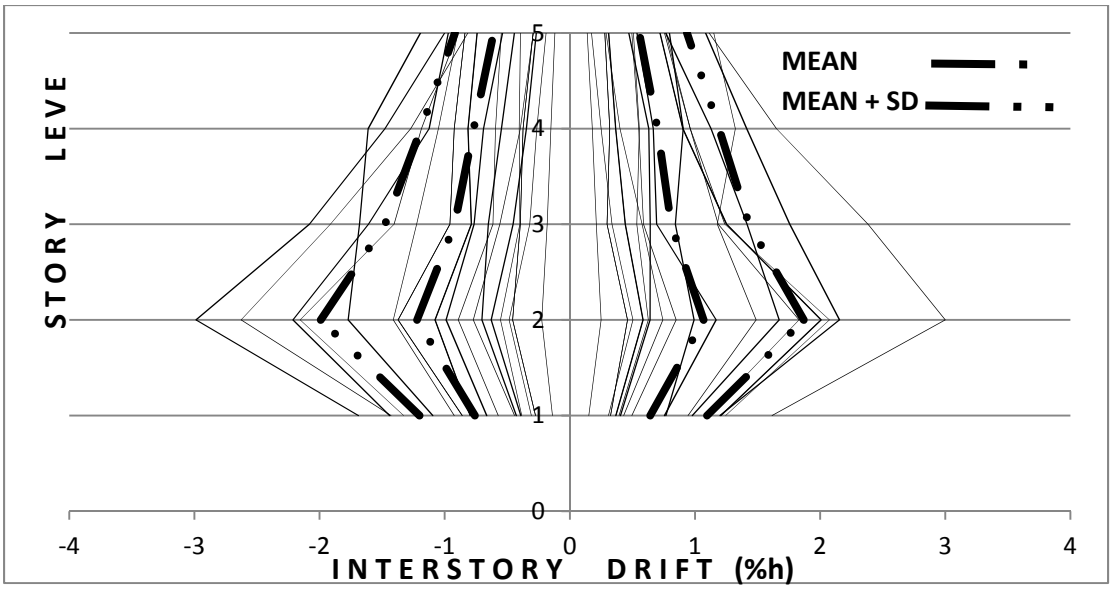

(a)

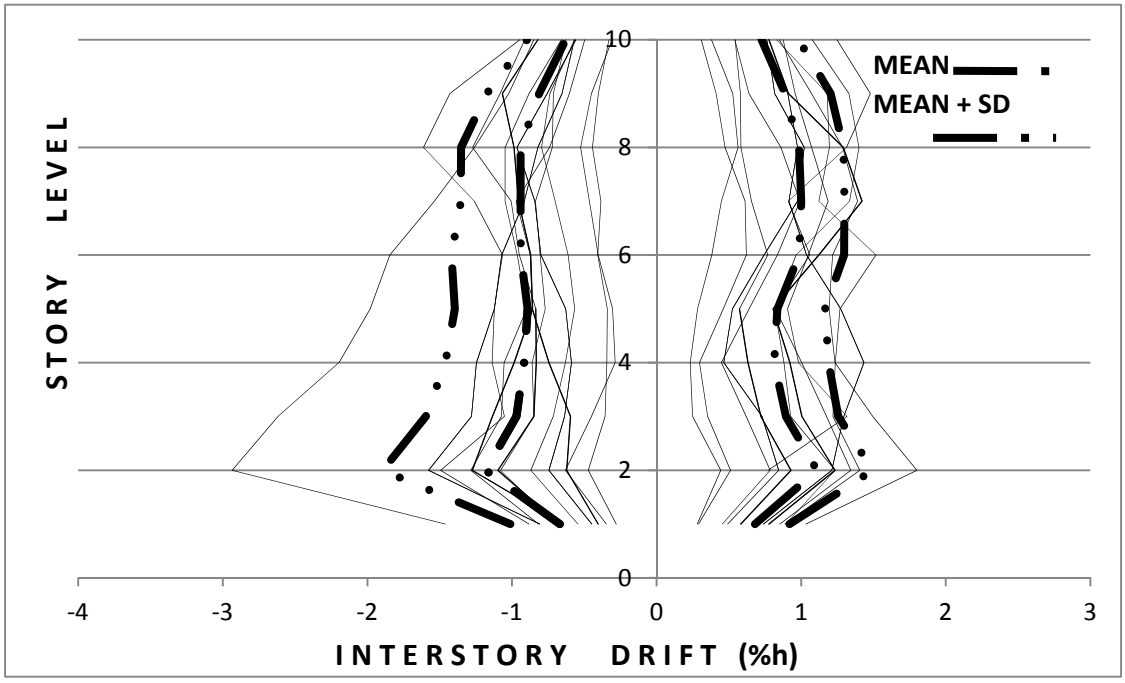

(b)

Figure 6.11 : Interstorey drift graphs from RHA of GMRs scaled using Least square scaling: (a) 5 storey SMRF (b) 10 storey SMRF

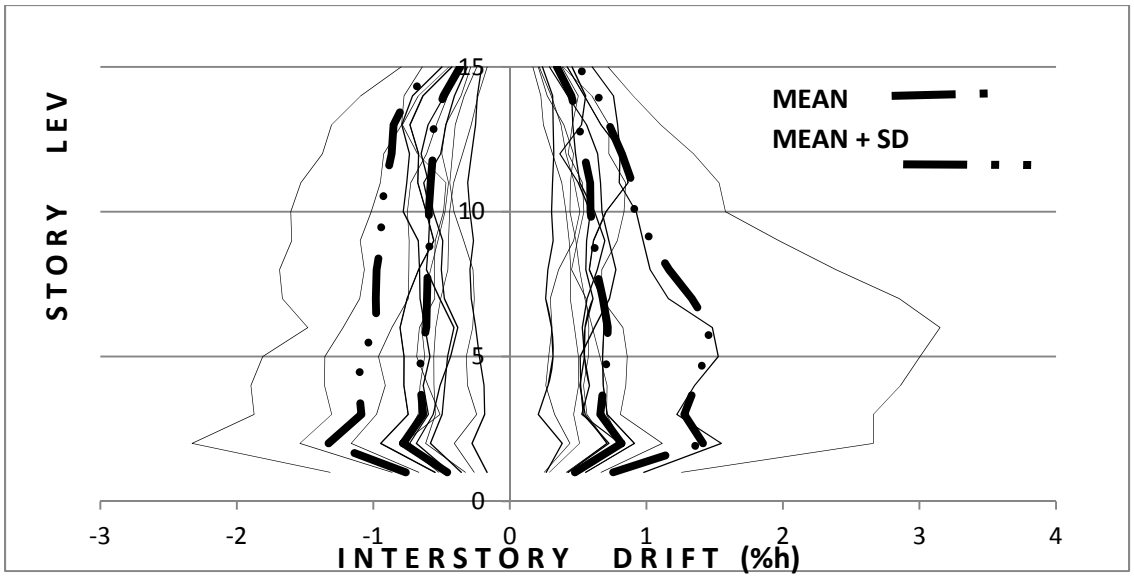

(a)

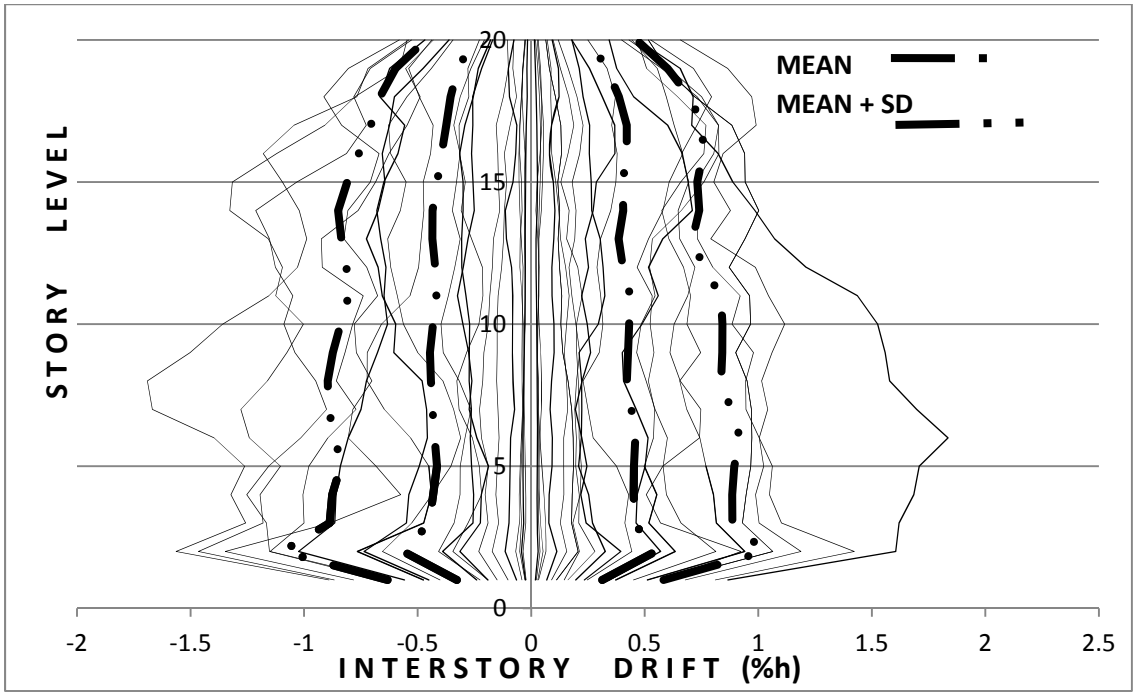

(b)

Figure 6.12: Interstorey drift graphs from RHA of GMRs scaled using Least square scaling (a) 15 storey SMRF (b) 20 storey SMRF

Table 6.12: Base shear (KN) from Least square scaling method

GMR	5 Storey	10 Storey	15 Storey	20 Storey
naver1	232	261	357	541
naver2	238	265	343	534
naver3	221	266	352	532
naver6	224	273	358	536
naver7	237	275	342	528
naver8	225	277	341	525
naver9	235	278	340	541
naver10	238	264	356	543
naver11	229	273	361	546
naver12	227	273	358	538
naver13	228	271	355	544
naver14	233	282	364	522
naver15	246	288	362	528
kobejap2	251	283	358	531
kobejap3	254	280	361	536
kobejap4	253	274	363	538
northdr1	257	277	372	529
northdr2	253	274	376	533
northdr3	251	279	374	537
northdr4	249	283	379	545

Table 6.12 gives the base shear values in the 5, 10, 15 and 20 storey buildings after the ground motions are scaled to the design spectrum using the Least square scaling method .

6.4 Discussion on the interstorey drift results from spectrum compatible records

6.4.1 Spectral matching using Seismo Match software

The interstorey drift graphs of the 5, 10, 15 and 20 storey frames have been plotted from the results of the Non-linear time history analysis for the selected GMR matched with the target spectrum using the Seismomatch software.

Table 6.13- Summary of Interstorey Drift for Real Ground Motion from Seismo Match Scaling method

SMRF	Interstorey Drifts (%hs) of SMRF			
	Spectral matching using Seismo match			
	Max. of Mean		Max. of (Mean+SD)	
	+	-	+	-
5 Storey	0.99	-0.56	1.46	-0.80
10 Storey	0.68	-0.40	0.82	-0.54
15 Storey	0.52	-0.30	0.63	-0.37
20 Storey	0.50	-0.32	0.56	-0.38

SD = Standard Deviation, h_s = Storey height.

Table 6.13 gives the values of mean , Sum of mean and the Standard deviation values of the interstorey drifts from the spectral matched records from the Seismomatch software .The Ground motion record NAVER8 is found to have the drift close to the mean value in the 5 storey frame, in the 10 storey frame NRD3 is found to have the drift close to the mean value, in the 15 storey frame the drift close to the mean value is obtained by scaling the record KOBJAP4, finally in the 20 storey fame NAVER1 ground motion record produces the modest drift in the building. . Figure 6.13 represents the Interstorey drift graphs from the time history analysis of GMRs scaled using the Seismomatch software for the 5 storey SMRF and the 10 storey SMRF, Figure 6.14 represents the interstorey drift graphs from the time history analysis of GMRs scaled using the Seismomatch software for the 15 storey SMRF and the 20 storey SMRF.

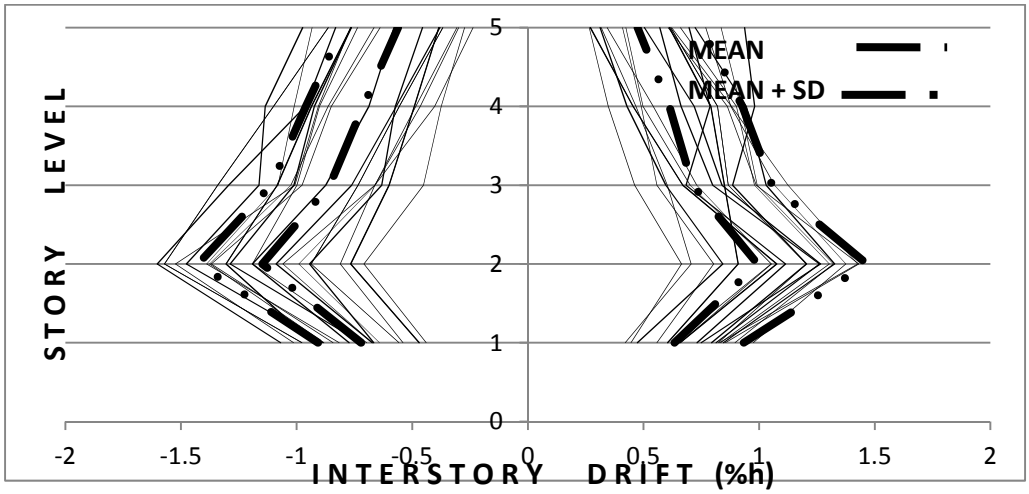

(a)

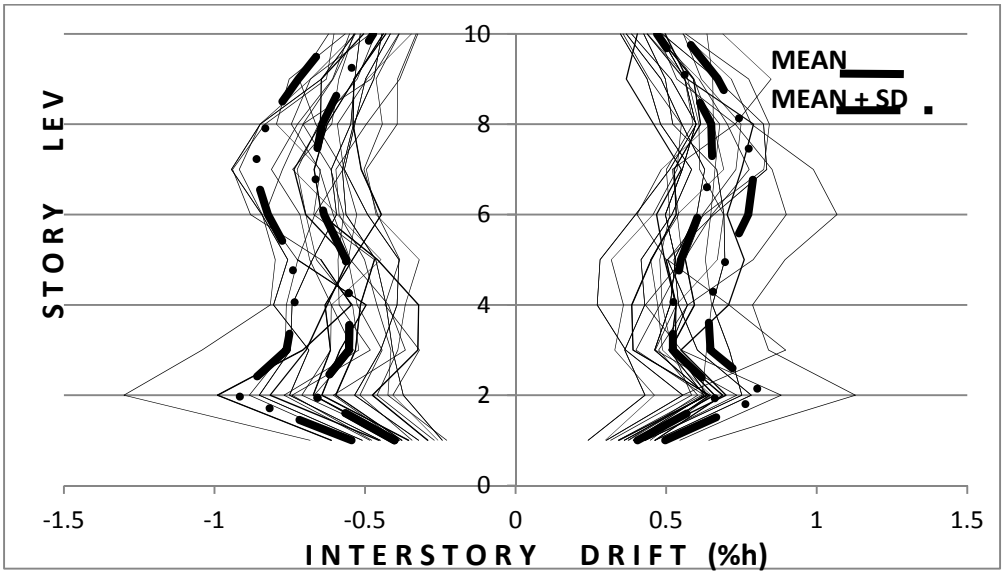

(b)

Figure 6.13: Interstorey drift graphs from RHA of Spectral matching using Seismo match

(a) 5 storey SMRF (b) 10 storey SMRF

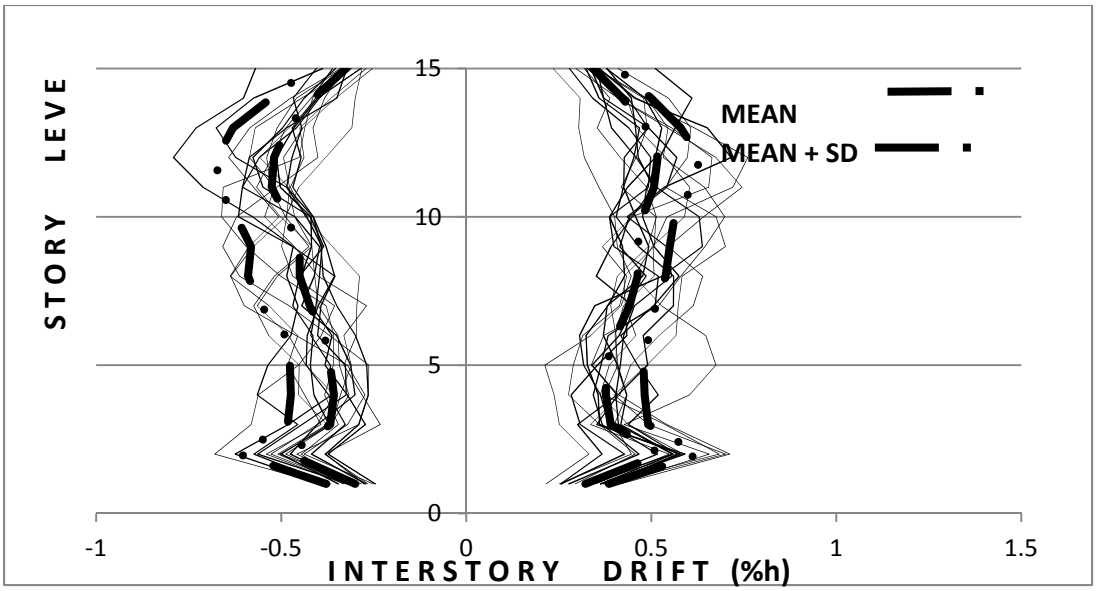

(a)

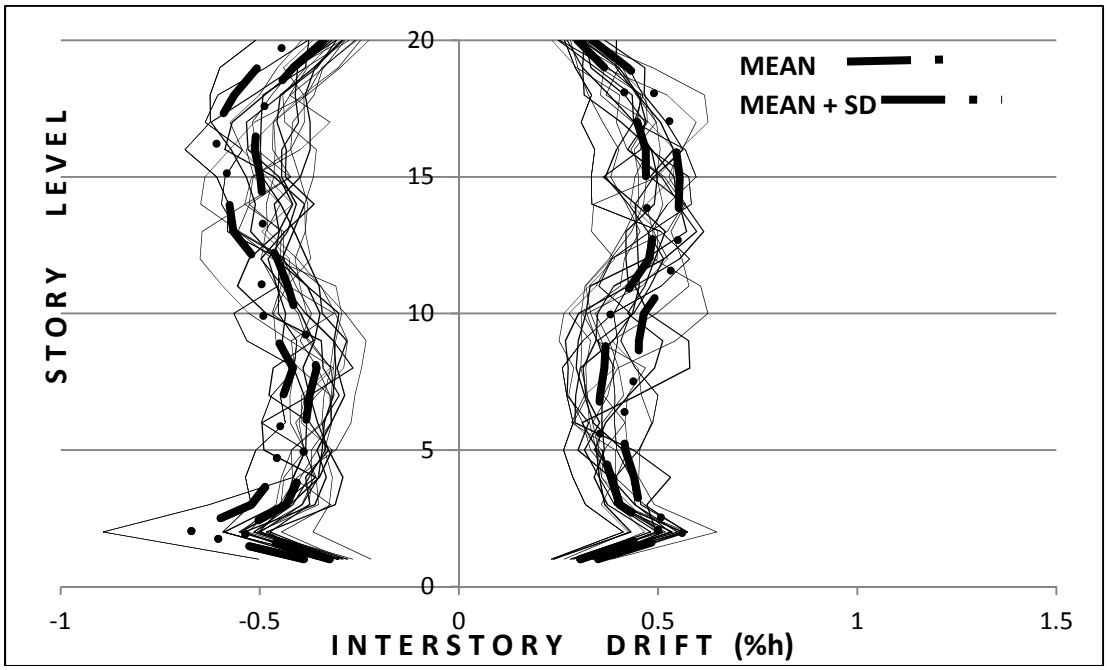

(b)

Figure 6.14: Interstorey drift graphs from RHA Spectral matching using Seismo match

(a) 15 storey SMRF (b) 20 storey SMRF

Table 6.14 - Base Shear (KN) from Seismo Match Spectral matching

GMRs	5 Storey	10 Storey	15 Storey	20 Storey
naver1	226	318	355	532
naver2	224	295	350	534
naver3	236	315	352	540
naver6	233	316	349	542
naver7	235	269	339	545
naver8	238	274	348	547
naver9	243	278	351	541
naver10	241	273	352	537
naver11	246	272	356	524
naver12	248	279	361	485
naver13	238	284	364	515
naver14	234	289	366	522
naver15	253	276	364	531
kobejap2	244	294	371	543
kobejap3	246	273	376	551
kobejap4	248	275	352	539
northdr1	254	278	357	538
northdr2	257	277	365	533
northdr3	249	285	344	528
northdr4	254	288	333	541

Table 6.14 gives the base shear values in the 5, 10, 15 and 20 storey buildings after the ground motions are scaled to the design spectrum using the Seismomatch software .

6.5 Discussion on the interstorey drift results from Atkinson's artificial records

6.5.1 Spectral matching using Atkinson's artificial records

The interstorey drift graphs of the 5, 10, 15 and 20 storey frames have been plotted from the results of the Non-linear time history analysis obtained using the Atkinson's artificial records.

Table 6.15 - Summary of Interstorey Drift for Real Ground Motion from Atkinson's artificial earthquake records

SMRF	Interstorey Drifts (%hs) of SMRF			
	Spectral matching using Atkinson's artificial records			
	Max. of Mean		Max. of (Mean+SD)	
	+	-	+	-
5 Storey	2.61	-0.99	3.48	-1.32
10 Storey	1.92	-0.61	2.71	-0.88
15 Storey	1.32	-0.43	1.82	-0.64
20 Storey	2.40	-0.45	3.76	-0.59

SD = Standard Deviation, h_s = Storey height.

Table 6.15 gives the values of mean, Sum of mean and the Standard deviation values of the interstorey drifts while using the Atkinson's artificial earthquake records . Figure 6.15 represents the Interstorey drift graphs from the time history analysis using Atkinson's artificial records for the 5 storey SMRF and the 10 storey SMRF, Figure 6.16 represents the Interstorey drift graphs from the time history analysis using the Atkinson's artificial records for the 15 storey SMRF and the 20 storey SMRF

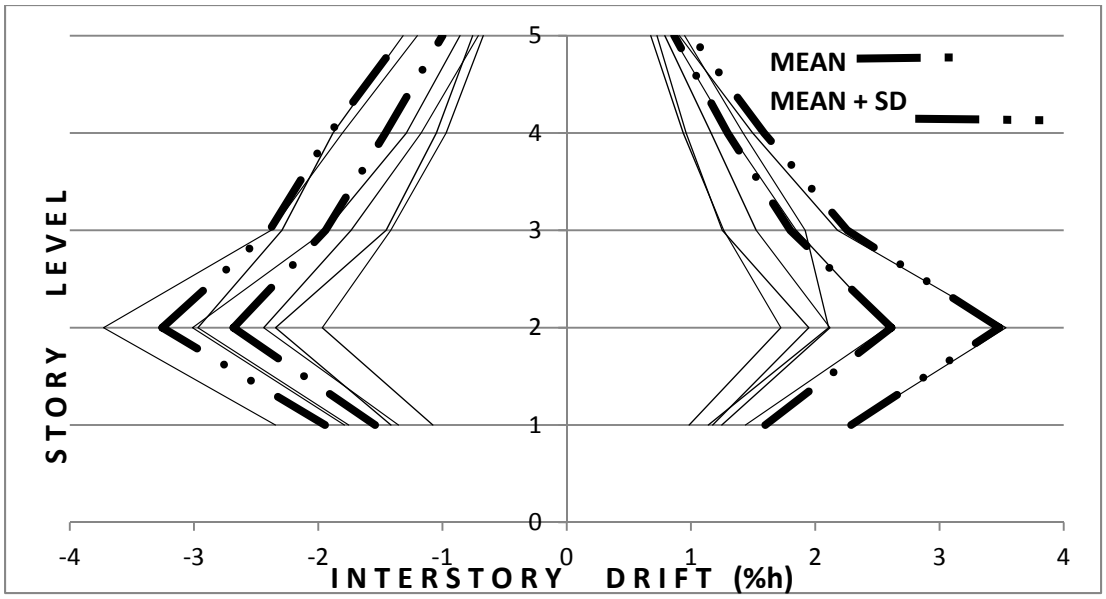

(a)

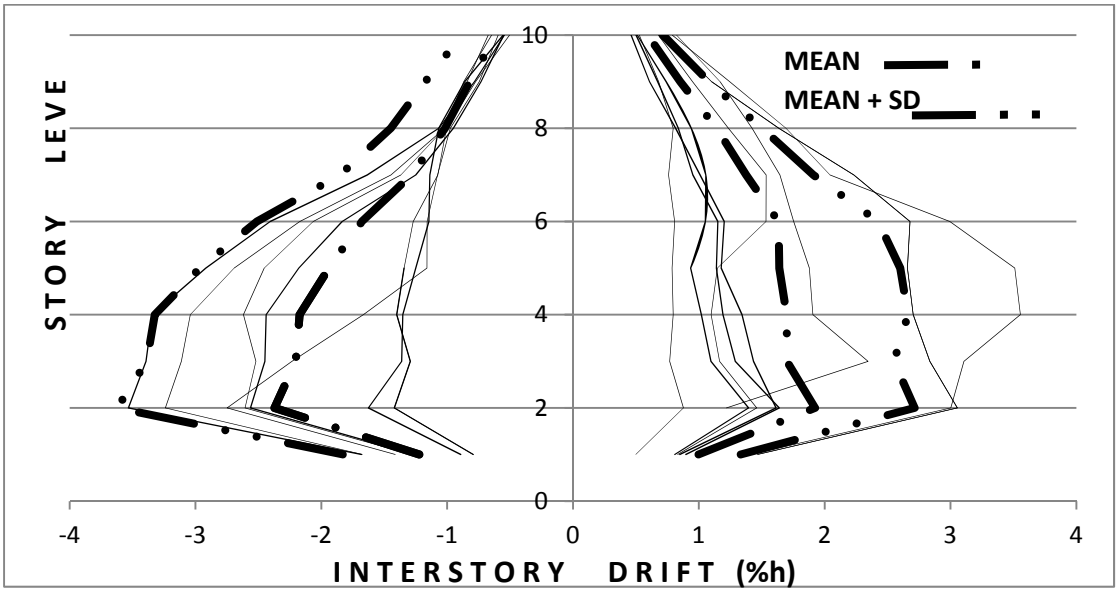

(b)

Figure 6.15: Interstorey drift graphs from RHA of Spectral matching using Atkinson's artificial earthquake records (a) 5 storey SMRF (b) 10 storey SMRF

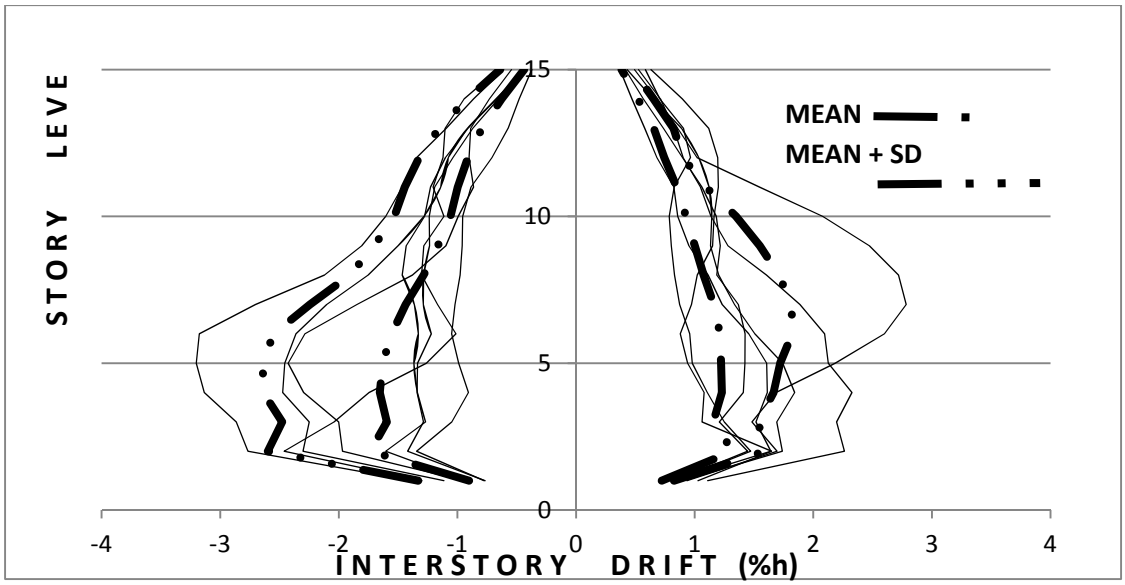

(a)

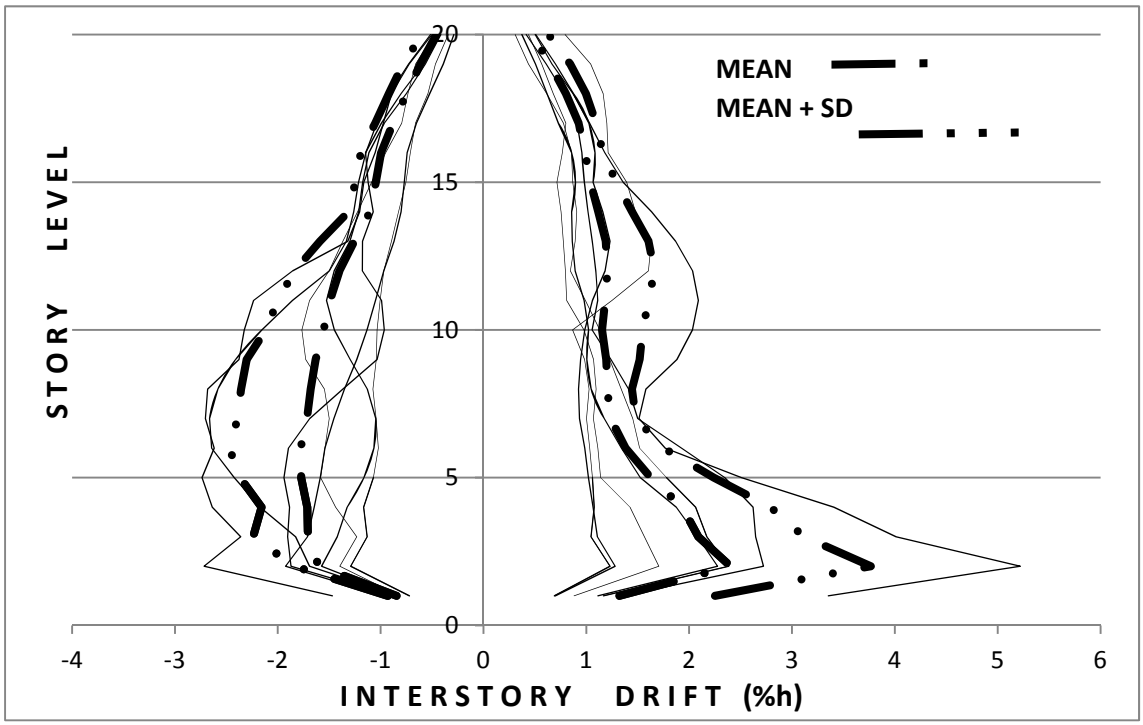

(b)

Figure 6.16: Interstorey drift graphs from RHA Spectral matching using Atkinson's artificial earthquake records (a) 15 storey SMRF (b) 20 storey SMRF

Table 6.16: Base Shear (KN) from Atkinson's artificial records

GMR	5 Storey	10 Storey	15 Storey	20 Storey
LP1	145	185	298	412
LP2	140	215	283	396
LP3	137	190	271	411
LP4	136	203	265	423
SP1	128	206	305	432
SP2	125	207	315	429
SP3	121	212	320	425
SP4	135	218	335	430

Table 6.16 gives the base shear values in the 5, 10, 15 and 20 storey buildings after the ground motions are scaled to the design spectrum using the Atkinson's artificial records .

6.6 Summary

The results of the response history analysis using scaled and artificial ground motion records are summarized in Tables 6.17 through 6.20. In these tables ISD indicates the mean values of the interstorey drift envelope, SD is standard deviation, Disp is the measure of dispersion which is defined here as the standard deviation expressed as a percentage of the mean value, and BS indicates the base shear obtained from the dynamic time history analysis.

Table 6.17: Summary of interstorey drift and base shear for the 5-storey frame

Scaling method	ISD, %h	SD, %h	Dispersion, %ISD	ISD+SD, %h	Min BS, kN	Max BS, kN
PGA	1.24	0.36	29.2	1.61	150	178
PSa	1.48	0.25	17.1	1.74	124	162
Ordinate	1.37	0.14	10.5	1.51	123	173
Partial Area	1.27	0.32	25.2	1.59	122	158
ASCE-7	1.22	0.61	50.0	1.83	210	255
Least Square	1.06	0.80	75.5	1.86	221	257
Spectrum Match	0.99	0.47	47.5	1.46	224	254
Atkinson	2.61	0.87	33.3	3.48	121	145

Table 6.18 : Summary of interstorey drift and base shear for the 10-storey frame

Scaling method	ISD, %h	SD, %h	Dispersion, %ISD	ISD+SD, %h	Min BS, kN	Max BS, kN
PGA	0.88	0.30	33.5	1.18	165	203
PSa	1.13	0.26	22.9	1.38	173	215
Ordinate	1.30	0.41	31.6	1.71	183	220
Partial Area	1.15	0.24	21.1	1.40	178	214
ASCE-7	1.08	0.22	20.4	1.30	264	283
Least Square	1.10	0.39	35.5	1.49	261	288
Spectrum Match	0.68	0.14	20.6	0.82	272	318
Atkinson	1.92	0.79	41.1	2.71	185	218

Table 6.19 : Summary of interstorey drift and base shear for the 15-storey frame

Scaling method	ISD, %h	SD, %h	Dispersion, %ISD	ISD+SD, %h	Min BS, kN	Max BS, kN
PGA	0.67	0.27	40.1	0.94	269	305
PSa	0.86	0.28	32.7	1.14	275	330
Ordinate	1.41	0.46	32.5	1.87	274	322
Partial Area	0.92	0.31	33.6	1.23	311	362
ASCE-7	0.89	0.18	20.2	1.07	332	357
Least Square	0.81	0.65	80.2	1.46	340	379
Spectrum Match	0.52	0.11	21.2	0.63	333	376
Atkinson	1.32	0.50	37.9	1.82	271	335

Table 6.20 : Summary of interstorey drift and base shear for the 20-storey frame

Scaling method	ISD, %h	SD, %h	Dispersion, %ISD	ISD+SD, %h	Min BS, kN	Max BS, kN
PGA	0.67	0.16	23.6	0.83	389	470
PSa	0.84	0.22	26.8	1.06	385	423
Ordinate	1.10	0.49	44.8	1.59	379	443
Partial Area	0.84	0.31	37.4	1.15	511	552
ASCE-7	1.00	0.18	18.0	1.18	512	555
Least Square	0.54	0.48	88.9	1.02	522	545
Spectrum Match	0.50	0.06	12.0	0.56	485	547
Atkinson	2.40	1.36	56.7	3.76	396	432

It is clear from these tables that the results of the dynamic time history analysis involves a significant uncertainty irrespective of the method used for scaling the ground motion records. Most methods produce large dispersion (i.e., more than 30%) in majority of the cases. Even the artificial records produce 33% to 57% dispersion of the interstorey drift values. Among all the methods used for scaling or matching the ground motion records to the design level of seismic hazard, the frequency domain matching of the spectral shape as performed here by Seismo Match seem to produce the best results by limiting the level of dispersion to less than 30% except in the case of the 5-storey frame. In case of the 5-storey frame, the ordinate method of scaling produces the best result (10.5% dispersion). In cases of the 10, 15 and 20 storey buildings, the spectral matching of the ground motion records by SeismoMatch produces the best results with the following levels of dispersion: 20.6%, 21.2% and 12.0%, respectively.

The ranges of the base shear (BS) obtained from the dynamic analysis using different methods of scaling of the ground motion records show a similar level of variability.

However, in comparison to the design base shear as reported in Table 5.2, the base shear from the dynamic analysis are found to be in the acceptable range. For example, the design base shear from the 5-storey building frame is 178 kN as shown in Table 5.2, while the minimum and maximum values of the base shear obtained from the time history analysis are found to be 121 kN and 254 kN, respectively (considering all methods as shown in Table 6.17). Similar observation can be made for the other buildings.

The scaling methods show different options available to the engineer to employ in scaling the GMR used in time history analysis. However, in controlling the response parameters and to minimize the effect of the scaling method employed engineering judgment has to be exercised under adequate supervision to obtain the design spectrum from the available ground motion. There is wide range of variability in the response quantities (e.g., interstorey drift) irrespective of the ground motion scaling techniques used. Among all the methods of scaling and spectral matching of the ground motion records, the frequency domain spectral matching seem to produce the best results as the dispersion in the results are observed to be lower than that in other cases. However, the interstorey drift obtained from the time history analysis using different scaling methods show a uniform and consistent pattern of deformation in low rise to medium rise frames, whereas a greater dispersion of the results has been observed in tall buildings. Although a similar level of variability is observed in the base shear obtained from the dynamic time history analysis, they are consistent with the design base shear from the corresponding buildings.

Chapter 7

Observations and Conclusions

7.1 Observations

In the present research the seismic response of steel buildings with moment resisting fames has been carried out using static and dynamic analysis procedures. Different methods available for the performance-based seismic design of buildings have been examined in the context of the buildings designed according to the current building code of Canada. In the nonlinear time history analysis, the effect of different available ground motion scaling techniques on the seismic response of the buildings has been studied. Four identical type of steel moment frames with varying height i.e., 5, 10, 15, 20 storey frames have been used in the study for the evaluation of seismic performance of moment resisting steel frame buildings. The force-based design provision or the equivalent static load method prescribed in the National Building Code of Canada (NBCC 2010) has been adopted in the design of the steel frames. The design of the building using the code based method is further evaluated through rigorous static and dynamic nonlinear analysis to check the performance of the buildings. The Nonlinear static Pushover analysis is carried out to evaluate the ductility capacity under seismic action. In this method the frame is pushed to a targeted roof displacement by applying the seismic force as lateral force varying in a inverted triangular shape, through the Nonlinear static pushover analysis the ductility capacity is obtained using the yield displacement and ultimate displacement of the SMRF. The ductility capacities as obtained from the pushover analysis obtained are 1.94, 2.10, 1.88 and 2.0 for twenty, fifteen, ten and five storey frames, respectively. Therefore, it is inferred that the ductility capacity of the buildings are lower than that assumed in the building design. A

range of performance-based design methodologies based on the static procedure has been examined in the context of the static pushover analysis and it is observed that the design procedure as provided in the current code NBCC 2010 can be used for producing a building design to achieve the life safety and collapse prevention levels of performance.

In the next step, Nonlinear Time history analysis (RHA) has been carried out for each of the real ground motion used coupled with every scaling techniques considered for the study to evaluate the seismic demand of the buildings to consider the effect of scaling technique used. The real ground motions are scaled to make them compatible to the specified location of the buildings beforehand whereas the synthesized ground motions are readily compatible to be used in the RHA . The mean interstorey drift value (M) and the mean plus standard deviation (M+SD) are computed from the RHA of the real ground motions. It is further noted that any of the eight scaling technique tested in the study can be easily used for scaling real ground motions in practice, the study also reveals that response from the scaled ground motions are observed to be more coherent and less dispersed in 5 and 10 storey frames whereas the dispersion was found to be deviant in 15 and 20 storey frames, the interstorey drift obtained from the tested scaling methods confirmed to the code NBCC 2010 specified limit of 2.5% interstorey drift. However the Least square scaling method and the synthesized records displayed interstorey drift exceeding 2.5% in certain ground motions. The value of mean plus standard deviation of the interstorey drift for real ground motion varies from 1.55% of storey height to 2.5% of storey height. The maximum value of interstorey drift for long period synthesized records varies from 1.20% to 2.18% and the maximum value of the interstorey drift for short period records varies from 1.93% of height of the storey to 2.35%.

The NBCC 2010 specifies only one performance objective - collapse limit at 2.5% interstorey drift. On the other hand, other standards like FEMA-273 (1997) and Vision 2000 (SEAOC, 1995) specify different level of performance with different performance objectives for a more robust design. FEMA-273 (1997) specifies the interstorey drift limit for Immediate Occupancy (IO) performance objective as less than 2%. NBCC 2010 drift specification of 2.5% for collapse prevention (CP) is considered is considered to in line with those standards. However, it may produce a conservative design in some cases such as the low rise building (e.g., the five storey building considered here). The Non-linear static analysis carried out in the light of the performance-based design of structures also shows that NBCC design procedure is conservative in some cases.

7.2 Conclusions

It is important to note that while the techniques utilized in the present work are available in the literature, the main contribution of the present work lies in the study of the effect of ground motion scaling methods in estimating the seismic response of a set of buildings designed according to the latest version of the Canadian code, and the interpretation of the seismic response of these buildings estimated using static procedures in the context of performance-based design. The present study provides an important insight into the sensitivity of the estimated dynamic response of buildings to ground motion scaling. It also shows how the existing performance-based methods can be utilized in the design and evaluation of the new

buildings based on the static pushover analysis. Based on the present study, the following conclusions are drawn.

- The code prescribed force-based design procedure is found to be slightly conservative. However, it can be used to predict or ensure the performance of the structure for life safety and collapse prevention.
- Non-linear static and nonlinear dynamic analysis in time domain are required to design the building in order to achieve the stated performance objective, the code based equivalent static load procedure holds good for a large class of conventional and simple structures with no complexities in design or geometry .
- The ductility capacity assumed in the force-based design is also unrealistic and the assumed ductility is hard to achieve
- It is a noted observation in pushover analysis that the roof displacement corresponding to instability or 2.5% interstorey drift is greater than the roof displacement corresponding to maximum of M+SD. Where, M & SD are the mean and standard deviation of the interstorey obtained from Response History Analysis
- The chosen method of scaling the real ground motion has a direct effect on the seismic demand of the building which usually varies widely for different methods of scaling. Hence a suitable scaling technique has to be chosen so as to keep the seismic demand and the related dispersion in control.
- Artificial or synthesized records may be chosen in absence of real records as they are known to give distorted dispersion of the seismic demand. However, the artificial records may not necessarily produce better results. It may produce the same level of uncertainty as for the scaled real records.

- Ground motions produced from a suit of real records by changing them in the frequency domain to match the design spectrum seem to work better and the level of dispersion produced by these records is found to be lower than the cases when other scaling methods are used.

7.3 Scope for future work

The scope for further research lies in exploring ways to the possibility of new scaling techniques that can control the dispersion in the response more effectively. Also, other types of buildings should be studied to understand the effect of ground motion scaling such that a coherent scaling technique can be developed in the future.

REFERENCES

Abrahamson, N.A. (1992). Software program – RSPMatch, Non-Stationary Spectral Matching. Seismological Research Letters, 63:1, 30.

Abrahamson, N.A., Hancock , J., Watson-Lamprey J., Markatis, A., McCOY, E., MENDIS, R., 2006. Program SeismoMatch v2 – software capable of adjusting earthquake accelerograms to match a specific design response spectrum, using the wavelets algorithm proposed by Abrahamson [1992] and Hancock et al. [2006]. http://www.seismosoft.com/en/SeismoMatch.aspx (cited October 2005).

Akbas B., Shen J., Kara FéI., Tugsal U.M., 2003, Seismic *behavior and Pushover Analyses in Steel Frames*, fifth National Conference on Earthquake Engineering, 26-30 May, Istanbul, Turkey, Paper No: AT-053

Alavi, B., and Krawinkler, H. (2000). "Consideration of near-fault ground motion effects in seismic design." Proc. of the 12th World Conf. on Earthquake Engineering, Paper No. 2665, New Zealand Society of Earthquake Engineering, Silverstream, New Zealand.

Ambraseys, N. N., Douglas, J., Rinaldis, D., Berge-Thierry, C., Suhadolc, P., Costa, G.,Sigb jomsson, R. and Smit , P. [ZOO41 "Dissemination of European strong-mot ion data,Vol. 2,". CD-ROM Collection, Engineering and Physical Sciences Research Council,United Kingdom.

ASCE, 2000. Standard ASCE 4-98, Seismic analysis of safety-related nuclear structures and commentary, American Society of Civil Engineers, Reston, VA.

ASCE, 2005, ASCE Standard ASCE/SEI 7-05. Minimum Design Loads for Buildings and Other Structures, Including Supplement No.1, American Society of Civil Engineers, Reston, VA.

Aschheim M., 2004, *Yield Point Spectra: A Simple Alternative to the Capacity Spectrum Method*, ASCE online research library http://www.ascelibrary.org (cited October 2005)

ATC, 1978. Tentative Provisions for the Development of Seismic Regulations for Buildings (ATC 3-06), Applied Technology Council, Redwood City, CA. (A second printing, in 1984, includes 1982 amendments).

Atkinson, G.M. 2009. Earthquake time histories compatible with the 2005 National Building Code of Canada uniform hazard spectrum. Canadian Journal of Civil Engineering, 36: 991-1000.

Bagchi, 2001, *Evaluation of the Seismic Performance of Reinforced Concrete Buildings*, Ph. D thesis, Department of Civil and Environmental Engineering, Carlton University, Ottawa, Canada

Beresnev, I., and G. Atkinson (1998). Stochastic finite-fault modeling of ground motions from the 1994 Northridge, California earthquake. I.Validation on rock sites, Bull. Seism. Soc. Am. 88, 1392–1401.

Beyer, K., and Bommer, J. 2007. Selection and scaling of real accelerograms for bi-directional loading: a review of current practice and code provisions. Journal of Earthquake Engineering, 11: 13-45.

Bommer, J.J. and Aceveo, A.B., 2004. The use of real earthquake accelerograms as input to dynamic analysis. Journal of Earthquake Engineering, 8(1), 43–91.

Boore, D. (2003). Prediction of ground motion using the stochastic method, Pure Appl. Geophys. 160, 635–676.

Bozorgnia, Y., and Mahin, S. A. (1998). “Ductility and strength demands of near-fault ground structure-specific scalar intensity measures 389 motions of the Northridge earthquake.”

Proc. of the 6th U.S. National Conf. on Earthquake Engineering, Earthquake Engineering Research Institute, Seattle.

Bozorgnia, Y.A., Bertero, V.V.A., 2004. Earthquake Engineering: From Engineering Seismology to Performance-Based Engineering , Text Book , CRC Press.

Chopra A.K. and Goel R.K., 1999, *Capacity-Demand-Diagram Method for Estimating Seismic deformation of Inelastic Structures: SDF systems*, Report No.PEER-1999/02 Pacific Earthquake Engineering Research Center, University of California, Berkeley, USA

Chopra, A. K., and Chinatanapakdee, C. 2004. "Inelastic deformation ratios for design and evaluation of structures: Single-degree-of-freedom bilinear systems." J. Struct. Eng., 130(9), 1309–1319.

CISC, 2010. *Handbook of Steel Construction*, Canadian Institute of Steel Construction, Willowdale, Ontario, Canada.

Cornell, C.A. (1968). Engineering seismic risk analysis, Bull. Seism. Soc. Am., 58, 1583-1606.

CSA. 2009. Design of Steel Structures, CSA-S16-09, Canadian Standards Association, Toronto, ON.

CSI, 2012a, ETABS v9.5 Integrated analysis, design and drafting of building systems, Computer Software, Computers and Structures, Inc., http://www.csiberkeley.com/ (cited Dec 2012).

CSI, 2012b, PERFORM 3D v5 NONLINEAR ANALYSIS AND PERFORMANCE ASSESSMENT FOR 3D STRUCTURES, Computer Software, Computers and Structures, Inc., 2012, http://www.csiberkeley.com/ (cited Dec 2012).

DeVall R.H, 2003, *Background information for some of the proposed earthquake design provisions for the 2005 edition of the National Building Code of Canada*, Canadian Journal of Civil Engineering. **30**: 279-286,

EC8, 2004. Eurocode 8: Design of structures for earthquake resistance, Part 1 – General rules, seismic actions and rules for buildings, European Committee for Standardization, Brussels, Belgium.

Fahjan, Y.M., Ozdemir, Z. and Keypour, H. 2007. Procedures for real earthquake time histories scaling and applicationto fit iranian design spectra, 5th International Conference on Seismology and Earthquake Engineering (SEE5), May 14-16, Tehran, Iran.

Fahjan Y. and Ozdemir Z., 2008. "Scaling of earthquake accelerograms for non linear dynamic analyses to match the earthquake design spectra", The 14th World Conference on Earthquake Engineering (14WCEE), Beijing, China.

Fajfar P.,2000, *A Nonlinear Analysis Method for Performance Based Seismic Design*, Earthquake Spectra, Vol.16, No.3pp.573-592

FEMA-273, 1997, *NEHRP Guidelines for the Seismic Rehabilitation of the Buildings*, prepared for the Building Seismic Safety Council (BSSC), Washington, D.C. USA

Gasparini, D.A., and Vanmarcke, E.H. 1976. SIMQKE: A program for artificial motion generation. User's manual and documentation, Department of Civil Engineering, Massachusetts Institute of Technology, Cambridge, Massachusetts.

Ghobarah A., 2001, *Performance-based design in earthquake engineering: state of development*, Engineering Structures 23 : 878-884.

Gupta A. and Krawinkler H.,2000,*Estimation of seismic drift demands for frame structures*, Earthquake Engineering and Structural Dynamics, Earthquake Engng Struct.Dyn.2000; 29:1287-1305

Hancock J, Bommer JJ. A state-of-knowledge review of the influence of strong-motion duration on structural damage. Earthquake Spectra 2006;22(3):827–45.

Hannan M., 2006, *Earthquake Resistant Design of a Twenty Story Building with Steel Moment Resisting Frames*, M.Eng. Project , Department of Building Civil and Environmental Engineering, Concordia University, Montreal, Canada

Herrera R., Ricles J. M., Sause R., Lewis B., 2003, *Seismic Performance Evaluation of Steel Moment Resisting Frames With Concrete Filled Tube Columns* ', Dept. of Civil Eng., Lehigh University, Bethlehem, Pennsylvania, http://www.ncree.org.tw (cited October 2005)

Humar, J. and Mahgoub M. A., 2003, *Determination of seismic design forces by equivalent static load method*, Canadian Journal of Civil Engineering, Volume 30 287-307.

Humar J. and Ghorbanie-Asl M., 2005, *A New Displacement-Based Design Method for Building*, 33rd Annual General Conference of the Canadian Society for Civil Engineering, GC-136, Toronto, Ontario, Canada.

Idriss, I.M, 1993. "Procedures for selecting ground motions at rock sites, "Report to the U.S. Department of Commerce . National Institute of Standards and Technology .

Kalkan, E. and Chopra, A. (2011). "Modal-Pushover-Based Ground-Motion Scaling Procedure." J. Struct. Eng. 137, SPECIAL ISSUE: Earthquake Ground Motion Selection and Modification for Nonlinear Dynamic Analysis of Structures, 298–310.

Katsanos, E.I., Sextos, A.G., and Manolis, G.D. 2010. Selection of earthquake ground motion records: a state-of-the-art review from a structural engineering perspective. Soil Dynamics and Earthquake Engineering, 30: 157-169.

Kaul, M.K. (1978). Spectrum consistent time-history generation, ASCE J. Eng Mech. EM4, 781-788.

Leger, P., Tremblay, R. 'Earthquake Ground Motions for Seismic Damage Assessment and Re-Evaluation of Existing Buildings and Critical Facilities", 2009, Book Section Page 193-219 - Damage Assessment and Reconstruction after War or Natural Disaster , Organisation - NATO Science for Peace and Security Series C: Environmental Security Edited by : Ibrahimbegovic, Adnan, Zlatar, Muhamed, Springer Netherlands 2009

Lilhanand, K. and Tseng, W. S. [I9881 "Development and application of realistic earthquake time histories' compatible with multiple-damping design spectra," Proceedings of the Ninth World Conference on Earthquake Engineering, Tokyo-Kyoto 2, 819-824.

Luco, N., and Cornell, A. C. (2007). "Structure-Specific Scalar Intensity Measures for Near-Source and Ordinary Earthquake Ground Motions," Earthquake Spectra, Vol. 23, No. 2, pp.357–392.

McGuire, R. K. [1995] "Probabilistic seismic hazard analysis and design earthquakes: Closing the loop,", Bulletin of the Seismological Society of America 85, 1275-1284.

Miranda, E. (1993). "Evaluation of site-dependent inelastic seismic designspectra." J. Struct. Eng., 119(5), 1319–1338.

Mukherjee, S. and Gupta, V.K., 2002. Wavelet-based generation of spectrum compatible time histories. Soil Dynamic and Earthquake Engineering, 22(9), 799–804.

Nau, J. and Hall, W. (1984). ”Scaling Methods for Earthquake Response Spectra.” J. Struct. Eng., 110(7), 1533–1548

Naumoski, N. 2001. Program SYNTH – Generation of artificial accelerograms compatible with a target spectrum. User's manual, Department of Civil Engineering, University of Ottawa, Ottawa, Ont., Canada.

Naumoski N., Saatcioglu M., and Amiri-Hormozaki K., 2004, *Effects of Scaling of Earthquake Excitations on the Dynamic Response of Reinforced Concrete Frame Buildings*, 13th World Conference on Earthquake Engineering, Vancouver, B.C., Canada, Paper No. 2917.

NBCC 2010, *National Building Code of Canada, 2005*, Canadian Commission on Building and Fire Codes, National Research Council of Canada, Ottawa

Nikolaou, A.S. (1998). A GIS Platform for Earthquake Risk Analysis, Ph.D.Thesis, State University of New York at Buffalo

Papageorgiou, A., Halldorsson, B. and Dong, G. (2002). TARSCTH (Target Acceleration Spectra Compatible Time Histories), Engineering Seismology Laboratory (ESL) at the State University of New York at Buffalo.

PEER, 2012, *Pacific Earthquake Engineering Research Center: NGA Database*, http://peer.berkeley.edu (cited October 2005).

Prakash V., Powell, Graham H, Campbell, Scott D., 1993, *Drain-2DX: Static and Dynamic analysis of Inelastic Plane Structure*, Department of Civil Engineering, University of California, Berkeley.

Priestley, M.J.N [2000].” Performance Based Seismic design” . Proceedings, 12 th WCEE, Auckland , New Zealand

Reitherman, R. (2008). International Aspects Of the History of Earthquake Engineering Part I February 12, Draft https://www.eeri.org/site/images/awards/reports/reithermanpart1.pdf (cited December, 2012).

Sawada T, Hirao K, Yamamoto H, Tsujihara O. Relation between maximum amplitude ratio and spectral parameters of earthquake ground motion. In: Proceedings of 10th world conference of earthquake engineering. Madrid, Spain, vol. 2, 1992.

SEAOC, 1995. Performance-based seismic engineering, Vision 2000 Committee, Report prepared by Structural Engineers Association of California, Sacramento, CA

SEAOC, 2007. "Development of System Factors", Seismology Committee, The SEAOC Blue Book: Seismic Design Recommendations, Structural Engineers Association of California, Sacramento, CA. Accessible via the world wide web at: http://www.seaoc.org/bluebook

Shome, N., and Cornell, A. C. (1998). "Normalization and scaling accelerograms for nonlinear structural analysis." Proc. of the 6th U.S. National Conf. on Earthquake Engineering, Earthquake Engineering Research Institute, Seattle.

Somerville., P., N. C. Smith, and R. W. Graves, 1997a. Modification of Empirical Strong Ground Motion Attenuation Relations to Include the Amplitude and Duration Effects of Rupture Directivity, Seism. Res.Lett. 68, no. 1, 199–221.

Somerville, P., Smith, N., Punyamurthula, S. and Sun, J., 1997b. Development of ground motion time histories for phase 2 of the FEMA/SAC steel project. SAC Joint Venture, Report No.SAC/BD-97/04, California.

Somerville, P. G. (1998). Emerging Art: Earthquake Ground Motion. Geotechnical Earthquake Engineering and Soil Dynamics III, ASCE Geotechnical Special Publication No. 75, Vol. 1, 1-38.

Stewart, J.P., S.J. Chiou, J.D. Bray, R.W. Graves, P.G. Somerville, N.A. Abrahamson. (2001). "Ground motion evaluation procedures for performance-based design," PEER-2001/09, UC Berkeley.

Tso WK, Zhu TJ, Heidebrecht AC. Engineering application of ground motion A/V ratio. Soil Dynamics and Earthquake Engineering 1992; 11:133–44.

Tothong, P., and Luco, N., 2007. Probabilistic seismic demand analysis using advanced groundmotion intensity measures, Earthquake Eng. Struct. Dyn. 36, 1837–1860.

Tothong, P., and Cornell, A. C. (2008). "Structural performance assessment under near-sourcepulse-like ground motions using advanced ground motion intensity measures," Eq. Eng. And Str. Dyn. Vol. 37, No. 7, pp. 1013-1037.

Vidic, T., Fajfar, P., and Fischinger, M. (1994). "Consistent inelastic design spectra: Strength and displacement." Earthquake Eng. Struct. Dyn.,23(5), 507–521.

Yun S.Y., Hamburger R.O., Cornell C. A., and Foutch D.A., 2002, *Seismic Performance Evaluation for Steel Moment Frames,* Journal of Structural Engineering, Vol. 128, No. 4, pp. 534-545

Yousuf, M, 2006. "Md Yousuf, M.A.Sc. Seismic Performance of Steel Frame Buildings", M.A.Sc. thesis, Department of Building, Civil and Environmental Engineering, Concordia University, Montreal, Canada.

Yousuf, M. and Bagchi, A., 2009, "Seismic Design and Performance Evaluation of Steel-Frame Buildings Designed using NBCC-2005", *Canadian J of Civil Engineering*, 36: 280-294.

Yousuf, M. and Bagchi, A., 2010, "Seismic Performance of a Twenty Storey Steel Frame Building in Canada", *J of Structural Design of Tall and Special Building*, 19: 901-921.

Zeng, Y., J. Anderson, and G. Yu (1994). A composite source model forcomputing realistic synthetic strong ground motions, Geophys. Res.Lett. 21, 725–728.